



## Seismic stratigraphy of the post-breakup succession offshore Northeast Greenland: Links to margin uplift

**Petersen, Thomas Guldborg**

*Published in:*  
Marine and Petroleum Geology

*Link to article, DOI:*  
[10.1016/j.marpetgeo.2019.03.007](https://doi.org/10.1016/j.marpetgeo.2019.03.007)

*Publication date:*  
2019

*Document Version*  
Peer reviewed version

[Link back to DTU Orbit](#)

*Citation (APA):*  
Petersen, T. G. (2019). Seismic stratigraphy of the post-breakup succession offshore Northeast Greenland: Links to margin uplift. *Marine and Petroleum Geology*, 103, 422-437.  
<https://doi.org/10.1016/j.marpetgeo.2019.03.007>

---

### General rights

Copyright and moral rights for the publications made accessible in the public portal are retained by the authors and/or other copyright owners and it is a condition of accessing publications that users recognise and abide by the legal requirements associated with these rights.

- Users may download and print one copy of any publication from the public portal for the purpose of private study or research.
- You may not further distribute the material or use it for any profit-making activity or commercial gain
- You may freely distribute the URL identifying the publication in the public portal

If you believe that this document breaches copyright please contact us providing details, and we will remove access to the work immediately and investigate your claim.

Manuscript Number: JMPG-D-19-00073R2

Title: Seismic stratigraphy of the post-breakup succession offshore  
Northeast Greenland: Links to margin uplift

Article Type: Full Length Article

Keywords: Northeast Greenland; continental margin; seismic stratigraphy;  
tectonics; tectonostratigraphy; North Atlantic

Corresponding Author: Dr. Thomas Guldborg Petersen, Ph.D.

Corresponding Author's Institution: Technical University of Denmark

First Author: Thomas Guldborg Petersen, Ph.D.

Order of Authors: Thomas Guldborg Petersen, Ph.D.

Abstract: The timing of the continental breakup between Norway and Greenland and the subsequent plate tectonic motions are well understood. However, due to the remote location of the Northeast Greenland shelf, relatively few details about the tectonosedimentary response to the tectonism following the breakup have previously been published. This article gives new insights into the structural and sedimentary history of the Northeast Greenland shelf, with an emphasis on the post-breakup tectonics, using state of the art 2D seismic data. The results of this study clearly shows a highly dynamic post-breakup tectonic setting with pronounced, kilometre-scale fault offsets, tilting of the Danmarkshavn Basin and pronounced progradational events. The tectonosedimentary events are linked with the passage of the Icelandic mantle plume south of the Northeast Greenland shelf. Based on tectonostratigraphic interpretations and integration of data from ODP 913, this study constructs a temporally robust model for the post-breakup succession. Significant post-breakup uplift and tectonism related to thermal uplift is present on the margin. It is observed that the Icelandic hot spot passes relatively close by the Northeast Greenland shelf (<500 Km) during the Cenozoic. Its passage south of the shelf supports the observation of the northwards tilt of the shelf and associated northwards shift of the prograding clinofolds due to a combination of thermal uplift and possibly dynamic topography.

Research Data Related to this Submission

-----  
There are no linked research data sets for this submission. The following reason is given:

The data that has been used is confidential

**Detailed response**

This resubmission does not contain any major revisions of the manuscript. The resubmission is purely done so that all figures are contained in the revision. Please note that an outline of the salt affected area is included in figure 2, as a response to previous reviewer comments.

Best regards

Thomas Guldborg Petersen

Assistant Professor

## \*Highlights (for review)

- Significant vertical motions along faults after the continental break-up
- Seismic interpretations reveal northward moving progradational units
- Passage of Iceland plume responsible for post-breakup tectonics

- 1     **1     Seismic stratigraphy of the post-breakup succession offshore Northeast**
- 2
- 3     **2     Greenland: Links to margin uplift**
- 4
- 5
- 6
- 7     3     Corresponding author: Thomas Guldborg Petersen, thog@byg.dtu.dk
- 8
- 9
- 10    4     Technical University of Denmark, Anker Engelundsvej 1, 2800 Kongens Lyngby, Denmark
- 11
- 12
- 13
- 14    5
- 15
- 16
- 17
- 18
- 19
- 20
- 21
- 22
- 23
- 24
- 25
- 26
- 27
- 28
- 29
- 30
- 31
- 32
- 33
- 34
- 35
- 36
- 37
- 38
- 39
- 40
- 41
- 42
- 43
- 44
- 45
- 46
- 47
- 48
- 49
- 50
- 51
- 52
- 53
- 54
- 55
- 56
- 57
- 58
- 59
- 60
- 61
- 62
- 63
- 64
- 65

1

2  
3  
4 **2 Abstract**

5  
6  
7 3 The timing of the continental breakup between Norway and Greenland and the subsequent plate  
8  
9 4 tectonic motions are well understood. However, due to the remote location of the Northeast  
10  
11 5 Greenland shelf, relatively few details about the tectonosedimentary response to the tectonism  
12  
13 6 following the breakup have previously been published. This article gives new insights into the  
14  
15 7 structural and sedimentary history of the Northeast Greenland shelf, with an emphasis on the post-  
16  
17 8 breakup tectonics, using state of the art 2D seismic data. The results of this study clearly shows a  
18  
19 9 highly dynamic post-breakup tectonic setting with pronounced, kilometre-scale fault offsets, tilting  
20  
21 10 of the Danmarkshavn Basin and pronounced progradational events. The tectonosedimentary events  
22  
23 11 are linked with the passage of the Icelandic mantle plume south of the Northeast Greenland shelf.  
24  
25 12 Based on tectonostratigraphic interpretations and integration of data from ODP 913, this study  
26  
27 13 constructs a temporally robust model for the post-breakup succession. Significant post-breakup  
28  
29 14 uplift and tectonism related to thermal uplift is present on the margin. It is observed that the  
30  
31 15 Icelandic hot spot passes relatively close by the Northeast Greenland shelf (<500 Km) during the  
32  
33 16 Cenozoic. Its passage south of the shelf supports the observation of the northwards tilt of the shelf  
34  
35 17 and associated northwards shift of the prograding clinoforms due to a combination of thermal uplift  
36  
37 18 and possibly dynamic topography.

38  
39  
40  
41  
42  
43  
44  
45  
46 **1 INTRODUCTION**

47  
48  
49 20 Passive margin tectonism is widely debated, especially in the North Atlantic realm. Conventional  
50  
51 21 models for continental breakup only predict thermally induced subsidence following the heating  
52  
53 22 caused by upwelling mantle (e.g. McKenzie, 1978). However, observations around the margins of the  
54  
55 23 North Atlantic suggest that significant tectonics and vertical motion occurred after the breakup  
56  
57 24 (Lundin and Doré, 2002; Tsikalas et al., 2012). The term breakup, or continental breakup is here

1 understood as the phase of separation between continental lithospheric plates, following the rift  
2 phase, *sensu* Cloetingh et al. (2013).

3 Although the Northeast Greenland shelf has been studied previously (e.g. Funck et al., 2017;  
4 Hamann et al., 2005; Petersen et al., 2015), very little is known about the tectonostratigraphic  
5 development of the shelf after the continental breakup. Based on a comprehensive seismic database  
6 consisting of the latest available data, this study yields new insights into the structural history and its  
7 influence on sedimentation. By conducting a thorough seismic stratigraphic study of the Northeast  
8 Greenland shelf, several seismic units significant to the understanding of the post-breakup  
9 development of Northeast Greenland are interpreted concerning depositional environment,  
10 tectonostratigraphy and relation to plate tectonics. A clear link between the passage of the Icelandic  
11 hotspot, uplift of the inner margin and a northward shift in prograding clinoforms is presented.

## 12 **2 REGIONAL GEOLOGY**

13 The North Atlantic plate tectonic history is described in multiple studies (e.g. Gaina et al., 2009;  
14 Matthews et al., 2016; Müller et al., 2016; Tsikalas et al., 2012). Evidence of rifting throughout the  
15 Paleozoic and Mesozoic along the margins of the North Atlantic is recorded as extensional tectonics  
16 both onshore (Stemmerik, 2000) and offshore (Tsikalas et al., 2012, 2005) as a part of the long-  
17 running opening of the Atlantic Ocean (Cloetingh et al., 2007). The rift to drift transition i.e. the  
18 continental breakup is dated by means of paleomagnetic anomalies to have occurred at 55.9 Ma  
19 (chron 24), at the Paleocene—Eocene transition (Gaina et al., 2009; Matthews et al., 2016; Ogg,  
20 2012; Olesen et al., 2007). This is associated with pronounced volcanism, dated to the earliest  
21 Eocene (Larsen et al., 2014). The shelf south of *ca.* 78° N is the conjugate margin to the Vøring and  
22 Lofoten margin in Norway, and is associated with extension of the Mohns Ridge segment of the mid  
23 ocean ridge system of the North Atlantic (e.g. Gaina et al., 2009; Talwani and Eldholm, 1977; Ziegler,  
24 1992). It is dominated by normal faulting prior to the continental breakup (Tsikalas et al., 2012).  
25 However, the shelf north of *ca.* 78° N is dominated by complex transpressional and transtensional

1 deformation during the opening of the Greenland Sea, where transverse deformation initially  
2 occurred along the East Greenland Ridge, before shifting to the Knipovich Ridge during the  
3 Oligocene. A slowing of the plate tectonic motion (Gaina et al., 2009; Tegner et al., 2011), dated to  
4 ca. 49-47 Ma, coincides with the peak in the Eureka Orogeny along the northernmost edge of  
5 Greenland. Absolute opposite plate motion, where Greenland drifts towards the Northwest and  
6 Norway towards the Southeast, was achieved during the earliest Oligocene (33.1 Ma), which implies  
7 that passive margin conditions were developed along the entire Northeast Greenland and North  
8 Greenland continental margin at this time (Gaina et al., 2009).

9 Pronounced progradation of clinoforms have been described previously, based on low density/low  
10 resolution seismic data, and attributed to a "Tertiary" age (Hamann et al., 2005). The pre-drift  
11 succession of the Northeast Greenland shelf have also been described in detail (Petersen et al.,  
12 2015), but very little has so far been published on the post-breakup seismic stratigraphy.

13 Sea level changes during the Cenozoic have been described previously (Miller et al., 2005) , and the  
14 effects of changing eustatic sea level obviously also had an impact on the sedimentation on the  
15 Northeast Greenland shelf. Even though this article focuses solely on the tectonic processes and on  
16 highlighting the vertical motions observed on the shelf during the post-breakup times, the author  
17 fully acknowledges the influence of eustatic sea level changes as well.

### 18 19 **3 DATA AND METHODS**

20 The database of this study is composed of the latest vintages of commercial 2D seismic data  
21 collected during a period from 2008-2014 by TGS, a commercial seismic data vendor, together with a  
22 scientific dataset collected by the Alfred Wegener Institute (AWI) during the early nineties (Berger  
23 and Jokat, 2009, 2008) (Fig.1). All seismic data are courtesy of TGS and Spectrum. The seismic data  
24 were supplied under the agreement that no shot points or navigational data are published. These



1 data are supplemented by free air gravity data from the DTU10 global gravity field model (Andersen,  
2 2010; Andersen et al., 2010). The locations of the North Atlantic hotspots are derived from  
3 Whittaker et al. (2013), and the locations of the magnetic anomalies are adopted from Müller et al.  
4 (2016). Plate tectonic reconstructions are based on Matthews et al. (2016). Reconstruction of the  
5 path of the hotspots was done using the open source software GPlates ([www.gplates.org](http://www.gplates.org)). The  
6 seismic interpretation was conducted using a seismic workstation (Petrel 2016). Standard seismic  
7 stratigraphic methods was applied as outlined by Emery and Myers (1996).

## 8 9 **4 OBSERVATIONS**

### 10 **4.1 Potential field data**

11 The use of free air gravity data gives excellent insights into the geometries of structural elements in  
12 the Northeast Greenland area (Fig. 2). The gravity data quite clearly show the location of the  
13 continental slope (Fig. 2), and the magnetic anomalies (Müller et al., 2016), shows the westward  
14 extent of the oceanic crust, as well as other key features of the Northeast Greenland shelf. The  
15 Danmarkshavn Basin stands out on the inner side of Northeast Greenland's continental shelf as a  
16 distinct low in the gravity field. In fact, the gravity low extends onshore Greenland, outlining the  
17 prominent sedimentary basins present there (Stemmerik, 2000). The Danmarkshavn Ridge is also  
18 outlined in detail as a positive gravity anomaly. The ridge is NE-SW striking and displays a noticeable  
19 right-lateral offset, separating the ridge into a north and a south segment (Fig. 2). It is also clear, that  
20 the deep faults observed on the shelf are parallel to the ridge, and that the faulting of the Cenozoic  
21 succession is focused at or near the ridge, with few exceptions (Fig. 2). Although a detailed  
22 description of the faults is given below, it is noted that faulting is also observed north of the  
23 Danmarkshavn Ridge gravity high. The Thetis Basin is seen as a relatively narrow, elongated gravity  
24 low parallel to the Danmarkshavn Ridge. This shape of the basin in the gravity data is controlled  
25 mostly by a very deep, narrow half graben created during the Mesozoic (Figs. 3a, b). The shape of

1 the basin during the Cenozoic is wider however, and spans from the Danmarkshavn Ridge to the  
2 continental slope.

### 3 **4.2 Seismic interpretation**

4 Based on the observed seismic facies of the individual units, the sedimentary facies, depositional  
5 environment and tectonic evolution are evaluated. The methodology is briefly described in Emery  
6 and Meyers (1996), where they highlight the seismic expression of various depositional  
7 environments. Due to the lack of well control, the seismic facies interpretations in this study are  
8 associated with some uncertainty.

9 This study is based on the mapping of several seismic horizons across the Northeast Greenland shelf  
10 and onto the oceanic crust (Figs. 3-7). The shown seismic horizons all hold significant information  
11 about the tectono-sedimentary history during the Neogene of Northeast Greenland. By using  
12 conventional seismic interpretation techniques and seismic stratigraphic principles, it is possible to  
13 describe exhumation, subsidence and the relative timing of tectonic events. This study establishes a  
14 regional framework of tectonic events with good confidence due to the inclusion of the most  
15 comprehensive, high quality seismic database currently available (fig. 1). The seismic observations  
16 correlates well with the gravity data, confirming the control of deeper structures on the depositional  
17 pattern. (Fig. 2). Examples of both the seismic horizons and the interpreted faults are presented in  
18 seismic cross sections (Figs. 3-7), and in map form (Figs. 8, 9). Only one borehole is available for age  
19 correlation, namely the ODP 913 borehole (Thiede et al., 1995). The location of ODP 913 on the  
20 oceanic crust means that the pre-breakup succession is not penetrated. Due to the absence of any  
21 deep well bores on the Northeast Greenland shelf, all the ages of the pre-early Eocene seismic  
22 horizons are associated with some uncertainty. This study infers the ages of the seismic horizons  
23 from published regional studies (Engen et al., 2008; Hamann et al., 2005; Petersen et al., 2015;  
24 Tsikalas et al., 2012), and by correlating with plate tectonic events highlighted in this study.

1 Structure maps of key surfaces are also presented (Fig. 8a, b). These maps are all in Two Way Time  
2 (TWT) reported in seconds. All structure and thickness maps are interpolations of seismic data,  
3 within the extent of the interpreted horizon. This means that the outer boundary of a surface is  
4 defined by the absence of the seismic horizon due to either erosion or condensation, or due to the  
5 lack of resolution in the seismic data. The study also includes thickness maps used to highlight areas  
6 of deposition (Figs. 10-12).

7 The seismic units described below, subdivide the Paleogene and Neogene succession of the  
8 Northeast Greenland margin into three seismic units significant for the understanding of the tectonic  
9 evolution after the continental breakup. The interpretation and definition of the seismic units was  
10 based on their importance concerning structural evolution of the margin, especially during post-  
11 breakup times. Pronounced unconformities was the central focus, as they play a significant role in  
12 the identification of the location and timing of tectonic events on the Northeast Greenland shelf.  
13 Seismic facies in the respective units are also described in order to interpret the depositional  
14 mechanisms responsible for the deposited sediments and to constrain the structural evolution of the  
15 Northeast Greenland margin after the breakup.

### 16 **4.3 Dating of the seismic units**

17 All dating of the seismic units is done by correlation with the plate tectonic evolution as well as  
18 understanding of regional tectonic events in conjunction with the previously mentioned ODP 913  
19 borehole. Previous studies have created a framework for the dating of the pre- and syn- breakup  
20 succession (Petersen et al., 2016, 2015). The current study further constrains the ages of the pre-  
21 breakup succession suggested in these studies by usage of better quality seismic data and closer  
22 correlation to the ODP 913 borehole. Furthermore, this study adds significant new knowledge about  
23 the post-breakup seismic units and their relative timing. The addition of reprocessed and recently  
24 acquired seismic data improves the reliability of these interpretations and adds additional  
25 information regarding the ages of the depositional events.

1 Prior to the onset of Paleocene deposition, a regional unconformity is observed in the Wandell Sea  
2 area, north of the current study area (Håkansson and Stemmerik, 1989). This and other observations  
3 are used by Hamann et al. (2005) to define the base of the Cenozoic succession in the Danmarkshavn  
4 Basin area. Furthermore, observations onshore Northeast Greenland in the Wollaston Foreland and  
5 Sabine Ø area (Fig. 2) confirms a hiatus between the Cretaceous and the Paleogene (Nøhr-Hansen  
6 et al., 2011). A change from syn-tectonic halfgraben infill to parallel reflections mark the Mesozoic-  
7 Cenozoic transition in the Thetis Basin. The accuracy of the age of the unconformity is uncertain due  
8 to the lack of any means of direct dating. Furthermore, the interface is most likely diachronous  
9 across most of the study area, although early Cenozoic deposits appear relatively conformable at  
10 their base, with the exception of the south part of the study area, where Petersen et. al (2015)  
11 describe progradation from the southwest.

12 The Early Eocene Unconformity is relatively well dated due to its association with the breakup  
13 volcanism. Compelling evidence of deepening of the erosion towards the centre of the magmatic  
14 intrusions in the Danmarkshavn Basin, (Petersen et al., 2015), together with the coinciding gas vent  
15 structures from the intrusions (Reynolds et al., 2017) yields a relatively tight constraint on the age of  
16 this horizon (Fig. 5). This is achieved by utilizing the well-known absolute ages of the peak in  
17 magmatic intrusions onshore Northeast Greenland (Larsen et al., 2014). These observations are  
18 further corroborated by the availability of the high quality data for this study. Especially the  
19 northwards correlation of this event makes it possible to constrain the ages of the  
20 tectonosedimentary events in the north of the study area (Fig. 7b).

21 There are no direct means of constraining the age of the Erosional incision seismic horizon, so a  
22 relative dating of the horizon is suggested. The Erosional incision horizon clearly truncates the well-  
23 dated Early Eocene Unconformity (Figs. 4a-c), thus a post- Early Eocene age can be initially  
24 suggested. The erosional incision also truncates strata younger than early Eocene, so the incision  
25 must post-date the Early Eocene Unconformity by some margin. The upwards constraint of the age

1 of the erosional incision is the Intra Miocene Unconformity, as this horizon is not truncated by the  
2 incision. However, a significant sedimentary succession is present between the two horizons, which  
3 hampers the possibility for a more accurate age for the Erosional incision horizon other than late  
4 Eocene—mid Miocene. An important observation in this context is that the Erosional incision  
5 horizon post-dates the continental breakup.

6 The Intra Miocene horizon is dated using the information from the ODP 913 borehole using the  
7 seismic tie from Berger and Jokat (2008). This is the only directly dated horizon in this study, but  
8 some uncertainty is still associated with the age of this horizon. Firstly, it is an unconformity, which is  
9 inherently a time-transgressive surface. Therefore significant lateral changes in the age of the  
10 horizon may occur. Secondly, the seismic correlation from the ODP 913 drill site and onto the  
11 Northeast Greenland shelf is associated with some uncertainty, due to sparse seismic data in the  
12 area and condensation across the continental slope. Still, this horizon remains possibly the most  
13 accurately dated seismic horizons of this study, and therefore it forms a significant anchor for the  
14 dating of the post-breakup events on the Northeast Greenland Shelf.

15 The youngest horizon interpreted in this study is the Top upper prograding unit seismic horizon. No  
16 direct methods for dating this horizon exists. It is clearly younger than the Intra Miocene  
17 unconformity horizon and it was affected by the uplift and rotation of the Danmarkshavn Basin and  
18 Ridge areas. This is evident from its location above a set of very steep clinofolds associated with the  
19 uplift (Fig. 3a). The only age constraint of this horizon is an age younger than mid Miocene, and  
20 predating the Quaternary glaciations of the shelf, since the shallow Quaternary erosion does not  
21 incise deeply into the unit (Fig. 4a).

#### 22 **4.4 Pre-Cenozoic units**

23 It is beyond the scope of this study to conduct a detailed interpretation of the Palaeozoic and  
24 Mesozoic succession on the Northeast Greenland shelf. However, some general observations are of  
25 relevance to the further interpretation, and will be summarised here. For a more complete

1 understanding of the pre-Cenozoic geology of the Northeast Greenland shelf, see e.g. Hamann et al.  
2 (2005). The Palaeozoic—Mesozoic Succession is largely conformable, but minor angular  
3 unconformities exist near the presumed Palaeozoic—Mesozoic transition (Figs. 3a, b). The  
4 succession is intersected and rotated by normal faults near the Danmarkshavn Ridge. The faults are  
5 all apparently deeply rooted (e.g. Fig. 5). The pre-Cenozoic succession of the Thetis Basin is largely  
6 deposited in a rotated half graben setting, with the controlling fault located along the east margin of  
7 the Danmarkshavn Ridge (Fig. 3b). The Cenozoic succession is thus underlain by several kilometres of  
8 Palaeozoic and Mesozoic sediments, intersected by faults mostly generated during Mesozoic rifting  
9 (Hamann et al., 2005).

#### 10 **4.5 Paleocene(?)—Early Eocene seismic unit**

11 The unit is partially described in Petersen et al. (2015), in the southern part of the Danmarkshavn  
12 Basin. A more regionally cohesive interpretation is included in this study since it is important for  
13 understanding the structural framework, and it forms an important temporal constraint of the  
14 continental breakup. The Base Paleogene horizon is the base of this unit and is regionally extensive  
15 and observed across most of the Northeast Greenland shelf area. It is primarily defined as an erosive  
16 unconformity, with a deepening incision towards the west in the Danmarkshavn Basin (Fig. 3a, b). A  
17 significant topographic break is observed at the transition from the Danmarkshavn  
18 Basin/Danmarkshavn Ridge and into the Thetis Basin (Figs. 3a, 8a), where the Base Paleogene lies  
19 significantly deeper. Towards the south, faulting offsets the Base Paleogene in the west part of the  
20 Thetis Basin (Figs. 3b, 4c). The Base Paleogene is delimited towards the west by erosion due to uplift  
21 and tilting of the Cenozoic succession. Towards the east, i.e. towards the continental slope, the Base  
22 Paleogene is truncated, since the continental rifting did not occur before the earliest Eocene (Gaina  
23 et al., 2009). The north and south extent of the unconformity is not resolved by the current data set.  
24 In the Thetis Basin, east of the basin bounding fault system (Fig. 2), the Base Paleogene Horizon  
25 seems to be mostly conformable with the underlying Mesozoic sediments. There are however some

1 evidence of faulting below the Base Paleogene, especially along the western margin of the Thetis  
2 Basin (Fig. 5). The Danmarkshavn Basin displays clear evidence of inversion following the Mesozoic  
3 rift phases, creating compressional structures such as folds and domes below the Base Paleogene  
4 (Fig. 5). These structures were subsequently eroded during a Late Cretaceous—Paleogene (?) and  
5 early Eocene erosional events (Figs. 3b, 4a). This compressional event is focused in the  
6 Danmarkshavn Basin and Ridge areas, in comparison with the more conformable nature of the Base  
7 Paleogene in the Thetis Basin. The seismic facies below the Base Paleogene show frequent examples  
8 of high amplitude, discontinuous reflections, often intersecting the bedding. These structures have  
9 previously been described as magmatic intrusions (Fig. 7b), (Petersen et al., 2015; Reynolds et al.,  
10 2017). Towards the eastern margin of the Thetis Basin, the seismic data show a rise of the Base  
11 Paleogene (Fig. 8a). This rise coincides with the shelf to continental slope transition, which is also  
12 coinciding with a gravity high (Fig. 2). The high-amplitude, discontinuous reflectors are also very  
13 prominent below the rise.

14 The unit mostly consists of parallel, medium to high amplitude reflections, with the high amplitudes  
15 focused mainly in the Danmarkshavn Basin and the Danmarkshavn Ridge areas. The unit is thinning  
16 across the eastern margin of the Danmarkshavn Ridge, and there is evidence of internal erosion  
17 along the ridge margin, especially to the north (Fig. 3a).

18 The thickness map (Fig. 10) show a southerly-located depo-centre in the Thetis Basin, with a distinct  
19 thinning across the Danmarkshavn Ridge, and smaller depo-centres in the Danmarkshavn Basin,  
20 consistent with previous observations (Petersen et al., 2015). Diverging internal reflections towards  
21 the faults separating the Danmarkshavn Ridge from the Danmarkshavn Basin indicate syn-tectonic  
22 deposition related to normal faulting (Fig. 5). The truncation of the seismic unit that deepens  
23 towards the south is mostly controlled by structural rotation and uplift (Fig. 5). The horizon is heavily  
24 disturbed in some places, where deep (100-200ms TWT, *ca.* 100-200 m) and laterally extensive (<2  
25 km) depressions or pockmarks are observed specifically at this level (Fig. 5). These features have

1 been mapped previously and been interpreted as gas escape structures related to the earliest  
2 Eocene volcanism (Reynolds et al., 2017).

### 3 **4.6 Early Eocene Unconformity**

4 The Early Eocene Unconformity is a very prominent angular unconformity in the southern area of the  
5 Danmarkshavn Basin (Fig. 5), whereas it is mostly conformable across the Danmarkshavn Ridge and  
6 in the northern part of the Danmarkshavn Basin (Fig. 3a, b). It forms the upper boundary of the  
7 Paleocene(?)—Early Eocene seismic unit described above. Some indications of an angular  
8 unconformity below the horizon is also observed on the southern part of the Danmarkshavn Ridge  
9 (Fig. 4c). The Early Eocene Unconformity is truncated by the same tilt-induced incision along the  
10 western margin of the Danmarkshavn Basin as the underlying Base Paleogene horizon. The  
11 truncation occurs further east compared to the Base Paleogene, which inhibits interpretation of the  
12 Early Eocene Unconformity in most of the Danmarkshavn Basin (Fig. 3a).

13 The horizon is offset by deep-rooted, reactivated faults on both the west and east sides of the  
14 Danmarkshavn Ridge (Fig. 5). The angular unconformity in the Danmarkshavn Basin deepens  
15 towards the southwest. Towards the south, the Early Eocene Unconformity is erosionally truncated  
16 by the Erosional Incision horizon observed along the boundary between the Danmarkshavn Ridge  
17 and the Thetis Basin (Fig. 3b). Faulting of the Early Eocene Unconformity is also observed along the  
18 Intra Danmarkshavn Basin Fault (Fig. 6).

### 19 **4.7 Erosional incision**

20 This seismic horizon is a very distinct feature along the south segment of the Danmarkshavn Ridge,  
21 where it truncates the Early Eocene Unconformity and overlying strata (Fig. 3b). The incision is  
22 concave down towards the west and becomes subparallel to the bedding towards the Thetis Basin  
23 (Figs. 4a-c). The incision is clearly associated with the westwards bounding fault system of the Thetis  
24 Basin. Uplift of the Danmarkshavn Basin and Ridge created a dip along the eastern edge of the ridge  
25 (Figs 8a) above the angle of repose of the strata on the Danmarkshavn Ridge, which caused



1 extensive mass wasting of material from the elevated Danmarkshavn Ridge and into the Thetis Basin  
2 (Fig. 5). The westward extent of the horizon is defined by the onset of the incision, and the eastward  
3 extent of the incision is defined by the transition to conformity (Fig. 3b). The incision is located  
4 further east of the Danmarkshavn Ridge and into the Thetis Basin towards the south. In the north,  
5 the incision is located on the eastern margin of the Danmarkshavn Ridge (Fig. 4a), whereas the  
6 incision is located about 10 km east of the ridge in the south (Fig. 4c). Furthermore, the mass  
7 wasting event seems more related to the Intra Thetis Basin Fault observed in the south Thetis Basin  
8 (Fig. 4c). The incision is a noticeable unconformity below the horizon, with very pronounced  
9 downlaps across the horizon (Figs. 4a-c). The steep incision is not observed north of the central part  
10 of the study area (Fig. 7a). However, other local erosional incisions are found along the north  
11 segment of the Danmarkshavn Ridge, and although they cannot be correlated with the incision seen  
12 in the south, this study indicates they are of similar age as the Erosional incision horizon and related  
13 to faulting between the Danmarkshavn Ridge and the Thetis Basin.

#### 14 **4.8 Eocene—Middle Miocene**

15 The Eocene—Middle Miocene seismic unit directly overlies the Paleogene—Early Eocene unit, and is  
16 therefore bounded at its base by the Early Eocene Unconformity. The top of the unit is defined by  
17 the Intra Miocene Unconformity. The seismic facies in the Danmarkshavn Basin area are very similar  
18 to the underlying unit, with high amplitude, parallel reflectors (Figs. 3b, 4a). The Erosional incision  
19 horizon across the Danmarkshavn Ridge to Thetis basin transition is associated with steep,  
20 prograding clinoforms, extending out into the central part of the Thetis Basin (Figs. 4a-b). The  
21 clinoforms are most pronounced in the south of the study area, whereas they are absent in the  
22 north (Fig. 3a). The clinoforms are very specifically linked to the erosional incision horizon described  
23 above (Fig. 3b). The earliest clinoforms show very little accretion in the topsets, indication of a very  
24 rapid initial progradation. The later clinoforms are associated with more topset aggradation and less  
25 progradation. The eastern part of the Thetis Basin is dominated by the sub-parallel reflections of the  
26 toesets associated with the clinoforms, with a gradual condensation and thinning towards the

1 continental slope (Fig. 3b). A very well defined depo-center along the south margin of the  
2 Danmarkshavn Ridge (Fig. 11) correlates with the location of the clinoforms. The thinning towards  
3 the shelf edge is also noticeable in the thickness map, as well as the fault control. Minor east-dipping  
4 normal faults with a relatively small offset (ca. 100 ms TWT, ca. 100 m) and no deep roots are  
5 present in several location above the steep prograding clinoforms (Figs. 4c-b). These faults appear to  
6 terminate in the Eocene—Middle Miocene seismic unit, and are thus not related to deep-rooted  
7 tectonics.

8 The upper boundary of this unit is the Intra Middle Miocene Unconformity, and is primarily defined  
9 based on correlation with the ODP 913 borehole, located on the oceanic crust (Fig. 1), and is thus  
10 temporally relatively well constrained based on an unconformity observed in the cores (Berger and  
11 Jokat, 2008; Døssing et al., 2016; Thiede et al., 1995). The incision caused by the structural tilt  
12 mentioned previously also truncates the Intra Miocene Unconformity along the centre of the  
13 Danmarkshavn Ridge. The horizon extends beyond the continental slope to the east, and mimics the  
14 same general topographic trends as the underlying horizons, with a steep, fault related slope along  
15 the Danmarkshavn/Thetis Basin interface, a deepening in the central Thetis Basin, and a topographic  
16 rise towards the shelf edge. The Intra Miocene Unconformity is a prominent downlap surface in the  
17 north of the study area. (Fig. 3a). In the south however, the horizon is located at the top of a  
18 prograding interval, and is largely conformable both below and above (Fig. 3b). The horizon is often  
19 intersected by minor faults, with offsets around 50-250 ms (or ca. 50-250 m). The faults are all  
20 located where the underlying clinoforms display the strongest progradation, and on a relatively  
21 steep slope (Figs. 4b-c, Fig. 5). In the northern part, where the Intra Miocene Unconformity is mainly  
22 overlying gently dipping strata, no evidence of faulting of the horizon is observed in the Thetis Basin  
23 (Fig. 3a, 4a).

#### 1 **4.9 Middle Miocene—Top Prograding Unit**

2 The Top Prograding Unit seismic horizon defines the upper boundary of the upper prograding  
3 seismic unit, the Middle Miocene—Top Prograding Unit. When comparing the horizon north to south,  
4 it is evident that very steep clinforms are present immediately below the horizon in the north (Fig.  
5 3a), but the seismic unit is approaching subparallel reflections to the south (Fig. 3b). In the  
6 southernmost part of the study area, evidence of most likely Quaternary erosional truncation of the  
7 Top upper prograding unit horizon is observed at the sea floor as well (Fig. 4c). The horizon is only  
8 observed in the Thetis Basin and along the eastern margin of the Danmarkshavn Basin (Fig. 8b). A  
9 combination of either erosional incision or condensation defines the westwards extent of the  
10 horizon (Fig. 4a-c). Onlap of the Top Prograding Unit horizon onto the shelf edge high defines the  
11 eastwards extent, effectively constraining the top of this upper prograding unit to the Thetis Basin.  
12 Towards the south, the seismic facies show a more or less continuous and conformable deposition  
13 with slight progradation and aggradation (Fig. 4c, b). The toesets thin considerably over the marginal  
14 high, where the unit condenses beyond seismic resolution. Towards the north, the unit is dominated  
15 by steep, rapidly prograding clinforms, with very little topset accommodation (Fig. 3a, 7b). The  
16 upper part of the clinforms show very high amplitudes, with a noticeable drop in amplitudes below  
17 the offlap break, indicative of either a facies change or simply scattering of seismic energy due to the  
18 steep geometry of the clinforms (Fig. 7b). This unit displays a close correlation between the  
19 locations of the clinforms and the depocentre, similar to that of the underlying unit. It is clear that  
20 the main progradation is located along the northern part of the Danmarkshavn Ridge (Fig. 12) as  
21 opposed to the underlying unit, where a more southerly depocentre is observed (Fig. 11).

#### 22 **4.10 Faulting and structures**

23 This study maps a significant number of faults active during the post-breakup phase of the Northeast  
24 Greenland shelf. The fault pattern is used to constrain the timing, location and mechanisms related  
25 to the post-breakup tectonism and vertical motions observed. The faulting observed on the

1 Northeast Greenland shelf is mostly extensional, with some indication of transverse movement in  
2 the Danmarkshavn Basin (Fig. 6, 9). This is consistent with the tectonic setting of the North Atlantic  
3 since the Carboniferous, where rifting and continental spreading dominated (Ziegler and Cloetingh,  
4 2004).

5 A prominent structural break is observed between the Danmarkshavn Ridge and the Thetis Basin,  
6 which affects the geometry of the seismic units described above significantly (Figs. 3a-b, 8a-b). West  
7 of this break, the Cenozoic succession in the Danmarkshavn Basin is dominated by a significant  
8 structural tilt and uplift towards the west (Fig. 3b), whereas the Thetis Basin remains mostly sub-  
9 horizontal. This in turn is associated with a westwards deepening erosional truncation of the  
10 Cenozoic succession. Cenozoic deposits are thus only preserved in the westernmost part of the  
11 Danmarkshavn Basin (Fig. 9). Seismic horizons up to and including the Top Upper prograding unit are  
12 affected by the tilt, although it is not possible to constrain it further due to the erosional incision.

13 The Danmarkshavn Ridge is a relatively complex structure. It is primarily a horst structure (Fig. 5)  
14 extending about 200 km across the Northeast Greenland shelf (Fig. 2). The Danmarkshavn Ridge also  
15 defines the orientation and dip of the main, basin bounding faults (Type 1 on Fig. 9). Towards the  
16 North, the ridge is dominated by inverted Palaeozoic—Mesozoic sedimentary basins overlying an  
17 uplifted crystalline basement (Fig. 3a), whereas the south segment of the ridge consists mostly of  
18 crystalline basement (Fig. 3b). The faults east of the ridge dips to the east to southeast, thus forming  
19 the border faults to the Mesozoic half graben Thetis Basin (Fig. 3b, 9). The faults separating the  
20 Thetis Basin and the Danmarkshavn Ridge show larger offsets in the seismic data towards the south,  
21 although seismic reflection patterns suggest that similar faults also exist to the north. The base  
22 Cenozoic reflector is clearly downthrown from the Danmarkshavn Ridge (Fig. 5), although the  
23 structural style varies across the fault zone. The central section of the ridge show a complex  
24 transition with several listric faults constituting the border fault system (Fig. 7b). To the north, the  
25 vertical movement between the Thetis Basin and the Danmarkshavn Ridge is mostly accommodated

1 by folding of Paleogene—middle Miocene strata across the transition from the Danmarkshavn Ridge  
2 and into the Thetis Basin (Fig. 3a). The Intra Thetis Basin fault parallel to the southern segment of  
3 the Danmarkshavn Ridge is located about 25 km east of the Danmarkshavn Ridge (Figs. 3b, 4c). The  
4 Intra Thetis Basin fault is aligned with the main fault system east of the northern segment of the  
5 Danmarkshavn Ridge (Fig. 9). It shows that the southern segment of the Danmarkshavn Ridge was  
6 not involved in the reactivation of the faulting along the east margin of the Thetis Basin during the  
7 Cenozoic.

8 The faults on the west side of the Danmarkshavn Ridge are all west dipping normal faults (Fig. 9),  
9 with the exception of a few antithetic faults (Fig. 3a). The faults clearly define the transition from the  
10 Danmarkshavn Ridge and into the deep Danmarkshavn Basin (Fig. 3b) in the south, whereas the  
11 northern segment is more ambiguous (Fig. 3a). The observation of faulting of the Cenozoic  
12 succession in the Danmarkshavn Basin is limited due to thinning and erosion. However, a fault on-  
13 trend with the south segment of the Danmarkshavn Ridge is observed in the Danmarkshavn Basin  
14 (Type 2, Fig. 9). It is tentatively suggested to be transpressional due to the localised, but intense  
15 compressional deformation in combination with a limited vertical offset of the deformed succession  
16 (Fig. 6). The fault is part of a zone that accommodates some shortening of the Danmarkshavn Basin,  
17 where the footwall block show strong eastwards tilting of Cenozoic strata close to the fault (Fig. 6). It  
18 is also observed that the Danmarkshavn Basin fault is associated with basin inversion of the  
19 Paleozoic—Mesozoic succession as well as a basement high (Fig. 3b).

20 The northwards termination of the Danmarkshavn Ridge is marked by increasing depth to the  
21 basement north of the ridge. This is also observed in the gravity field as a reduced positive gravity  
22 anomaly north of the Danmarkshavn Ridge (Fig. 9). Numerous faults intersect the Cenozoic  
23 succession north of the Danmarkshavn Ridge (Fig. 2, Fig. 9, Fault type 5), but show lower lateral  
24 extent and less organised orientations, although an easterly dip is prevailing. The less organised  
25 nature of the faults in the north of the study area is largely attributed to the presence of salt in this

1 area (Figs. 7a-b). Diapirism is frequently observed, with salt diapirs rising close to the sea floor in  
2 many occasions. The faulting appear to be thin-skinned with a sole-out in the salt of most of the  
3 faults (Fig. 7a). The salt tectonics appear to have initiated during either Palaeozoic or Mesozoic  
4 times, which is confirmed by previous studies (Rowan and Lindsø, 2017). It is beyond the scope of  
5 the current study to give a detailed interpretation of the salt tectonics, but it would appear as if the  
6 Paleogene—earliest Eocene succession does not display any signs of salt-related thickness changes  
7 towards the salt diapirs (Fig. 7b, far left). Furthermore, the salt related faulting (Fig. 7a) shows little  
8 to no syn-tectonic deposition during this time. This indicates that the salt may have been activated  
9 during the post-breakup phase.

## 10 **5 DISCUSSION**

11 The results of this study of recent seismic data clearly shows a highly dynamic post-breakup tectonic  
12 setting with pronounced, kilometre-scale fault offsets, uplift and tilting of the Danmarkshavn Basin  
13 and pronounced progradational events. The large-scale structures and pre-breakup  
14 tectonostratigraphy have previously been described (Hamann et al., 2005; Petersen et al., 2015;  
15 Tsikalas et al., 2005). This study however presents new details on the causes and timing of the post-  
16 breakup tectonics. Based on tectonostratigraphic interpretations and integration of data from the  
17 ODP 913 borehole, this study constructs a temporally robust model for the tectonosedimentary  
18 evolution during the late Palaeogene—Early Neogene period.

### 19 **5.1 Seismic facies**

20 The plane-parallel, high amplitude seismic facies of the Paleocene—early Eocene succession  
21 indicates deposition of well-bedded, laterally cohesive sediments in a quiet setting, such as a marine  
22 setting below wave base. However, previous studies find small-scale, prograding clinoforms in the  
23 southwest of the study area (Petersen et al., 2016, 2015). This is confirmed in the current study both  
24 in map view (Fig. 10), where the clinoforms correlate with depo-centres, and in seismic section (Fig.  
25 6). Such clinoforms indicate that initial infill of the Danmarkshavn basin was controlled by a

1 channelized system, most likely in a shallow water setting. Such clinofolds are likely to be sand  
2 prone, whereas the plane parallel seismic facies present elsewhere is more consistent with a clay  
3 prone sedimentary facies.

4 Cenozoic deposits are very scarce onshore East and Northeast Greenland, but Nøhr-Hansen et al.  
5 (2011) describes early Paleocene fluvial deposits in the Wollaston Forland and Sabine Ø Area, south-  
6 west of the study area (Fig. 2). A sediment fairway from the south-west during the Paleocene is  
7 consistent with the prograding clinofolds observed in the seismic data in the southwest part of the  
8 study area.

9 The Eocene—mid Miocene succession is comprised of two main seismic facies types. In the  
10 Danmarkshavn Basin and Ridge, the facies strongly resemble that of the underlying unit, suggesting  
11 a continued deposition in a marine, sub-wave base, clay-rich environment. In the Thetis Basin  
12 however, the seismic facies are dominated by the steep, prograding clinofolds (*e.g.* Figs. 5, 7)  
13 associated with the uplift and tilting of the Danmarkshavn Basin and the faulting that intersects the  
14 Cenozoic deposits across the east margin of the Danmarkshavn Ridge. Evidence of one or several  
15 mass wasting events following rapid motion on the fault system east of the Danmarkshavn Ridge is  
16 observed (Fig. 5).

17 The prograding clinofolds are indicative of more coarse-grained material, most likely sand prone in  
18 the proximal part, and fining in the distal direction, i.e. towards the centre of the Thetis Basin. The  
19 topsets of the prograding succession (Fig. 4b) may be composed of either typical delta top deposits  
20 such as overbank fines and fluvial deposits, or alternatively a form of sub-marine fine-grained top-  
21 set deposit.

22 The focus of the prograding clinofolds during the Eocene—mid Miocene is located in the south part  
23 of the Thetis Basin, along the edge of the Danmarkshavn Ridge (Fig. 11). This implies that the south  
24 Danmarkshavn Ridge, Danmarkshavn Basin and the area onshore Northeast Greenland south of

1  
2  
3  
4  
5  
6  
7  
8  
9  
10  
11  
12  
13  
14  
15  
16  
17  
18  
19  
20  
21  
22  
23  
24  
25  
26  
27  
28  
29  
30  
31  
32  
33  
34  
35  
36  
37  
38  
39  
40  
41  
42  
43  
44  
45  
46  
47  
48  
49  
50  
51  
52  
53  
54  
55  
56  
57  
58  
59  
60  
61  
62  
63  
64  
65

1 Store Koldewey most likely acted as the source area for this progradational event. The presence of  
2 fluvial deposits of an latest Paleocene—earliest Eocene age in the Wollastand Forland and Sabine Ø  
3 area (Nøhr-Hansen et al., 2011), highlights the presence of a fluvial system southwest of the study  
4 area during the time of deposition of the clinoforms. It seems highly likely that this fluvial system  
5 transported the sediment forming the Eocene—mid Miocene clinoforms to the margin.

6 The interpretation of whether the erosional incision of the uplifted footwall of the Danmarkshavn  
7 Ridge occurred in a marine or terrigenous environment have obvious implications for the  
8 understanding of the depositional evolution of the Northeast Greenland margin. If the erosional  
9 incision was terrigenous, it would imply a very dramatic change in depositional environment, from  
10 below (storm) wave base to subaerial exposure due to fault related uplift of the Danmarkshavn  
11 Ridge. However, erosional incision and prograding clinoforms may as well occur in a marine setting,  
12 and the continuous, uniform nature of the topsets and the overlying strata seems to be more  
13 consistent with deposition in a marine environment. This does not however imply that there was no  
14 tectonic motion. In fact, the steepness of the incision, in combination with the chaotic nature of the  
15 material transported into the Thetis Basin resulting from the mass wasting event, indicates a rapid  
16 and significant tectonic movement (Fig. 5).

17 The post-mid Miocene, upper prograding unit, displays very similar facies patterns as the underlying  
18 unit. However, as described above, the location of the clinoforms are shifted further north in the  
19 Thetis Basin (Fig. 12). The seismic facies of the clinoform-dominated northern part of the unit show a  
20 very distinct proximal to distal facies change (Figs. 3a, 7b). The high amplitudes of the topsets  
21 indicate a highly heterogenic depositional environment, with interbedded sand and shale. The  
22 foresets are most likely dominated by lateral sand-on-sand contacts, as the amplitudes show a  
23 marked dimming, resulting from relatively homogenous sediments. The chaotic to moderately well  
24 bedded topsets are consistent with basin floor fan deposition dominated by various mass wasting  
25 deposition such as slides, slumps and turbidites. The northwards shift of the clinoforms indicates a



1 change in the drainage pattern of the Northeast Greenland shelf, and possibly also onshore  
2 Northeast Greenland, from mainly focused south of Store Koldewey for the lower prograding unit to  
3 north of Store Koldewey for the upper.

## 4 **5.2 Structural evolution**

5 The seismic data offshore Northeast Greenland clearly demonstrate that tectonics play a prominent  
6 role in the sedimentation pattern after the continental breakup. The post-breakup faulting observed  
7 mainly around the Danmarkshavn Ridge is extensional in nature, as all faults have some degree of a  
8 normal motion on them. However, the total extension of the shelf after the continental breakup is  
9 interpreted to be relatively modest due to the steep dips of the fault planes and low amount of  
10 heave on the individual faults.

11 The two main tectonic events are the tilting and uplift of the strata in the Danmarkshavn Basin, and  
12 the 1-2 s TWT throw on the western boundary fault system in the Thetis Basin. Both events clearly  
13 post-date the Early Eocene Unconformity, as this horizon is involved in both the structural tilt and  
14 intersected by the faulting. The relative timing between these two events indicates that the western  
15 boundary fault of the Thetis Basin was reactivated prior to any significant tilting in the  
16 Danmarkshavn Ridge or Danmarkshavn Basin area. Tilting might however have initiated west of the  
17 Danmarkshavn Basin at an earlier stage.

18 The intra-Thetis Basin fault (Fig. 4c) display normal faulting of the entire Cenozoic succession in the  
19 southern area of the basin. Although the fault throw is relatively modest, the initiation of the fault is  
20 significant, as it controls the location of the footwall erosional escarpment, and seems to be aligned  
21 with the northern segment of the Danmarkshavn Ridge. It also indicates that the southern segment  
22 of the Danmarkshavn Ridge was not tectonically active after the breakup.

23 A significant amount of vertical offset has accumulated between the Thetis Basin and the  
24 Danmarkshavn Ridge during the Eocene—Miocene(?) period, amounting to 1-2 s TWT. By assuming

1 an average seismic velocity of 2000 m/s (Berger and Jokat, 2008) this equates to 1-2km of vertical  
2 offset. As mentioned above, extension appear to be limited during the Cenozoic. Therefore, it seems  
3 likely that the vertical offset was created by a steep, listric fault with a sole-out at the base of the  
4 crust. This is consistent with the seismic observations in this study and with other geophysical  
5 observations (Tsikalas et al., 2005). Some of the post-breakup subsidence may be caused by  
6 differential compaction between the Danmarkshavn Ridge and the Thetis Basin. However, the  
7 abrupt nature of the subsidence, causing slope failure on the footwall, seems in contrast to relatively  
8 slow and continuous compaction-related subsidence.

9 In a regional perspective, it is apparent that the extensional faulting observed around the  
10 Danmarkshavn Ridge and in the Thetis basin is oriented sub-parallel to the main extensional axis  
11 created during continental breakup (Fig. 2), even though some of the faulting post-dates the  
12 breakup by >40 Ma. This is clear evidence that the structural grain created during the Mesozoic  
13 rifting (Tsikalas et al., 2012) was reactivated during the post-breakup extensional tectonics.

14 The timing of the salt movement can in the context of the current study yield important information  
15 about tectonic events. Remobilised salt is observed throughout the northern part of the study area  
16 (Fig. 2), and is associated with a complex fault pattern (Fig. 9). Salt diapirs frequently rise to or close  
17 to the sea floor, indicating that salt mobilisation has been occurring close to present time, although  
18 presumed Quaternary erosion truncates the crests of the diapirs, hampering a more accurate  
19 constraint on the timing (Figs. 7a, b). Since there is no evidence of Paleocene—Eocene rim synclines,  
20 no pre-breakup salt mobilisation is interpreted. Since the salt was not activated during the  
21 continental breakup, it seems likely that most of the tectonic deformation during the breakup (at *ca.*  
22 55 Ma) was focused along the margin of the shelf, away from the Danmarkshavn Basin. The lack of  
23 pre-breakup tectonism on the shelf, apart from the thermally induced uplift in the earliest Eocene,  
24 further confirms this observation. It then seems more likely that the salt mobilisation is linked to the

1 same post-breakup tectonics seen in the data as movement of the Thetis Basin boundary fault and  
2 tilting of the Danmarkshavn Basin.

### 3 **5.3 Uplift and erosion**

4 The Northeast Greenland shelf displays a series of uplift events from the Late Cretaceous through  
5 the Neogene (Hamann et al., 2005; Petersen et al., 2016, 2015). The unconformity below the  
6 Cenozoic succession is a surface of regional significance, also observed onshore Northeast Greenland  
7 (Nøhr-Hansen et al., 2011). In the current study, the unconformity is mostly observed in the  
8 Danmarkshavn Basin and on the Danmarkshavn Ridge, and is particularly well developed in the  
9 south of the study area. This trend is seen in subsequent uplift events as well, where uplift events  
10 are most pronounced towards the south. The uplift and related intrusions of hot magma, peaking  
11 around *ca.* 55 Ma (Larsen et al., 2014) reported previously (Petersen et al., 2015; Reynolds et al.,  
12 2017), also display a deepening incision in the south part of the Danmarkshavn Basin, associated  
13 with progradation of clinoforms into the Danmarkshavn Basin (Petersen et al., 2016, 2015). Some  
14 minor basin inversion is also observed at the earliest Eocene times (Fig. 5), although this is in  
15 contrast to the generally extensional tectonic regime of the shelf during the Cenozoic. However,  
16 compression may be caused by counter-clockwise rotation of Greenland during the Palaeocene,  
17 which may have caused minor NE-SW compressional stresses to be transmitted onto the Northeast  
18 Greenland shelf (Guarnieri, 2015). However, this mechanism seems unable to account for neither  
19 the geometry nor the amount of uplift observed on the Northeast Greenland shelf.

20 The gradual uplift and associated denudation of the Cenozoic deposits of the Danmarkshavn Basin  
21 and Ridge area most likely post-dates the intra Miocene unconformity. The exhumation of the inner  
22 part of the shelf and its association with steep, prograding clinoforms with downlaps onto the Intra  
23 Miocene Unconformity (Fig. 3a), points to a post-mid Miocene age for the cessation of the uplift of  
24 the inner Northeast Greenland shelf. The vertical motions seems to stop or slow significantly around  
25 the time of the Top upper prograding unit seismic horizon (Fig. 7b). The end of the main denudation

1 phase is therefore poorly constrained, since the age of the Top upper prograding unit can only be  
2 attributed to a post-mid Miocene age. It is suggested in this study, that the main cause of uplift and  
3 tectonics following the continental breakup is caused by thermal uplift and dynamic topographic  
4 effects associated with the Icelandic mantle plume. (Fig. 13)

5 A central feature of the post-breakup denudation of the inner Northeast Greenland shelf is the time  
6 transgressive nature of the uplift, as indicated by the prograding units and their migration  
7 northwards over time. This is evident when comparing the thickness maps of the two uppermost  
8 late Paleogene—Neogene units (Figs. 11 and 12), but in fact, the north to south migration of  
9 clinofolds seems to start potentially as early as the Palaeocene (Petersen et al., 2015). This  
10 northwards move of the main depocentre indicates that the uplift and exhumation of the Northeast  
11 Greenland shelf must have been focused east, southeast or south of the current study area. This  
12 initially created a structural tilt of the Danmarkshavn Basin towards the west, but with a minor  
13 northwards component as well. The earliest observations of clinofolds in the south is dated as  
14 Paleocene, and the youngest clinofolds are post mid-Miocene, a period of about 45 Ma. This implies  
15 a slow northwards tilting of the Northeast Greenland shelf. Alternatively, it is possible that the  
16 northwards tilting occurred much faster, but that the sedimentation occurred in pulses related to  
17 hinterland uplift.

#### 18 **5.4 Effect of mantle plume path on deposition**

19 The Icelandic hotspot and its effect in the North Atlantic realm, in particular in relation to the  
20 continental breakup, has been the source of much debate (Campbell, 2007; Clift et al., 1998; Storey  
21 et al., 2007). In the current study, it is suggested that the mantle plume system at present day  
22 located beneath Iceland and Jan Mayen (Rickers et al., 2013), was instrumental in the uplift of the  
23 inner Northeast Greenland shelf, and that it was responsible for a gradual, northwards shift of the  
24 main sediment fairway. The central argument for this interpretation is that the Icelandic plume  
25 system moved along a trajectory south of the study area during the Cenozoic, which is in good

1 agreement with the time-transgressive northward movement of the prograding units observed in  
2 this study.

3 The plume activity, its trajectory and its morphology are all influencing the depositional patterns  
4 observed during the Cenozoic on the Northeast Greenland shelf. The plume underneath the North  
5 Atlantic show a significant lateral extent, with an origin observed down to the lower mantle (Rickers  
6 et al., 2013). Døssing et al (2016) concludes that the thermal perturbation at 2-15 Ma ( mid Miocene-  
7 -Pliocene) is linked to the IMU (Intra Miocene Unconformity) observed around the East Greenland  
8 Ridge, indicating a clear link between the thermal perturbations of the passing hotspot and tectonism  
9 in the region.

10 The coupling between the Atlantic mantle plume system and the North Atlantic Igneous Province is  
11 well established (e.g. Ganerød et al., 2010; Hansen et al., 2009; Larsen et al., 2014; Storey et al.,  
12 2007). Onshore Northeast Greenland, the accurately dated igneous rocks show a distinct trend of  
13 younger igneous rocks towards the north (Larsen et al., 2014). The youngest igneous rocks (40-20  
14 Ma) observed according to Larsen et al.(2014) are all found north of 67° N (Fig. 13), further  
15 indicating a south to north time transgressive impact of the passing Icelandic mantle plume system.  
16 The location of the Icelandic and Jan Mayen hotspots directly south of the study area during mid  
17 Miocene times (Fig. 13), is in very good agreement with uplift in the south and tilting of the margin  
18 towards the north during the mid Miocene—Quaternary.

## 19 **6 CONCLUSIONS**

20 This study utilizes a vast database of the most recent seismic data and presents a series of novel  
21 observations on the tectonosedimentary development of the Northeast Greenland shelf following  
22 the continental breakup. A summary of the tectonic and sedimentary events described in the current  
23 study is presented in Fig. 15.

1 It is demonstrated that significant vertical motion and associated extensional faulting are observed  
2 after the continental breakup at *ca.* 55 Ma. Differential subsidence, some of which may be  
3 attributed to deep-rooted faults, in the order of 1-2 km is observed along the west boundary of the  
4 Thetis Basin, during the Eocene to post-Miocene times. The faulting occurred simultaneously with a  
5 pronounced uplift and eastward tilt of the inner Northeast Greenland shelf.

6 Several progradational events are interpreted based on the seismic data. The earliest clinoforms are  
7 of a pre-breakup age, and located in the south Danmarkshavn Basin. The clinoforms are however  
8 more pronounced after the earliest Eocene breakup, where steep, rapidly prograding clinoforms  
9 oversteps the Danmarkshavn Ridge and progrades into the Thetis Basin. These clinoforms display a  
10 northward migration over time, with a significant clinoform succession formed in the north of the  
11 Thetis Basin sometime after the mid Miocene.

12 The Icelandic hot spot is suggested as the main cause of uplift, rotation and extensional faulting of  
13 the shelf. The trajectory of the Icelandic hot spot south of the Northeast Greenland shelf during the  
14 Neogene fits very well with a gradual, northwards shift of progradation due to thermally induced  
15 uplift and dynamic topography. This is observed in the seismic data as northwards tilting of the shelf  
16 during post-breakup times. Lastly, the reactivation of the fault system separating the Danmarkshavn  
17 Ridge and the Thetis Basin is also attributed to the thermal uplift caused by the passage of the  
18 Icelandic hotspot.

19 **Acknowledgements**

20 The author wishes to thank TGS and Spectrum for supplying the seismic database for this study, and  
21 for allowing the publication of the data with very limited constraints. The author also wishes to  
22 thank Schlumberger for providing the workstation software Petrel. For obvious reasons this study  
23 could not have taken place without their support. This paper benefitted greatly from anonymous  
24 reviews.

1

1  
2  
3  
4  
5  
6  
7  
8  
9  
10  
11  
12  
13  
14  
15  
16  
17  
18  
19  
20  
21  
22  
23  
24  
25  
26  
27  
28  
29  
30  
31  
32  
33  
34  
35  
36  
37  
38  
39  
40  
41  
42  
43  
44  
45  
46  
47  
48  
49  
50  
51  
52  
53  
54  
55  
56  
57  
58  
59  
60  
61  
62  
63  
64  
65

1 **Captions**

2  
3 2 Fig. 1. Overview of the study area and the seismic database. The data are composed of two vintages.  
4  
5 3 The AWI seismic data, collected during the nineties, and the TGS data collected 2008-2014. The TGS  
6  
7 4 data are of both better quality and much higher density, as shown on the map. The AWI data covers  
8  
9 5 the important transition from continental to oceanic crust however. All data are courtesy of TGS and  
10  
11 6 Spectrum. Approximate locations of the seismic cross sections are also highlighted.  
12  
13  
14  
15

16 7 Fig. 2. Map of the main structural elements, traces of the interpreted faults, free air gravity  
17  
18 8 anomalies, as well as magnetic isochrons. The map shows the NNE-SSW elongated Danmarkshavn  
19  
20 9 Basin (DKHB), the Danmarkshavn Ridge (DKHR), right-lateral transfer zone (TS) and the Thetis Basin  
21  
22 10 located on the easternmost side of the shelf. The East Greenland Ridge (EGR), Store Koldewey (SKW)  
23  
24 11 and Wollaston Forland (WSF) are also shown. Gravity data are courtesy of DTU Space DNSC08GRA  
25  
26 12 and DTU10 data sets (Andersen 2010 and Andersen et al 2010).  
27  
28  
29  
30

31 13 Fig. 3. (a) Regional west to east oriented seismic profile through the northern part of the study area.  
32  
33 14 The section shows a thick Palaeozoic and Mesozoic succession that overlies the northernmost extent  
34  
35 15 of the Danmarkshavn Ridge basement high. The section shows a distinct step down of the Base  
36  
37 16 Paleogene horizon from the Danmarkshavn Ridge and into the Thetis basin caused by ductile  
38  
39 17 accommodation of normal reactivation of faults at the Danmarkshavn Ridge to Thetis Basin  
40  
41 18 transition. To the west, in the Danmarkshavn Basin, the Cenozoic succession shows evidence of  
42  
43 19 tilting and erosional incision, associated with pronounced progradation in the Thetis Basin, above  
44  
45 20 the Intra Middle Miocene reflection. (b) Regional west to east oriented seismic profile through the  
46  
47 21 southern part of the study area. The Cenozoic succession displays a significant uplift and tilt to the  
48  
49 22 east across the Danmarkshavn Basin and Danmarkshavn Ridge. Faulting is present in the  
50  
51 23 Danmarkshavn Basin, where it offsets the Cenozoic succession (IDBF: Intra Danmarkshavn Basin  
52  
53 24 Fault). Faulting is also present between the Danmarkshavn Ridge and Thetis Basin, as well as in the  
54  
55 25 Thetis Basin, with the faults downfaulting the Cenozoic succession towards the East along the Intra  
56  
57  
58  
59  
60  
61  
62  
63  
64  
65



1 Thetis Basin Fault (ITBF). Evidence of a steep erosional scar infilled with prograding clinoforms is  
2 present across the Danmarkshavn Ridge. Seismic data are courtesy of TGS and Spectrum.  
3  
4  
5  
6 Fig. 4. Seismic examples of the Danmarkshavn Ridge to Thetis Basin transition at the southern  
7 segment of the Danmarkshavn Ridge. (a) The Palaeocene to Miocene(?) seismic facies across the  
8 Danmarkshavn Ridge is dominated by parallel, high amplitude reflections unconformably overlying  
9 the Danmarkshavn Ridge. A concave erosional truncation of the Palaeocene to Miocene(?) marks the  
10 transition from the Danmarkshavn Ridge to the Thetis Basin, where two east dipping normal faults  
11 off sets the Paleogene succession by >1 s TWT down into the Thetis Basin. Steep, prograding  
12 clinoforms fills out the accommodation space created by the erosional incision and extends out into  
13 the Thetis Basin. (b) Seismic section further south compared to (a). The two faults still mark the  
14 transition from the Danmarkshavn Ridge to the Thetis Basin. The prograding clinoforms persist,  
15 reaching far out into the Thetis Basin. Small-scale faults intersect the succession between the Early  
16 Eocene Unconformity and the Top upper prograding unit. (c) Seismic example from the  
17 southernmost Danmarkshavn Ridge. Note the increase in distance between the Danmarkshavn Ridge  
18 and the Intra Thetis Basin Fault (ITBF). The erosional incision is located east of the Danmarkshavn  
19 Ridge, indicating that the ITBF triggered the incision. Note the pronounced angular unconformity  
20 below the Early Eocene Unconformity to the far west. Seismic data are courtesy of TGS and  
21 Spectrum.

22  
23  
24  
25 Fig. 5. Seismic section through the central study area covering the Danmarkshavn Basin, the  
26 Danmarkshavn Ridge and the Thetis Basin. The seismic section clearly show domal uplift and  
27 truncation below the Early Eocene Unconformity in the Danmarkshavn Basin, with some indications  
28 of minor compression and inversion are observed along the west margin of the Danmarkshavn  
29 Ridge. To the far NW of the profile, disturbances in the reflections below the Early Eocene  
30 Unconformity indicates gas venting and a pockmark associated with volcanic activity. The bounding  
31 fault between the Danmarkshavn Ridge and the Thetis Basin offsets the entire succession above the

1 Base Paleogene, but the Erosional incision seismic horizon and prograding clinoforms are confined to  
2 the Thetis Basin. Chaotic seismic facies indicate mass deposited sediments below the Erosional  
3 incision reflection. Seismic data are courtesy of TGS and Spectrum.

4 Fig. 6. Seismic profile across the largest fault in the Danmarkshavn Basin, the Intra Danmarkshavn  
5 Basin Fault (IDBF). There is a distinct offset of the Palaeogene succession along the fault, and several  
6 minor associated faults are present. Also, notice the prograding clinoforms west of the fault. Seismic  
7 data are courtesy of TGS and Spectrum.

8 Fig. 7. (a) Seismic example north of the Danmarkshavn Ridge. The structural style here is heavily  
9 affected by the salt, which forms a detachment plane at the base of the faults. Salt diapirism is also  
10 observed. (b) Seismic section showing the structural complexity of the Danmarkshavn Ridge in the  
11 central part of the study area. Several eastwards dipping, listric faults comprise the Danmarkshavn  
12 Ridge to Thetis Basin transition. At the westernmost edge of the profile, a salt diapir rises close to  
13 the seafloor. Note how the main progradational event is now above the Intra Miocene  
14 Unconformity. For comparison, see fig. 4. Seismic data are courtesy of TGS and Spectrum.

15 Fig. 8. (a) Structure map of the Base Palaeogene horizon in TWT with fault traces of the main faults  
16 that outline the Danmarkshavn Ridge overlain. The map clearly shows the steep transition from the  
17 relatively elevated Danmarkshavn Basin/Ridge area and lower lying Thetis Basin. Also, note the  
18 coincidence between the faulting and the steep transition zone. (b) Structure map of the Upper  
19 prograding unit horizon in TWT with fault traces of the main faults that outline the Danmarkshavn  
20 Ridge trace overlain. The steep slope along the northern Danmarkshavn Ridge is due to steep,  
21 prograding clinoforms rather than structural deformation. Note the eastwards movement of the  
22 western limit of the unit.

23 Fig. 9. Overview and classification of the faults interpreted in this study overlain the free air gravity  
24 data. Faults are subdivided into five categories: Main, ridge-delineating faults (type 1, black), Intra-

1 Danmarkshavn Basin faults (type 2, green), pre-Cenozoic faults that are not reactivated (type 3,  
2 grey), Intra-Thetis Basin faults (type 4, blue), and salt related faults (type 5, magenta). The white  
3 fault is a hybrid between the ridge delineating fault and the salt related fault types. The ridge  
4 delineating faults are all located on the margins of the NE-SW oriented positive gravity anomaly  
5 associated with the Danmarkshavn Ridge. A right-lateral transfer zone between the north and south  
6 segments of the Danmarkshavn Ridge is highlighted. Note that all the salt related faults are located  
7 in the northern part of the study area, where the gravity anomaly is relatively low. The westwards  
8 erosional truncation of the Cenozoic deposits is also highlighted (grey line).

9 Fig. 10. Thickness map (in TWT) of the succession between the Early Eocene and the Base Paleogene,  
10 corresponding to the Palaeocene—lowermost Eocene. The main depo-center is located in the  
11 southernmost part of the Thetis Basin, and thins substantially on the Danmarkshavn Ridge. A  
12 potential northerly depo-center is also tentatively interpreted from the data. The Location of the  
13 Danmarkshavn Ridge and the right-lateral transfer zone are shown for reference together with the  
14 main, basin delineating faults.

15 Fig. 11. Thickness map (in TWT) of the succession between the Early Eocene and the Intra middle  
16 Miocene horizons, corresponding to the Eocene—lower Miocene interval dominated by early  
17 prograding clinofolds. The main depo-center is prominently located immediately west of the  
18 southern segment of the Danmarkshavn Ridge. The Location of the Danmarkshavn Ridge and the  
19 right-lateral transfer zone are shown for reference together with the main, basin delineating faults.

20 Fig. 12. Thickness map (in TWT) of the succession between the Intra middle Miocene and Upper  
21 prograding unit horizons, dominated by the late prograding event. The upper age of this interval is  
22 poorly constrained to a post-Miocene age. The depo-centre is located NE of the Danmarkshavn  
23 Ridge. Compared to fig. 11, it is evident that the depo-center shifts further north and further into the  
24 Thetis Basin. The Location of the Danmarkshavn Ridge and the right-lateral transfer zone are shown  
25 for reference together with the main, basin delineating faults.

1 Fig. 13. Overview map showing the path and estimated extent of the Jan Mayen-Iceland hotspot  
2 system after Rickers et al. 2013, shown together with free air gravity anomalies. Ages of the  
3 observed, onshore volcanics (Larsen et al. 2014) show a trend of younger magmatic rocks towards  
4 the north (italics, stars and horizontal lines). A relatively good correlation between the passage of  
5 the hot spots and the ages of the intrusions are seen, with the Jan Mayen plume branch a likely  
6 candidate for the northern (and younger intrusions). The observed northwards shift in prograding  
7 clinofolds, southwards deepening erosion during the latest Eocene and the area with seismic  
8 observations of volcanics are shown as reference.

9 Fig. 14. Summary of tectonostratigraphic events during the early-mid Cenozoic period of the  
10 Northeast Greenland shelf. Red arrows show uplift, blue arrows show normal faulting/subsidence.  
11 Note how the clinofolds shift northwards during Eocene—Miocene period. The Thetis Basin is  
12 dominated by varying degrees of subsidence (blue minus), but the Danmarkshavn Ridge and  
13 Danmarkshavn Basin show a more complicated history of uplift (red plus) and erosion (grey  
14 hatched).

## 15 **References**

- 16 Andersen, O.B., 2010. The DTU10 Gravity field and Mean sea surface, in: Second International  
17 Symposium of the Gravity Field of the Earth (IGFS2). Fairbanks, Alaska.
- 18 Andersen, O.B., Knudsen, P., Berry, P.A.M., 2010. The DNSC08GRA global marine gravity field from  
19 double retracked satellite altimetry. *J. Geod.* 84, 191–199. [https://doi.org/10.1007/s00190-  
20 009-0355-9](https://doi.org/10.1007/s00190-009-0355-9)
- 21 Berger, D., Jokat, W., 2009. Sediment deposition in the northern basins of the North Atlantic and  
22 characteristic variations in shelf sedimentation along the East Greenland margin. *Mar. Pet.  
23 Geol.* 26, 1321–1337. <https://doi.org/10.1016/j.marpetgeo.2009.04.005>

- 1 Berger, D., Jokat, W., 2008. A seismic study along the East Greenland margin from 72°N to 77°N.  
2 Geophys. J. Int. 174, 733–748. <https://doi.org/10.1111/j.1365-246X.2008.03794.x>  
3  
4  
5  
6 3 Campbell, I.H., 2007. Testing the plume theory. Chem. Geol. 241, 153–176.  
7  
8 4 <https://doi.org/10.1016/j.chemgeo.2007.01.024>  
9  
10  
11 5 Clift, P.D., Carter, A., Hurford, A.J., P.D. Clift, A.C. and A.J.H., 1998. The erosional and uplift history of  
12 NE Atlantic passive margins: constraints on a passing plume. J. Geol. Soc. London. 155, 788–  
13 800. <https://doi.org/10.1144/gsjgs.155.5.0787>  
14  
15  
16 7  
17  
18  
19 8 Cloetingh, S., Burov, E., Matenco, L., Beekman, F., Roure, F., Ziegler, P.A., 2013. The Moho in  
20 extensional tectonic settings: Insights from thermo-mechanical models. Tectonophysics 609,  
21 558–604. <https://doi.org/10.1016/j.tecto.2013.06.010>  
22  
23  
24 10  
25  
26  
27 11 Cloetingh, S.A.P.L., Ziegler, P.A., Bogaard, P.J.F., Andriessen, P.A.M., Artemieva, I.M., Bada, G., van  
28 Balen, R.T., Beekman, F., Ben-Avraham, Z., Brun, J.P., Bunge, H.P., Burov, E.B., Carbonell, R.,  
29 Facenna, C., Friedrich, A., Gallart, J., Green, A.G., Heidbach, O., Jones, A.G., Matenco, L., Mosar,  
30 J., Oncken, O., Pascal, C., Peters, G., Sliampa, S., Soesoo, A., Spakman, W., Stephenson, R.A.,  
31 Thybo, H., Torsvik, T., de Vicente, G., Wenzel, F., Wortel, M.J.R., 2007. TOPO-EUROPE: The  
32 geoscience of coupled deep Earth-surface processes. Glob. Planet. Change 58, 1–118.  
33  
34  
35 14  
36  
37 15  
38  
39 16  
40  
41  
42 17 <https://doi.org/10.1016/j.gloplacha.2007.02.008>  
43  
44  
45 18 Døssing, A., Japsen, P., Watts, A.B., Nielsen, T., Jokat, W., Thybo, H., Dahl-Jensen, T., 2016. Miocene  
46 uplift of the NE Greenland margin linked to plate tectonics: Seismic evidence from the  
47 Greenland Fracture Zone, NE Atlantic. Tectonics 35, 257–282.  
48  
49  
50 20  
51  
52 21 <https://doi.org/10.1002/2015TC004079>  
53  
54  
55  
56 22 Emery, D., Myers, K., Bertram, G.T., 1996. Sequence stratigraphy. Blackwell Science.  
57  
58  
59 23 Engen, Ø., Faleide, J.I., Dyreng, T.K., 2008. Opening of the Fram Strait gateway: A review of plate  
60  
61  
62  
63  
64  
65

- 1 tectonic constraints. *Tectonophysics* 450, 51–69. <https://doi.org/10.1016/j.tecto.2008.01.002>
- 2  
3  
4 2 Funck, T., Erlendsson, Ö., Geissler, W.H., Gradmann, S., Kimbell, G.S., McDermott, K., Petersen, U.K.,  
5  
6 3 2017. A review of the NE Atlantic conjugate margins based on seismic refraction data. *Geol.*  
7  
8 4 *Soc. London, Spec. Publ.* 447, 171–205. <https://doi.org/10.1144/SP447.9>
- 9  
10  
11 5 Gaina, C., Gernigon, L., Ball, P., 2009. Palaeocene-Recent plate boundaries in the NE Atlantic and the  
12  
13 6 formation of the Jan Mayen microcontinent. *J. Geol. Soc. London.* 166, 601–616.  
14  
15 7 <https://doi.org/10.1144/0016-76492008-112>
- 16  
17  
18  
19 8 Ganerød, M., Smethurst, M.A., Torsvik, T.H., Prestvik, T., Rouse, S., McKenna, C., van Hinsbergen,  
20  
21 9 D.J.J., Hendriks, B.W.H., 2010. The North Atlantic Igneous Province reconstructed and its  
22  
23 10 relation to the Plume Generation Zone: The Antrim Lava Group revisited. *Geophys. J. Int.* 182,  
24  
25 11 183–202. <https://doi.org/10.1111/j.1365-246X.2010.04620.x>
- 26  
27  
28  
29  
30 12 Guarnieri, P., 2015. Pre-break-up palaeostress state along the East Greenland margin. *J. Geol. Soc.*  
31  
32 13 *London.* 172, 727–739. <https://doi.org/10.1144/jgs2015-053>
- 33  
34  
35  
36 14 Håkansson, E., Stemmerik, L., 1989. Wandel Sea Basin - a new synthesis of the Late Paleozoic to  
37  
38 15 Tertiary accumulation in North Greenland. *Geology* 17, 683–686.  
39  
40 16 [https://doi.org/10.1130/0091-7613\(1989\)017<0683:WSBANS>2.3.CO;2](https://doi.org/10.1130/0091-7613(1989)017<0683:WSBANS>2.3.CO;2)
- 41  
42  
43  
44 17 Hamann, N.E., Whittaker, R.C., Stemmerik, L., 2005. Geological development of the Northeast  
45  
46 18 Greenland Shelf, in: *Petroleum Geology: North-West Europe and Global Perspectives –*  
47  
48 19 *Proceedings of the 6th Petroleum Geology Conference.* pp. 887–902.  
49  
50 20 <https://doi.org/10.1144/0060887>
- 51  
52  
53  
54 21 Hansen, J., Jerram, D.A., McCaffrey, K., Passey, S.R., 2009. The onset of the North Atlantic Igneous  
55  
56 22 Province in a rifting perspective. *Geol. Mag.* 146, 309–325.  
57  
58 23 <https://doi.org/10.1017/S0016756809006347>
- 59  
60  
61  
62  
63  
64  
65

1 Larsen, L.M., Pedersen, A.K., Tegner, C., Duncan, R.A., 2014. Eocene to Miocene igneous activity in  
2 NE Greenland: northward younging of magmatism along the East Greenland margin. *J. Geol.*  
3 *Soc. London.* 171, 539–553. <https://doi.org/10.1144/jgs2013-118>  
4  
5  
6  
7  
8 4 Lundin, E., Doré, A.G., 2002. Mid -Cenozoic post -breakup deformation in the ` passive ' margins  
9 bordering the Norwegian- Greenland Sea 19, 79–93.  
10  
11  
12  
13  
14 6 Matthews, K.J., Maloney, K.T., Zahirovic, S., Williams, S.E., Seton, M., Müller, R.D., 2016. Global plate  
15 boundary evolution and kinematics since the late Paleozoic. *Glob. Planet. Change* 146, 226–  
16 250. <https://doi.org/10.1016/j.gloplacha.2016.10.002>  
17  
18  
19  
20  
21  
22 9 McKenzie, D., 1978. Some remarks on the development of sedimentary basins. *Earth Planet. Sci.*  
23 *Lett.* 40, 25–32. [https://doi.org/10.1016/0012-821X\(78\)90071-7](https://doi.org/10.1016/0012-821X(78)90071-7)  
24  
25  
26  
27  
28 11 Miller, K.G., Kominz, M.A., Browning, J. V., Wright, J.D., Mountain, G.S., Katz, M.E., Sugarman, P.J.,  
29 Cramer, B.S., Christie-Blick, N., Pekar, S.F., 2005. The phanerozoic record of global sea-level  
30 change. *Science* (80- ). 310, 1293–1298. <https://doi.org/10.1126/science.1116412>  
31  
32  
33  
34  
35  
36 14 Müller, R.D., Seton, M., Zahirovic, S., Williams, S.E., Matthews, K.J., Wright, N.M., Shephard, G.E.,  
37 Maloney, K.T., Barnett-Moore, N., Hosseinpour, M., Bower, D.J., Cannon, J., 2016. Ocean Basin  
38 Evolution and Global-Scale Plate Reorganization Events Since Pangea Breakup. *Annu. Rev. Earth*  
39 *Planet. Sci.* 44, 107–138. <https://doi.org/10.1146/annurev-earth-060115-012211>  
40  
41  
42  
43  
44  
45  
46 18 Nøhr-Hansen, H., Nielsen, L.H., Sheldon, E., Hovikoski, J., Alsen, P., 2011. Palaeogene deposits in  
47 North-East Greenland. *Geol. Surv. Denmark Greenl. Bull.* 23, 61–64.  
48  
49  
50  
51  
52 20 Ogg, J.G., 2012. *Geomagnetic Polarity Time Scale, The Geologic Time Scale 2012.* Elsevier.  
53 <https://doi.org/10.1016/B978-0-444-59425-9.00005-6>  
54  
55  
56  
57  
58 22 Olesen, O., Ebbing, J., Lundin, E., Mauring, E., Skilbrei, J.R., Torsvik, T.H., Hansen, E.K., Henningsen,

1 T., Midbøe, P., Sand, M., 2007. An improved tectonic model for the Eocene opening of the  
2 Norwegian-Greenland Sea: Use of modern magnetic data. *Mar. Pet. Geol.* 24, 53–66.  
3 <https://doi.org/10.1016/j.marpetgeo.2006.10.008>  
4 Petersen, T.G., Hamann, N.E., Stemmerik, L., 2016. Correlation of the Palaeogene successions on the  
5 North-East Greenland and Barents Sea margins. *Bull. Geol. Soc. Denmark* 64, 77–96.  
6 Petersen, T.G., Hamann, N.E., Stemmerik, L., 2015. Tectono-sedimentary evolution of the Paleogene  
7 succession offshore Northeast Greenland. *Mar. Pet. Geol.* 67, 481–497.  
8 <https://doi.org/10.1016/j.marpetgeo.2015.05.033>  
9 Reynolds, P., Planke, S., Millett, J.M., Jerram, D.A., Trulsvik, M., Schofield, N., Myklebust, R., 2017.  
10 Hydrothermal vent complexes offshore Northeast Greenland: A potential role in driving the  
11 PETM. *Earth Planet. Sci. Lett.* 467, 72–78. <https://doi.org/10.1016/j.epsl.2017.03.031>  
12 Rickers, F., Fichtner, A., Trampert, J., 2013. The Iceland-Jan Mayen plume system and its impact on  
13 mantle dynamics in the North Atlantic region: Evidence from full-waveform inversion. *Earth*  
14 *Planet. Sci. Lett.* 367, 39–51. <https://doi.org/10.1016/j.epsl.2013.02.022>  
15 Rowan, M.G., Lindsø, S., 2017. Salt Tectonics of the Norwegian Barents Sea and Northeast Greenland  
16 Shelf, Permo-Triassic Salt Provinces of Europe, North Africa and the Atlantic Margins: Tectonics  
17 and Hydrocarbon Potential. Elsevier Inc. <https://doi.org/10.1016/B978-0-12-809417-4.00013-6>  
18 Stemmerik, L., 2000. Late Palaeozoic evolution of the North Atlantic margin of Pangea. *Palaeogeogr.*  
19 *Palaeoclimatol. Palaeoecol.* 161, 95–126. [https://doi.org/10.1016/S0031-0182\(00\)00119-X](https://doi.org/10.1016/S0031-0182(00)00119-X)  
20 Storey, M., Duncan, R.A., Tegner, C., 2007. Timing and duration of volcanism in the North Atlantic  
21 Igneous Province: Implications for geodynamics and links to the Iceland hotspot. *Chem. Geol.*  
22 241, 264–281. <https://doi.org/10.1016/j.chemgeo.2007.01.016>



1 Talwani, M., Eldholm, O., 1977. Evolution of the Norwegian-Greenland Sea. *Bull. Geol. Soc. Am.* 88,  
2 969–999. [https://doi.org/10.1130/0016-7606\(1977\)88<969:EOTNS>2.0.CO;2](https://doi.org/10.1130/0016-7606(1977)88<969:EOTNS>2.0.CO;2)  
3  
4  
5  
6 3 Tegner, C., Storey, M., Holm, P.M., Thorarinsson, S.B., Zhao, X., Lo, C.H., Knudsen, M.F., 2011.  
7  
8 4 Magmatism and Eureka deformation in the High Arctic Large Igneous Province: <sup>40</sup>Ar-<sup>39</sup>Ar age  
9  
10 5 of Kap Washington Group volcanics, North Greenland. *Earth Planet. Sci. Lett.* 303, 203–214.  
11  
12 6 <https://doi.org/10.1016/j.epsl.2010.12.047>  
13  
14  
15  
16 7 Thiede, J., Myhre, A.M., Firth, J.V. and the S.S.P., 1995. Cenozoic northern hemisphere polar and  
17  
18 8 subpolar ocean paleoenvironments (summary of ODP Leg 151 drilling results). *Proc. Ocean*  
19  
20 9 *Drill. Program, Initial Reports 151*, 397–420.  
21  
22  
23  
24 10 Tsikalas, F., Faleide, J.I., Eldholm, O., Antonio Blaich, O., 2012. The NE Atlantic conjugate margins,  
25  
26 11 Regional Geology and Tectonics. <https://doi.org/10.1016/B978-0-444-56357-6.00004-4>  
27  
28  
29  
30 12 Tsikalas, F., Faleide, J.I., Eldholm, O., Wilson, J., 2005. Late Mesozoic–Cenozoic structural and  
31  
32 13 stratigraphic correlations between the conjugate mid-Norway and NE Greenland continental  
33  
34 14 margins. *Pet. Geol. North-West Eur. Glob. Perspect. – Proc. 6th Pet. Geol. Conf.* 785–801.  
35  
36 15 <https://doi.org/10.1144/0060785>  
37  
38  
39  
40 16 Whittaker, J.M., Williams, S., Masterton, S.M., Afonso, J.C., Seton, M., Landgrebe, T.C., Coffin, M.F.,  
41  
42 17 Müller, D., 2013. Interactions among plumes, mantle circulation and mid-ocean ridges. *AGU*  
43  
44 18 *Fall Meet. Abstr. DI13A–04*.  
45  
46  
47  
48  
49 19 Ziegler, P.A., 1992. European Cenozoic rift system. *Tectonophysics* 208, 91–111.  
50  
51 20 [https://doi.org/10.1016/0040-1951\(92\)90338-7](https://doi.org/10.1016/0040-1951(92)90338-7)  
52  
53  
54 21 Ziegler, P.A., Cloetingh, S., 2004. Dynamic processes controlling evolution of rifted basins. *Earth-*  
55  
56 22 *Science Rev.* 64, 1–50. [https://doi.org/10.1016/S0012-8252\(03\)00041-2](https://doi.org/10.1016/S0012-8252(03)00041-2)  
57  
58  
59  
60  
61  
62  
63  
64  
65

1

1  
2  
3  
4  
5  
6  
7  
8  
9  
10  
11  
12  
13  
14  
15  
16  
17  
18  
19  
20  
21  
22  
23  
24  
25  
26  
27  
28  
29  
30  
31  
32  
33  
34  
35  
36  
37  
38  
39  
40  
41  
42  
43  
44  
45  
46  
47  
48  
49  
50  
51  
52  
53  
54  
55  
56  
57  
58  
59  
60  
61  
62  
63  
64  
65

1  
2  
3  
4  
5  
6  
7  
8  
9  
10  
11  
12  
13  
14  
15  
16  
17  
18  
19  
20  
21  
22  
23  
24  
25  
26  
27  
28  
29  
30  
31  
32  
33  
34  
35  
36  
37  
38  
39  
40  
41  
42  
43  
44  
45  
46  
47  
48  
49  
50  
51  
52  
53  
54  
55  
56  
57  
58  
59  
60  
61  
62  
63  
64  
65

1 **Seismic stratigraphy of the post-breakup succession offshore Northeast**

2 **Greenland: Links to margin uplift**

3 Corresponding author: Thomas Guldborg Petersen, thog@byg.dtu.dk

4 Technical University of Denmark, Anker Engelundsvej 1, 2800 Kongens Lyngby, Denmark

5

1  
2  
3  
4  
5  
6  
7  
8  
9  
10  
11  
12  
13  
14  
15  
16  
17  
18  
19  
20  
21  
22  
23  
24  
25  
26  
27  
28  
29  
30  
31  
32  
33  
34  
35  
36  
37  
38  
39  
40  
41  
42  
43  
44  
45  
46  
47  
48  
49  
50  
51  
52  
53  
54  
55  
56  
57  
58  
59  
60  
61  
62  
63  
64  
65

1

2 **Abstract**

3 The timing of the continental breakup between Norway and Greenland and the subsequent plate  
4 tectonic motions are well understood. However, due to the remote location of the Northeast  
5 Greenland shelf, relatively few details about the tectonosedimentary response to the tectonism  
6 following the breakup have previously been published. This article gives new insights into the  
7 structural and sedimentary history of the Northeast Greenland shelf, with an emphasis on the post-  
8 breakup tectonics, using state of the art 2D seismic data. The results of this study clearly shows a  
9 highly dynamic post-breakup tectonic setting with pronounced, kilometre-scale fault offsets, tilting  
10 of the Danmarkshavn Basin and pronounced progradational events. The tectonosedimentary events  
11 are linked with the passage of the Icelandic mantle plume south of the Northeast Greenland shelf.  
12 Based on tectonostratigraphic interpretations and integration of data from ODP 913, this study  
13 constructs a temporally robust model for the post-breakup succession. Significant post-breakup  
14 uplift and tectonism related to thermal uplift is present on the margin. It is observed that the  
15 Icelandic hot spot passes relatively close by the Northeast Greenland shelf (<500 Km) during the  
16 Cenozoic. Its passage south of the shelf supports the observation of the northwards tilt of the shelf  
17 and associated northwards shift of the prograding clinoforms due to a combination of thermal uplift  
18 and possibly dynamic topography.

19 **1 INTRODUCTION**

20 Passive margin tectonism is widely debated, especially in the North Atlantic realm. Conventional  
21 models for continental breakup only predict thermally induced subsidence following the heating  
22 caused by upwelling mantle (e.g. McKenzie, 1978). However, observations around the margins of the  
23 North Atlantic suggest that significant tectonics and vertical motion occurred after the breakup  
24 (Lundin and Doré, 2002; Tsikalas et al., 2012). The term breakup, or continental breakup is here

1  
2 1 understood as the phase of separation between continental lithospheric plates, following the rift  
3  
4 2 phase, *sensu* Cloetingh et al. (2013).  
5  
6  
7 3 Although the Northeast Greenland shelf has been studied previously (e.g. Funck et al., 2017;  
8  
9 4 Hamann et al., 2005; Petersen et al., 2015), very little is known about the tectonostratigraphic  
10  
11 5 development of the shelf after the continental breakup. Based on a comprehensive seismic database  
12  
13 6 consisting of the latest available data, this study yields new insights into the structural history and its  
14  
15 7 influence on sedimentation. By conducting a thorough seismic stratigraphic study of the Northeast  
16  
17 8 Greenland shelf, several seismic units significant to the understanding of the post-breakup  
18  
19 9 development of Northeast Greenland are interpreted concerning depositional environment,  
20  
21 10 tectonostratigraphy and relation to plate tectonics. A clear link between the passage of the Icelandic  
22  
23 11 hotspot, uplift of the inner margin and a northward shift in prograding clinoforms is presented.  
24  
25

## 26 12 **2 REGIONAL GEOLOGY**

27  
28 13 The North Atlantic plate tectonic history is described in multiple studies (e.g. Gaina et al., 2009;  
29  
30 14 Matthews et al., 2016; Müller et al., 2016; Tsikalas et al., 2012). Evidence of rifting throughout the  
31  
32 15 Paleozoic and Mesozoic along the margins of the North Atlantic is recorded as extensional tectonics  
33  
34 16 both onshore (Stemmerik, 2000) and offshore (Tsikalas et al., 2012, 2005) as a part of the long-  
35  
36 17 running opening of the Atlantic Ocean (Cloetingh et al., 2007). The rift to drift transition i.e. the  
37  
38 18 continental breakup is dated by means of paleomagnetic anomalies to have occurred at 55.9 Ma  
39  
40 19 (chron 24), at the Paleocene—Eocene transition (Gaina et al., 2009; Matthews et al., 2016; Ogg,  
41  
42 20 2012; Olesen et al., 2007). This is associated with pronounced volcanism, dated to the earliest  
43  
44 21 Eocene (Larsen et al., 2014). The shelf south of *ca.* 78° N is the conjugate margin to the Vøring and  
45  
46 22 Lofoten margin in Norway, and is associated with extension of the Mohs Ridge segment of the mid  
47  
48 23 ocean ridge system of the North Atlantic (e.g. Gaina et al., 2009; Talwani and Eldholm, 1977; Ziegler,  
49  
50 24 1992). It is dominated by normal faulting prior to the continental breakup (Tsikalas et al., 2012).  
51  
52 25 However, the shelf north of *ca.* 78° N is dominated by complex transpressional and transtensional  
53  
54  
55  
56  
57  
58  
59  
60  
61  
62  
63  
64  
65

Formatted: Danish (Denmark)

Formatted: Danish (Denmark)

1  
2 1 deformation during the opening of the Greenland Sea, where transverse deformation initially  
3  
4 2 occurred along the East Greenland Ridge, before shifting to the Knipovich Ridge during the  
5  
6 3 Oligocene. A slowing of the plate tectonic motion (Gaina et al., 2009; Tegner et al., 2011), dated to  
7  
8 4 ca. 49-47 Ma, coincides with the peak in the Eurekan Orogeny along the northernmost edge of  
9  
10 5 Greenland. Absolute opposite plate motion, where Greenland drifts towards the Northwest and  
11  
12 6 Norway towards the Southeast, was achieved during the earliest Oligocene (33.1 Ma), which implies  
13  
14 7 that passive margin conditions were developed along the entire Northeast Greenland and North  
15  
16 8 Greenland continental margin at this time (Gaina et al., 2009).  
17  
18  
19 9 Pronounced progradation of clinoforms have been described previously, based on low density/low  
20  
21 10 resolution seismic data, and attributed to a "Tertiary" age (Hamann et al., 2005). The pre-drift  
22  
23 11 succession of the Northeast Greenland shelf have also been described in detail (Petersen et al.,  
24  
25 12 2015), but very little has so far been published on the post-breakup seismic stratigraphy.

26  
27  
28 13 Sea level changes during the Cenozoic have been described previously (Miller et al., 2005), and the  
29  
30 14 effects of changing eustatic sea level obviously also had an impact on the sedimentation on the  
31  
32 15 Northeast Greenland shelf. Even though this article focuses solely on the tectonic processes and on  
33  
34 16 highlighting the vertical motions observed on the shelf during the post-breakup times, the author  
35  
36 17 fully acknowledges the influence of eustatic sea level changes as well.  
37  
38  
39 18

### 42 19 **3 DATA AND METHODS**

43  
44 20 The database of this study is composed of the latest vintages of commercial 2D seismic data  
45  
46 21 collected during a period from 2008-2014 by TGS, a commercial seismic data vendor, together with a  
47  
48 22 scientific dataset collected by the Alfred Wegener Institute (AWI) during the early nineties (Berger  
49  
50 23 and Jokat, 2009, 2008) (Fig.1). All seismic data are courtesy of TGS and Spectrum. The seismic data  
51  
52 24 were supplied under the agreement that no shot points or navigational data are published. These  
53  
54  
55  
56  
57  
58  
59  
60  
61  
62  
63  
64  
65

1  
2 1 data are supplemented by free air gravity data from the DTU10 global gravity field model (Andersen,  
3  
4 2 2010; Andersen et al., 2010). The locations of the North Atlantic hotspots are derived from  
5  
6 3 Whittaker et al. (2013), and the locations of the magnetic anomalies are adopted from Müller et al.  
7  
8 4 (2016). Plate tectonic reconstructions are based on Matthews et al. (2016). Reconstruction of the  
9  
10 5 path of the hotspots was done using the open source software GPlates ([www.gplates.org](http://www.gplates.org)). The  
11  
12 6 seismic interpretation was conducted using a seismic workstation (Petrel 2016). Standard seismic  
13  
14 7 stratigraphic methods was applied as outlined by Emery and Myers (1996).  
15  
16  
17 8

## 20 9 **4 OBSERVATIONS**

### 22 10 **4.1 Potential field data**

24 11 The use of free air gravity data gives excellent insights into the geometries of structural elements in  
25  
26 12 the Northeast Greenland area (Fig. 2). The gravity data quite clearly show the location of the  
27  
28 13 continental slope (Fig. 2), and the magnetic anomalies (Müller et al., 2016), shows the westward  
29  
30 14 extent of the oceanic crust, as well as other key features of the Northeast Greenland shelf. The  
31  
32 15 Danmarkshavn Basin stands out on the inner side of Northeast Greenland's continental shelf as a  
33  
34 16 distinct low in the gravity field. In fact, the gravity low extends onshore Greenland, outlining the  
35  
36 17 prominent sedimentary basins present there (Stemmerik, 2000). The Danmarkshavn Ridge is also  
37  
38 18 outlined in detail as a positive gravity anomaly. The ridge is NE-SW striking and displays a noticeable  
39  
40 19 right-lateral offset, separating the ridge into a north and a south segment (Fig. 2). It is also clear, that  
41  
42 20 the deep faults observed on the shelf are parallel to the ridge, and that the faulting of the Cenozoic  
43  
44 21 succession is focused at or near the ridge, with few exceptions (Fig. 2). Although a detailed  
45  
46 22 description of the faults is given below, it is noted that faulting is also observed north of the  
47  
48 23 Danmarkshavn Ridge gravity high. The Thetis Basin is seen as a relatively narrow, elongated gravity  
49  
50 24 low parallel to the Danmarkshavn Ridge. This shape of the basin in the gravity data is controlled  
51  
52 25 mostly by a very deep, narrow half graben created during the Mesozoic (Figs. 3a, b). The shape of  
53  
54  
55  
56  
57  
58  
59  
60  
61  
62  
63  
64  
65

1  
2 1 the basin during the Cenozoic is wider however, and spans from the Danmarkshavn Ridge to the  
3  
4 2 continental slope.  
5  
6

#### 7 3 **4.2 Seismic interpretation**

8  
9 4 Based on the observed seismic facies of the individual units, the sedimentary facies, depositional  
10  
11 5 environment and tectonic evolution are evaluated. The methodology is briefly described in Emery  
12  
13 6 and Meyers (1996), where they highlight the seismic expression of various depositional  
14  
15 7 environments. Due to the lack of well control, the seismic facies interpretations in this study are  
16  
17 8 associated with some uncertainty.  
18  
19

20 9 This study is based on the mapping of several seismic horizons across the Northeast Greenland shelf  
21  
22 10 and onto the oceanic crust (Figs. 3-7). The shown seismic horizons all hold significant information  
23  
24 11 about the tectono-sedimentary history during the Neogene of Northeast Greenland. By using  
25  
26 12 conventional seismic interpretation techniques and seismic stratigraphic principles, it is possible to  
27  
28 13 describe exhumation, subsidence and the relative timing of tectonic events. This study establishes a  
29  
30 14 regional framework of tectonic events with good confidence due to the ~~availability~~inclusion of the  
31  
32 15 most comprehensive, high quality seismic database currently available (fig. 1). The seismic  
33  
34 16 observations correlates well with the gravity data, confirming the control of deeper structures on  
35  
36 17 the depositional pattern. (Fig. 2). Examples of both the seismic horizons and the interpreted faults  
37  
38 18 are presented in seismic cross sections (Figs. 3-7), and in map form (Figs. 8, 9). Only one borehole is  
39  
40 19 available for age correlation, namely the ODP 913 borehole (Thiede et al., 1995). The location of ODP  
41  
42 20 913 on the oceanic crust means that the pre-break-up succession is not penetrated. Due to the  
43  
44 21 absence of any deep well bores on the Northeast Greenland shelf, all the ages of the pre-early  
45  
46 22 Eocene seismic horizons are associated with some uncertainty. This study infers the ages of the  
47  
48 23 seismic horizons from published regional studies (Engen et al., 2008; Hamann et al., 2005; Petersen  
49  
50 24 et al., 2015; Tsikalas et al., 2012), and by correlating with plate tectonic events highlighted in this  
51  
52 25 study.  
53  
54  
55  
56  
57  
58  
59  
60  
61  
62  
63  
64  
65



1  
2 1 Structure maps of key surfaces are also presented (Fig. 8a, b). These maps are all in Two Way Time  
3  
4 2 (TWT) reported in seconds. All structure and thickness maps are interpolations of seismic data,  
5  
6 3 within the extent of the interpreted horizon. This means that the outer boundary of a surface is  
7  
8 4 defined by the absence of the seismic horizon due to either erosion or condensation, or due to the  
9  
10 5 lack of resolution in the seismic data. The study also includes thickness maps used to highlight areas  
11  
12 6 of deposition (Figs. 10-12).

13  
14  
15 7 The seismic units described below, subdivide the Paleogene and Neogene succession of the  
16  
17 8 Northeast Greenland margin into three seismic units significant for the understanding of the tectonic  
18  
19 9 evolution after the continental breakup. The interpretation and definition of the seismic units was  
20  
21 10 based on their importance concerning structural evolution of the margin, especially during post-  
22  
23 11 breakup times. Pronounced unconformities was the central focus, as they play a significant role in  
24  
25 12 the identification of the location and timing of tectonic events on the Northeast Greenland shelf.  
26  
27 13 Seismic facies in the respective units are also described in order to interpret the depositional  
28  
29 14 mechanisms responsible for the deposited sediments and to constrain the structural evolution of the  
30  
31 15 Northeast Greenland margin after the breakup.

### 32 33 34 16 **4.3 Dating of the seismic units**

35  
36 17 All dating of the seismic units is done by correlation with the plate tectonic evolution as well as  
37  
38 18 understanding of regional tectonic events in conjunction with the previously mentioned ODP 913  
39  
40 19 borehole. Previous studies have created a framework for the dating of the pre- and syn- breakup  
41  
42 20 succession (Petersen et al., 2016, 2015). The current study further constrains the ages of the pre-  
43  
44 21 breakup succession suggested in these studies by usage of better quality seismic data and closer  
45  
46 22 correlation to the ODP 913 borehole. Furthermore, this study adds significant new knowledge about  
47  
48 23 the post-breakup seismic units and their relative timing. The addition of reprocessed and recently  
49  
50 24 acquired seismic data improves the reliability of these interpretations and adds additional  
51  
52 25 information regarding the ages of the depositional events.

1  
2 1 Prior to the onset of Paleocene deposition, a regional unconformity is observed in the Wandell Sea  
3  
4 2 area, north of the current study area (Håkansson and Stemmerik, 1989). This and other observations  
5  
6 3 are used by Hamann et al. (2005) to define the base of the Cenozoic succession in the Danmarkshavn  
7  
8 4 Basin area. Furthermore, observations onshore Northeast Greenland in the Wollaston Foreland and  
9  
10 5 Sabine Ø area (Fig. 2) confirms a hiatus between the Cretaceous and the Paleogene (Nøhr-Hansen  
11  
12 6 et al., 2011). A change from syn-tectonic halfgraben infill to parallel reflections mark the Mesozoic-  
13  
14 7 Cenozoic transition in the Thetis Basin. The accuracy of the age of the unconformity is uncertain due  
15  
16 8 to the lack of any means of direct dating. Furthermore, the interface is most likely diachronous  
17  
18 9 across most of the study area, although early Cenozoic deposits appear relatively conformable at  
19  
20 10 their base, with the exception of the south part of the study area, where Petersen et. al (2015)  
21  
22 11 describe progradation from the southwest.

23  
24  
25 12 The Early Eocene Unconformity is relatively well dated due to its association with the breakup  
26  
27 13 volcanism. Compelling evidence of deepening of the erosion towards the centre of the magmatic  
28  
29 14 intrusions in the Danmarkshavn Basin, (Petersen et al., 2015), together with the coinciding gas ~~vent~~  
30  
31 15 structures from the intrusions (Reynolds et al., 2017) yields a relatively tight constraint on the age of  
32  
33 16 this horizon (Fig. 5). This is achieved by utilizing the well-known absolute ages of the peak in  
34  
35 17 magmatic intrusions onshore Northeast Greenland (Larsen et al., 2014). These observations are  
36  
37 18 further corroborated by the availability of the high quality data for this study. Especially the  
38  
39 19 northwards correlation of this event makes it possible to constrain the ages of the  
40  
41 20 tectonosedimentary events in the north of the study area (Fig. 7b).

42  
43  
44 21 There are no direct means of constraining the age of the Erosional incision seismic horizon, so a  
45  
46 22 relative dating of the horizon is suggested. The Erosional incision horizon clearly truncates the well-  
47  
48 23 dated Early Eocene Unconformity (Figs. 4a-c), thus a post- Early Eocene age can be initially  
49  
50 24 suggested. The erosional incision also truncates strata younger than early Eocene, so the incision  
51  
52 25 must post-date the Early Eocene Unconformity by some margin. The upwards constraint of the age

1  
2 1 of the erosional incision is the Intra Miocene Unconformity, as this horizon is not truncated by the  
3  
4 2 incision. However, a significant sedimentary succession is present between the two horizons, which  
5  
6 3 hampers the possibility for a more accurate age for the Erosional incision horizon other than late  
7  
8 4 Eocene—mid Miocene. An important observation in this context is that the Erosional incision  
9  
10 5 horizon post-dates the continental breakup.

11  
12  
13 6 The Intra Miocene horizon is dated using the information from the ODP 913 borehole using the  
14  
15 7 seismic tie from Berger and Jokat (2008). This is the only directly dated horizon in this study, but  
16  
17 8 some uncertainty is still associated with the age of this horizon. Firstly, it is an unconformity, which is  
18  
19 9 inherently a time-transgressive surface. Therefore significant lateral changes in the age of the  
20  
21 10 horizon may occur. Secondly, the seismic correlation from the ODP 913 drill site and onto the  
22  
23 11 Northeast Greenland shelf is associated with some uncertainty, due to sparse seismic data in the  
24  
25 12 area and condensation across the continental slope. Still, this horizon remains possibly the most  
26  
27 13 accurately dated seismic horizons of this study, and therefore it forms a significant anchor for the  
28  
29 14 dating of the post-breakup events on the Northeast Greenland Shelf.

30  
31  
32 15 The youngest horizon interpreted in this study is the Top upper prograding unit seismic horizon. No  
33  
34 16 direct methods for dating this horizon exists. It is clearly younger than the Intra Miocene  
35  
36 17 unconformity horizon and it was affected by the uplift and rotation of the Danmarkshavn Basin and  
37  
38 18 Ridge areas. This is evident from its location above a set of very steep clinoforms associated with the  
39  
40 19 uplift (Fig. 3a). The only age constraint of this horizon is an age younger than mid Miocene, and  
41  
42 20 predating the Quaternary glaciations of the shelf, since the shallow Quaternary erosion does not  
43  
44 21 incise deeply into the unit (Fig. 4a).

#### 47 22 **4.4 Pre-Cenozoic units**

48  
49 23 It is beyond the scope of this study to conduct a detailed interpretation of the Palaeozoic and  
50  
51 24 Mesozoic succession on the Northeast Greenland shelf. However, some general observations are of  
52  
53 25 relevance to the further interpretation, and will be summarised here. For a more complete  
54

1  
2 1 understanding of the pre-Cenozoic geology of the Northeast Greenland shelf, see e.g. Hamann et al.  
3  
4 2 (2005). The Palaeozoic—Mesozoic Succession is largely conformable, but minor angular  
5  
6 3 unconformities exist near the presumed Palaeozoic—Mesozoic transition (Figs. 3a, b). The  
7  
8 4 succession is intersected and rotated by normal faults near the Danmarkshavn Ridge. The faults are  
9  
10 5 all apparently deeply rooted (e.g. Fig. 5). The pre-Cenozoic succession of the Thetis Basin is largely  
11  
12 6 deposited in a rotated half graben setting, with the controlling fault located along the east margin of  
13  
14 7 the Danmarkshavn Ridge (Fig. 3b). The Cenozoic succession is thus underlain by several kilometres of  
15  
16 8 Palaeozoic and Mesozoic sediments, intersected by faults mostly generated during Mesozoic rifting  
17  
18 9 (Hamann et al., 2005).

#### 21 10 **4.5 Paleocene(?)—Early Eocene seismic unit**

22  
23 11 The unit is partially described in Petersen et al. (2015), in the southern part of the Danmarkshavn  
24  
25 12 Basin. A more regionally cohesive interpretation is included in this study since it is important for  
26  
27 13 understanding the structural framework, and it forms an important temporal constraint of the  
28  
29 14 continental breakup. The Base Paleogene horizon is the base of this unit is and is regionally extensive  
30  
31 15 and observed across most of the Northeast Greenland shelf area. It is primarily defined as an erosive  
32  
33 16 unconformity, with a deepening incision towards the west in the Danmarkshavn Basin (Fig. 3a, b). A  
34  
35 17 significant topographic break is observed at the transition from the Danmarkshavn  
36  
37 18 Basin/Danmarkshavn Ridge and into the Thetis Basin (Figs. 3a, 8a), where the Base Paleogene lies  
38  
39 19 significantly deeper. Towards the south, faulting offsets the Base Paleogene in the west part of the  
40  
41 20 Thetis Basin (Figs. 3b, 4c). The Base Paleogene is delimited towards the west by erosion due to uplift  
42  
43 21 and tilting of the Cenozoic succession. Towards the east, i.e. towards the continental slope, the Base  
44  
45 22 Paleogene is truncated, since the continental rifting did not occur before the earliest Eocene (Gaina  
46  
47 23 et al., 2009). The north and south extent of the unconformity is not resolved by the current data set.  
48  
49  
50 24 In the Thetis Basin, east of the basin bounding fault system (Fig. 2), the Base Paleogene Horizon  
51  
52 25 seems to be mostly conformable with the underlying Mesozoic sediments. There are however some  
53  
54  
55  
56  
57  
58  
59  
60  
61  
62  
63  
64  
65

1  
2 1 evidence of faulting below the Base Paleogene, especially along the western margin of the Thetis  
3  
4 2 Basin (Fig. 5). The Danmarkshavn Basin displays clear evidence of inversion following the Mesozoic  
5  
6 3 rift phases, creating compressional structures such as folds and domes below the Base Paleogene  
7  
8 4 (Fig. 5). These structures were subsequently eroded during a Late Cretaceous—Paleogene (?) and  
9  
10 5 early Eocene erosional events (Figs. 3b, 4a). This compressional event is focused in the  
11  
12 6 Danmarkshavn Basin and Ridge areas, in comparison with the more conformable nature of the Base  
13  
14 7 Paleogene in the Thetis Basin. The seismic facies below the Base Paleogene show frequent examples  
15  
16 8 of high amplitude, discontinuous reflections, often intersecting the bedding. These structures have  
17  
18 9 previously been described as magmatic intrusions (Fig. 7b), (Petersen et al., 2015; Reynolds et al.,  
19  
20 10 2017). Towards the eastern margin of the Thetis Basin, the seismic data shows a rise of the Base  
21  
22 11 Paleogene (Fig. 8a). This rise coincides with the shelf to continental slope transition, which is also  
23  
24 12 coinciding with a gravity high (Fig. 2). The high-amplitude, discontinuous reflectors are also very  
25  
26 13 prominent below the rise.

27  
28  
29 14 The unit mostly consists of parallel, medium to high amplitude reflections, with the high amplitudes  
30  
31 15 focused mainly in the Danmarkshavn Basin and the Danmarkshavn Ridge areas. The unit is thinning  
32  
33 16 across the eastern margin of the Danmarkshavn Ridge, and there is evidence of internal erosion  
34  
35 17 along the ridge margin, especially to the north (Fig. 3a).

36  
37  
38 18 The thickness map (Fig. 10) show a southerly-located depo-centre in the Thetis Basin, with a distinct  
39  
40 19 thinning across the Danmarkshavn Ridge, and smaller depo-centres in the Danmarkshavn Basin,  
41  
42 20 consistent with previous observations (Petersen et al., 2015). Diverging internal reflections towards  
43  
44 21 the faults separating the Danmarkshavn Ridge from the Danmarkshavn Basin indicate syn-tectonic  
45  
46 22 deposition related to normal faulting (Fig. 5). The truncation of the seismic unit that deepens  
47  
48 23 towards the south is mostly controlled by structural rotation and uplift (Fig. 5). The horizon is heavily  
49  
50 24 disturbed in some places, where deep (100-200ms TWT, ca. 100-200 m) and laterally extensive (<2  
51  
52 25 km) depressions or pockmarks are observed specifically at this level (Fig. 5). These features have

1  
2 1 been mapped previously and been interpreted as gas escape structures related to the earliest  
3  
4 2 Eocene volcanism (Reynolds et al., 2017).

#### 7 3 **4.6 Early Eocene Unconformity**

8  
9 4 The Early Eocene Unconformity is a very prominent angular unconformity in the southern area of the  
10  
11 5 Danmarkshavn Basin (Fig. 5), whereas it is mostly conformable across the Danmarkshavn Ridge and  
12  
13 6 in the northern part of the Danmarkshavn Basin (Fig. 3a, b). It forms the upper boundary of the  
14  
15 7 Paleocene(?)—Early Eocene seismic unit described above. Some indications of an angular  
16  
17 8 unconformity below the horizon is also observed on the southern part of the Danmarkshavn Ridge  
18  
19 9 (Fig. 4c). The Early Eocene Unconformity is truncated by the same tilt-induced incision along the  
20  
21 10 western margin of the Danmarkshavn Basin as the underlying Base Paleogene horizon. The  
22  
23 11 truncation occurs further east compared to the Base Paleogene, which inhibits interpretation of the  
24  
25 12 Early Eocene Unconformity in most of the Danmarkshavn Basin (Fig. 3a).

26  
27  
28 13 The horizon is offset by deep-rooted, reactivated faults on both the west and east sides of the  
29  
30 14 Danmarkshavn Ridge (Fig. 5). The angular unconformity in the Danmarkshavn Basin deepens  
31  
32 15 towards the southwest. Towards the south, the Early Eocene Unconformity is erosionally truncated  
33  
34 16 by the Erosional Incision horizon observed along the boundary between the Danmarkshavn Ridge  
35  
36 17 and the Thetis Basin (Fig. 3b). Faulting of the Early Eocene Unconformity is also observed along the  
37  
38 18 Intra Danmarkshavn Basin Fault (Fig. 6).

#### 41 19 **4.7 Erosional incision**

42  
43 20 This seismic horizon is a very distinct feature along the south segment of the Danmarkshavn Ridge,  
44  
45 21 where it truncates the Early Eocene Unconformity and overlying strata (Fig. 3b). The incision is  
46  
47 22 concave down towards the west and becomes subparallel to the bedding towards the Thetis Basin  
48  
49 23 (Figs. 4a-c). The incision is clearly associated with the westwards bounding fault system of the Thetis  
50  
51 24 Basin. Uplift of the Danmarkshavn Basin and Ridge created a dip along the eastern edge of the ridge  
52  
53 25 (Figs 8a) above the angle of repose of the strata on the Danmarkshavn Ridge, which caused

1  
2 1 extensive mass wasting of material from the elevated Danmarkshavn Ridge and into the Thetis Basin  
3  
4 2 (Fig. 5). The westward extent of the horizon is defined by the onset of the incision, and the eastward  
5  
6 3 extent of the incision is defined by the transition to conformity (Fig. 3b). The incision is located  
7  
8 4 further east of the Danmarkshavn Ridge and into the Thetis Basin towards the south. In the north,  
9  
10 5 the incision is located on the eastern margin of the ca. 5 km west of the Danmarkshavn Ridge (Fig.  
11  
12 6 4a), whereas the incision is located about 10 km east of the ridge in the south (Fig. 4c). Furthermore,  
13  
14 7 the mass wasting event seems more related to the Intra Thetis Basin Fault observed in the south  
15  
16 8 Thetis Basin (Fig. 4c). The incision is a noticeable unconformity below the horizon, with very  
17  
18 9 pronounced downlaps across the horizon (Figs. 4a-c). The steep incision is not observed north of the  
19  
20 10 in the central part of the study area (Fig. 7a). However, other local erosional incisions are found  
21  
22 11 along the north segment of the Danmarkshavn Ridge, and although they cannot be correlated with  
23  
24 12 the incision seen in the south, this study indicates they are of similar age as the Erosional incision  
25  
26 13 horizon and related to faulting between the Danmarkshavn Ridge and the Thetis Basin.  
27  
28

#### 29 14 **4.8 Eocene—Middle Miocene**

30  
31 15 The Eocene—Middle Miocene seismic unit directly overlies the Paleogene—Early Eocene unit, and is  
32  
33 16 therefore bounded at its base by the Early Eocene Unconformity. The top of the unit is defined by  
34  
35 17 the Intra Miocene Unconformity. The seismic facies in the Danmarkshavn Basin area are very similar  
36  
37 18 to the underlying unit, with high amplitude, parallel reflectors (Figs. 3b, 4a). The Erosional incision  
38  
39 19 horizon across the Danmarkshavn Ridge to Thetis basin transition is associated with steep,  
40  
41 20 prograding clinoforms, extending out into the central part of the Thetis Basin (Figs. 4a-b). The  
42  
43 21 clinoforms are most pronounced in the south of the study area, whereas they are absent in the  
44  
45 22 north (Fig. 3a). The clinoforms are very specifically linked to the erosional incision horizon described  
46  
47 23 above (Fig. 3b). The earliest clinoforms show very little accretion in the topsets, indication of a very  
48  
49 24 rapid initial progradation. The later clinoforms are associated with more topset aggradation and less  
50  
51 25 progradation. The eastern part of the Thetis Basin is dominated by the sub-parallel reflections of the  
52  
53 26 toesets associated with the clinoforms, with a gradual condensation and thinning towards the  
54

1  
2 1 continental slope (Fig. 3b). A very well defined depo-center along the south margin of the  
3  
4 2 Danmarkshavn Ridge (Fig. 11) correlates with the location of the clinoforms. The thinning towards  
5  
6 3 the shelf edge is also noticeable in the thickness map, as well as the fault control. Minor east-dipping  
7  
8 4 normal faults with a relatively small offset (ca. 100 ms TWT, ca. 100 m) and no deep roots are  
9  
10 5 present in several location above the steep prograding clinoforms (Figs. 4c-b). These faults appear to  
11  
12 6 terminate in the Eocene—Middle Miocene seismic unit, and are thus not related to deep-rooted  
13  
14 7 tectonics.  
15  
16  
17 8 The ~~is~~ upper boundary of this unit is the Intra Middle Miocene Unconformity, and is primarily defined  
18  
19 9 based on correlation with the ODP 913 borehole, located on the oceanic crust (Fig. 1), and is thus  
20  
21 10 temporally relatively well constrained based on an unconformity observed in the cores (Berger and  
22  
23 11 Jokat, 2008; Døssing et al., 2016; Thiede et al., 1995). The incision caused by the structural tilt  
24  
25 12 mentioned previously also truncates the Intra Miocene Unconformity along the centre of the  
26  
27 13 Danmarkshavn Ridge. The horizon extends beyond the continental slope to the east, and mimics the  
28  
29 14 same general topographic trends as the underlying horizons, with a steep, fault related slope along  
30  
31 15 the Danmarkshavn/Thetis Basin interface, a deepening in the central Thetis Basin, and a topographic  
32  
33 16 rise towards the shelf edge. The Intra Miocene Unconformity is a prominent downlap surface in the  
34  
35 17 north of the study area. (Fig. 3a). In the south however, the horizon is located at the top of a  
36  
37 18 prograding interval, and is largely conformable both below and above (Fig. 3b). The horizon is often  
38  
39 19 intersected by minor faults, with offsets around 50-250 ms (or ca. 50-250 m). The faults are all  
40  
41 20 located where the underlying clinoforms display the strongest progradation, and on a relatively  
42  
43 21 steep slope (Figs. 4b-c, Fig. 5). In the northern part, where the Intra Miocene Unconformity is mainly  
44  
45 22 overlying gently dipping strata, no evidence of faulting of the horizon is observed in the Thetis Basin  
46  
47 23 (Fig. 3a, 4a).  
48  
49  
50  
51  
52  
53  
54  
55  
56  
57  
58  
59  
60  
61  
62  
63  
64  
65



1  
2 1 **4.9 Middle Miocene—Top Prograding Unit**  
3  
4 2 The Top Prograding Unit seismic horizon defines the upper boundary of the upper prograding  
5  
6 3 seismic unit, the Middle Miocene—Top Prograding Unit. When comparing the horizon north to south,  
7  
8 4 it is evident that very steep clinoforms are present immediately below the horizon in the north (Fig.  
9  
10 5 3a), but the seismic unit is approaching subparallel reflections to the south (Fig. 3b). In the  
11  
12 6 southernmost part of the study area, evidence of most likely Quaternary erosional truncation of the  
13  
14 7 Top upper prograding unit horizon is observed at the sea floor as well (Fig. 4c). The horizon is only  
15  
16 8 observed in the Thetis Basin and along the eastern margin of the Danmarkshavn Basin (Fig. 8b). A  
17  
18 9 combination of either erosional incision or condensation defines the westwards extent of the  
19  
20 10 horizon (Fig. 4a-c). Onlap of the Top Prograding Unit horizon onto the shelf edge high defines the  
21  
22 11 eastwards extent, effectively constraining the top of this upper prograding unit to the Thetis Basin.  
23  
24  
25 12 Towards the south, the seismic facies show a more or less continuous and conformable deposition  
26  
27 13 with slight progradation and aggradation (Fig. 4c, b). The toesets thin considerably over the marginal  
28  
29 14 high, where the unit condenses beyond seismic resolution. Towards the north, the unit is dominated  
30  
31 15 by steep, rapidly prograding clinoforms, with very little topset accommodation (Fig. 3a, 7b). The  
32  
33 16 upper part of the clinoforms show very high amplitudes, with a noticeable drop in amplitudes below  
34  
35 17 the offlap break, indicative of either a facies change or simply scattering of seismic energy due to the  
36  
37 18 steep geometry of the clinoforms (Fig. 7b). This unit displays a close correlation between the  
38  
39 19 locations of the clinoforms and the depocentre, similar to that of the underlying unit. It is clear that  
40  
41 20 the main progradation is located along the northern part of the Danmarkshavn Ridge (Fig. 12) as  
42  
43 21 opposed to the underlying unit, where a more southerly depocentre is observed (Fig. 11).  
44  
45

#### 46 22 **4.10 Faulting and structures**

47

48 23 This study maps a significant number of faults active during the post-breakup phase of the Northeast  
49  
50 24 Greenland shelf. The fault pattern is used to constrain the timing, location and mechanisms related  
51  
52 25 to the post-breakup tectonism and vertical motions observed. The faulting observed on the  
53  
54  
55  
56  
57  
58  
59  
60  
61  
62  
63  
64  
65

1  
2 1 Northeast Greenland shelf is mostly extensional, with some indication of transverse movement in  
3  
4 2 the Danmarkshavn Basin (Fig. 6, 9). This is consistent with the tectonic setting of the North Atlantic  
5  
6 3 since the Carboniferous, where rifting and continental spreading dominated (Ziegler and Cloetingh,  
7  
8 4 2004).  
9  
10  
11 5 A prominent structural break is observed between the Danmarkshavn Ridge and the Thetis Basin,  
12  
13 6 which affects the geometry of the seismic units described above significantly (Figs. 3a-b, 8a-b). West  
14  
15 7 of this break, the Cenozoic succession in the Danmarkshavn Basin is dominated by a significant  
16  
17 8 structural tilt and uplift towards the west (Fig. 3b), whereas the Thetis Basin remains mostly sub-  
18  
19 9 horizontal. This in turn is associated with a westwards deepening erosional truncation of the  
20  
21 10 Cenozoic succession. Cenozoic deposits are thus only preserved in the westernmost part of the  
22  
23 11 Danmarkshavn Basin (Fig. 9). Seismic horizons up to and including the Top Upper prograding unit are  
24  
25 12 affected by the tilt, although it is not possible to constrain it further due to the erosional incision.  
26  
27  
28 13 The Danmarkshavn Ridge is a relatively complex structure. It is primarily a horst structure (Fig. 5)  
29  
30 14 extending about 200 km across the Northeast Greenland shelf (Fig. 2). The Danmarkshavn Ridge also  
31  
32 15 defines the orientation and dip of the main, basin bounding faults (Type 1 on Fig. 9). Towards the  
33  
34 16 North, the ridge is dominated by inverted Palaeozoic—Mesozoic sedimentary basins overlying an  
35  
36 17 uplifted crystalline basement (Fig. 3a), whereas the south segment of the ridge consists mostly of  
37  
38 18 crystalline basement (Fig. 3b). The faults east of the ridge dips to the east to southeast, thus forming  
39  
40 19 the border faults to the Mesozoic half graben Thetis Basin (Fig. 3b, 9). The faults separating the  
41  
42 20 Thetis Basin and the Danmarkshavn Ridge show larger offsets in the seismic data ~~in~~towards the  
43  
44 21 south, although seismic reflection patterns suggest that similar faults also exist to the north. The  
45  
46 22 base Cenozoic reflector is clearly downthrown from the Danmarkshavn Ridge (Fig. 5), although the  
47  
48 23 structural style varies across the fault zone. The central section of the ridge show a complex  
49  
50 24 transition with several listric faults constituting the border fault system (Fig. 7b). To the north, the  
51  
52 25 vertical movement between the Thetis Basin and the Danmarkshavn Ridge is mostly accommodated  
53  
54  
55  
56  
57  
58  
59  
60  
61  
62  
63  
64  
65

1  
2 1 by folding of Paleogene—middle Miocene strata across the transition from the Danmarkshavn Ridge  
3  
4 2 and into the Thetis Basin (Fig. 3a). The Intra Thetis Basin fault parallel to the southern segment of  
5  
6 3 the Danmarkshavn Ridge is located about 25 km east of the Danmarkshavn Ridge (Figs. 3b, 4c). The  
7  
8 4 Intra Thetis Basin fault is aligned with the main fault system east of the northern segment of the  
9  
10 5 Danmarkshavn Ridge (Fig. 9). It shows that the southern segment of the Danmarkshavn Ridge was  
11  
12 6 not involved in the reactivation of the faulting along the east margin of the Thetis Basin during the  
13  
14 7 Cenozoic.  
15  
16  
17 8 The faults on the west side of the Danmarkshavn Ridge are all west dipping normal faults (Fig. 9),  
18  
19 9 with the exception of a few antithetic faults (Fig. 3a). The faults clearly define the transition from  
20  
21 10 the Danmarkshavn Ridge and into the deep Danmarkshavn Basin (Fig. 3b) in the south, whereas the  
22  
23 11 northern segment is more ambiguous (Fig. 3a). The observation of faulting of the Cenozoic  
24  
25 12 succession in the Danmarkshavn Basin is limited due to thinning and erosion. However, a fault on-  
26  
27 13 trend with the south segment of the Danmarkshavn Ridge is observed in the Danmarkshavn Basin  
28  
29 14 (Type 2, Fig. 9). It is tentatively suggested to be transpressional due to the localised, but intense  
30  
31 15 compressional deformation in combination with a limited vertical offset of the deformed succession  
32  
33 16 (Fig. 6). The fault is part of a zone that accommodates some shortening of the Danmarkshavn Basin,  
34  
35 17 where the footwall block show strong eastwards tilting of Cenozoic strata close to the fault- (Fig. 6).  
36  
37 18 It is also observed that the Danmarkshavn Basin fault is associated with basin inversion of the  
38  
39 19 Paleozoic—Mesozoic succession as well as a basement high (Fig. 3b).  
40  
41  
42 20 The northwards termination of the Danmarkshavn Ridge is marked by increasing depth to the  
43  
44 21 basement north of the ridge. This is also observed in the gravity field as a reduced positive gravity  
45  
46 22 anomaly north of the Danmarkshavn Ridge (Fig. 9). Numerous faults intersect the Cenozoic  
47  
48 23 succession north of the Danmarkshavn Ridge (Fig. 2, Fig. 9, Fault type 5), but show lower lateral  
49  
50 24 extents and less organised orientations, although an easterly dip is prevailing. The less organised  
51  
52 25 nature of the faults in the north of the study area is largely attributed to the presence of salt in this  
53  
54  
55  
56  
57  
58  
59  
60  
61  
62  
63  
64  
65

1  
2 1 area (Figs. 7a-b). Diapirism is frequently observed, with salt diapirs rising close to the sea floor in  
3  
4 2 many occasions. The faulting appear to be thin-skinned with a sole-out in the salt of most of the  
5  
6 3 faults (Fig. 7a). The salt tectonics appear to have initiated during either Palaeozoic or Mesozoic  
7  
8 4 times, which is confirmed by previous studies (Rowan and Lindsø, 2017). It is beyond the scope of  
9  
10 5 the current study to give a detailed interpretation of the salt tectonics, but it would appear as if the  
11  
12 6 Paleogene—earliest Eocene succession does not display any signs of salt-related thickness changes  
13  
14 7 towards the salt diapirs (Fig. 7b, far left). Furthermore, the salt related faulting (Fig. 7a) shows little  
15  
16 8 to no syn-tectonic deposition during this time. This indicates that the salt may have been activated  
17  
18 9 during the post-breakup phase.

## 21 10 **5 DISCUSSION**

22  
23 11 The results of this study of recent seismic data clearly shows a highly dynamic post-breakup tectonic  
24  
25 12 setting with pronounced, kilometre-scale fault offsets, uplift and tilting of the Danmarkshavn Basin  
26  
27 13 and pronounced progradational events. The large-scale structures and pre-breakup  
28  
29 14 tectonostratigraphy have previously been described (Hamann et al., 2005; Petersen et al., 2015;  
30  
31 15 Tsikalas et al., 2005). This study however presents new details on the causes and timing of the post-  
32  
33 16 breakup tectonics. Based on tectonostratigraphic interpretations and integration of data from the  
34  
35 17 ODP 913 borehole, this study constructs a temporally robust model for the tectonosedimentary  
36  
37 18 evolution during the late Palaeogene—Early Neogene period.

### 40 19 **5.1 Seismic facies**

41  
42 20 The plane-parallel, high amplitude seismic facies of the Paleocene—early Eocene succession  
43  
44 21 indicates deposition of well-bedded, laterally cohesive sediments in a quiet setting, such as a marine  
45  
46 22 setting below wave base. However, previous studies find small-scale, prograding clinoforms in the  
47  
48 23 southwest of the study area (Petersen et al., 2016, 2015). This is confirmed in the current study both  
49  
50 24 in map view (Fig. 10), where the clinoforms correlate with depo-centres, and in seismic section (Fig.  
51  
52 25 6). Such clinoforms indicate that initial infill of the Danmarkshavn basin was controlled by a

1  
2 1 channelized system, most likely in a shallow water setting. Such clinoforms are likely to be sand  
3  
4 2 prone, whereas the plane parallel seismic facies present elsewhere is more consistent with a clay  
5  
6 3 prone sedimentary facies.  
7  
8  
9 4 Cenozoic deposits are very scarce onshore East and Northeast Greenland, but Nøhr-Hansen et al.  
10  
11 5 (2011) describes early Paleocene fluvial deposits in the Wollaston Forland and Sabine Ø Area, south-  
12  
13 6 west of the study area (Fig. 2). A sediment fairway from the south-west during the Paleocene is  
14  
15 7 consistent with the prograding clinoforms observed in the seismic data in the southwest part of the  
16  
17 8 study area.  
18  
19  
20 9 The Eocene—mid Miocene succession is comprised of two main seismic facies types. In the  
21  
22 10 Danmarkshavn Basin and Ridge, the facies strongly resemble that of the underlying unit, suggesting  
23  
24 11 a continued deposition in a marine, sub-wave base, clay-rich environment. In the Thetis Basin  
25  
26 12 however, the seismic facies are dominated by the steep, prograding clinoforms (*e.g.* Figs. 5, 7)  
27  
28 13 associated with the uplift and tilting of the Danmarkshavn Basin and the faulting that intersects the  
29  
30 14 Cenozoic deposits across the east margin of the Danmarkshavn Ridge. Evidence of one or several  
31  
32 15 mass wasting events following rapid motion on the fault system east of the Danmarkshavn Ridge is  
33  
34 16 observed (Fig. 5).  
35  
36  
37 17 The prograding clinoforms are indicative of more coarse-grained material, most likely sand prone in  
38  
39 18 the proximal part, and fining in the distal direction, i.e. towards the centre of the Thetis Basin. The  
40  
41 19 topsets of the prograding succession (Fig. 4b) may be composed of either typical delta top deposits  
42  
43 20 such as overbank fines and fluvial deposits, or alternatively a form of sub-marine fine-grained top-  
44  
45 21 set deposit.  
46  
47  
48 22 The focus of the prograding clinoforms during the Eocene—mid Miocene is located in the south part  
49  
50 23 of the Thetis Basin, along the edge of the Danmarkshavn Ridge (Fig. 11). This implies that the south  
51  
52 24 Danmarkshavn Ridge, Danmarkshavn Basin and the area onshore Northeast Greenland south of  
53  
54  
55  
56  
57  
58  
59  
60  
61  
62  
63  
64  
65

1  
2 1 Store Koldewey most likely acted as the source area for this progradational event. The presence of  
3  
4 2 fluvial deposits of an latest Paleocene—earliest Eocene age in the Wollastand Forland and Sabine Ø  
5  
6 3 area (Nøhr-Hansen et al., 2011), highlights the presence of a fluvial system southwest of the study  
7  
8 4 area during the time of deposition of the clinoforms. It seems highly likely that this fluvial system  
9  
10 5 transported the sediment forming the Eocene—mid Miocene clinoforms to the margin.  
11  
12  
13 6 The interpretation of whether the erosional incision of the uplifted footwall of the Danmarkshavn  
14  
15 7 Ridge occurred in a marine or terrigenous environment have obvious implications for the  
16  
17 8 understanding of the depositional evolution of the Northeast Greenland margin. If the erosional  
18  
19 9 incision ~~was were~~ terrigenous, it would imply a very dramatic change in depositional environment,  
20  
21 10 from below (storm) wave base to subaerial exposure due to fault related uplift of the Danmarkshavn  
22  
23 11 Ridge. However, erosional incision and prograding clinoforms may as well occur in a marine setting,  
24  
25 12 and the continuous, uniform nature of the topsets and the overlying strata seems to be more  
26  
27 13 consistent with deposition in a marine environment. This does not however imply that there was no  
28  
29 14 tectonic motion. In fact, the steepness of the incision, in combination with the chaotic nature of the  
30  
31 15 material transported into the Thetis Basin resulting from the mass wasting event, indicates a rapid  
32  
33 16 and significant tectonic movement (Fig. 5).  
34  
35  
36 17 The post-mid Miocene, upper prograding unit, displays very similar facies patterns as the underlying  
37  
38 18 unit. However, as described above, the location of the clinoforms are shifted further north in the  
39  
40 19 Thetis Basin (Fig. 12). The seismic facies of the clinoform-dominated northern part of the unit show a  
41  
42 20 very distinct proximal to distal facies change (Figs. 3a, 7b). The high amplitudes of the topsets  
43  
44 21 indicates a highly heterogenic depositional environment, with interbedded sand and shale. The  
45  
46 22 foresets are most likely dominated by lateral sand-on-sand contacts, as the amplitudes show a  
47  
48 23 marked dimming, resulting from relatively homogenous sediments. The chaotic to moderately well  
49  
50 24 bedded topsets are consistent with basin floor fan deposition dominated by various mass wasting  
51  
52 25 deposition such as slides, slumps and turbidites. The northwards shift of the clinoforms indicates a  
53  
54  
55  
56  
57  
58  
59  
60  
61  
62  
63  
64  
65

1  
2 1 change in the drainage pattern of the Northeast Greenland shelf, and possibly also onshore  
3  
4 2 Northeast Greenland, from mainly focused south of Store Koldewey for the lower prograding unit to  
5  
6 3 north of Store Koldewey for the upper.  
7  
8

## 9 4 **5.2 Structural evolution**

10 5 The seismic data offshore Northeast Greenland clearly demonstrate that tectonics play a prominent  
11  
12 6 role in the sedimentation pattern after the continental breakup. The post-breakup faulting observed  
13  
14  
15 7 mainly around the Danmarkshavn Ridge is extensional in nature, as all faults have some degree of a  
16  
17 8 normal motion on them. However, the total extension of the shelf after the continental breakup is  
18  
19 9 interpreted to be relatively modest due to the steep dips of the fault planes and low amount of  
20  
21 10 heave on the individual faults.  
22  
23

24 11 The two main tectonic events are the tilting and uplift of the strata in the Danmarkshavn Basin, and  
25  
26 12 the 1-2 s TWT throw on the western boundary fault system in the Thetis Basin. Both events clearly  
27  
28 13 post-date the Early Eocene Unconformity, as this horizon is involved in both the structural tilt and  
29  
30 14 intersected by the faulting. The relative timing between these two events indicates that the western  
31  
32 15 boundary fault of the Thetis Basin was reactivated prior to any significant tilting in the  
33  
34 16 Danmarkshavn Ridge or Danmarkshavn Basin area. Tilting might however have initiated west of the  
35  
36 17 Danmarkshavn Basin at an earlier stage.  
37  
38

39 18 The intra-Thetis Basin fault (Fig. 4c) display normal faulting of the entire Cenozoic succession in the  
40  
41 19 southern area of the basin. Although the fault throw is relatively modest, the initiation of the fault is  
42  
43 20 significant, as it controls the location of the footwall erosional escarpment, and seems to be aligned  
44  
45 21 with the northern segment of the Danmarkshavn Ridge. It also indicates that the southern segment  
46  
47 22 of the Danmarkshavn Ridge was not tectonically active after the breakup.  
48  
49

50 23 A significant amount of vertical offset has accumulated between the Thetis Basin and the  
51  
52 24 Danmarkshavn Ridge during the Eocene—Miocene(?) period, amounting to 1-2 s TWT. By assuming  
53  
54

1  
2 1 an average seismic velocity of 2000 m/s (Berger and Jokat, 2008) this equates to 1-2km of vertical  
3  
4 2 offset. As mentioned above, extension appear to be limited during the Cenozoic. Therefore, it seems  
5  
6 3 likely that the vertical offset was created by a steep, listric fault with a sole-out at the base of the  
7  
8 4 crust. This is consistent with the seismic observations in this study and with other geophysical  
9  
10 5 observations (Tsikalas et al., 2005). Some of the post-breakup subsidence may be caused by  
11  
12 6 differential compaction between the Danmarkshavn Ridge and the Thetis Basin. However, the  
13  
14 7 abrupt nature of the subsidence, causing slope failure on the footwall, seems in contrast to relatively  
15  
16 8 slow and continuous compaction-related subsidence.

17  
18  
19 9 In a regional perspective, it is apparent that the extensional faulting observed around the  
20  
21 10 Danmarkshavn Ridge and in the Thetis basin is oriented sub-parallel to the main extensional axis  
22  
23 11 created during continental breakup (Fig. 2), even though some of the faulting post-dates the  
24  
25 12 breakup by >40 Ma. This is clear evidence that the structural grain created during the Mesozoic  
26  
27 13 rifting (Tsikalas et al., 2012) was reactivated during the post-breakup extensional tectonics.

28  
29  
30 14 The timing of the salt movement can in the context of the current study yield important information  
31  
32 15 about tectonic events. Remobilised salt is observed throughout the northern part of the study area  
33  
34 16 (Fig. 2), and is associated with a complex fault pattern (Fig. 9). Salt diapirs frequently rise to or close  
35  
36 17 to the sea floor, indicating that salt mobilisation has been occurring close to present time, although  
37  
38 18 presumed Quaternary erosion truncates the crests of the diapirs, hampering a more accurate  
39  
40 19 constraint on the timing (Figs. 7a, b). Since there is no evidence of Paleocene—Eocene rim synclines,  
41  
42 20 no pre-breakup salt mobilisation is interpreted. Since the salt was not activated during the  
43  
44 21 continental breakup, it seems likely that most of the tectonic deformation during the breakup (at *ca.*  
45  
46 22 55 Ma) was focused along the margin of the shelf, away from the Danmarkshavn Basin. The lack of  
47  
48 23 pre-breakup tectonism on the shelf, apart from the thermally induced uplift in the earliest Eocene,  
49  
50 24 further confirms this observation. It then seems more likely that the salt mobilisation is linked to the  
51  
52  
53  
54  
55  
56  
57  
58  
59  
60  
61  
62  
63  
64  
65



1  
2 1 same post-breakup tectonics seen in the data as movement of the Thetis Basin boundary fault and  
3  
4 2 tilting of the Danmarkshavn Basin.  
5  
6

### 7 3 **5.3 Uplift and erosion**

8  
9 4 The Northeast Greenland shelf displays a series of uplift events from the Late Cretaceous through  
10  
11 5 the Neogene (Hamann et al., 2005; Petersen et al., 2016, 2015). The unconformity below the  
12  
13 6 Cenozoic succession is a surface of regional significance, also observed onshore Northeast Greenland  
14  
15 7 (Nøhr-Hansen et al., 2011). In the current study, the unconformity is mostly observed in the  
16  
17 8 Danmarkshavn Basin and on the Danmarkshavn Ridge, and is particularly well developed in the  
18  
19 9 south of the study area. This trend is seen in subsequent uplift events as well, where uplift events  
20  
21 10 are most pronounced towards the south. The uplift and related intrusions of hot magma, peaking  
22  
23 11 around *ca.* 55 Ma (Larsen et al., 2014) reported previously (Petersen et al., 2015; Reynolds et al.,  
24  
25 12 2017), also display a deepening incision in the south part of the Danmarkshavn Basin, associated  
26  
27 13 with progradation of clinofolds into the Danmarkshavn Basin (Petersen et al., 2016, 2015). Some  
28  
29 14 minor basin inversion is also observed at the earliest Eocene times (Fig. 5), although this is in  
30  
31 15 contrast to the generally extensional tectonic regime of the shelf during the Cenozoic. However,  
32  
33 16 compression may be caused by counter-clockwise rotation of Greenland during the Palaeocene,  
34  
35 17 which may have caused minor NE-SW compressional stresses to be transmitted onto the Northeast  
36  
37 18 Greenland shelf (Guarnieri, 2015). However, this mechanism seems unable to account for neither  
38  
39 19 the geometry nor the amount of uplift observed on the Northeast Greenland shelf.  
40  
41

42 20 The gradual uplift and associated denudation of the Cenozoic deposits of the Danmarkshavn Basin  
43  
44 21 and Ridge area most likely post-dates the intra Miocene unconformity. The exhumation of the inner  
45  
46 22 part of the shelf and its association with steep, prograding clinofolds with downlaps onto the Intra  
47  
48 23 Miocene Unconformity (Fig. 3a), points to a post-mid Miocene age for the cessation of the uplift of  
49  
50 24 the inner Northeast Greenland shelf. The vertical motions seems to stop or slow significantly around  
51  
52 25 the time of the Top upper prograding unit seismic horizon (Fig. 7b). The end of the main denudation  
53  
54  
55  
56  
57  
58  
59  
60  
61  
62  
63  
64  
65

1  
2 1 phase is therefore poorly constrained, since the age of the Top upper prograding unit can only be  
3  
4 2 attributed to a post-mid Miocene age. It is suggested in this study, that the main cause of uplift and  
5  
6 3 tectonics following the continental breakup is caused by thermal uplift and dynamic topographic  
7  
8 4 effects associated with the Icelandic mantle plume. (Fig. 13)  
9  
10  
11 5 A central feature of the post-breakup denudation of the inner Northeast Greenland shelf is the time  
12  
13 6 transgressive nature of the uplift, as indicated by the prograding units and their migration  
14  
15 7 northwards over time. This is evident when comparing the thickness maps of the two uppermost  
16  
17 8 late Paleogene—Neogene units (Figs. 11 and 12), but in fact, the north to south migration of  
18  
19 9 clinoforms seems to start potentially as early as the Palaeocene (Petersen et al., 2015). This  
20  
21 10 northwards move of the main depocentre indicates that the uplift and exhumation of the Northeast  
22  
23 11 Greenland shelf must have been focused east, southeast or south of the current study area. This  
24  
25 12 initially created a structural tilt of the Danmarkshavn Basin towards the west, but with a minor  
26  
27 13 northwards component as well. The earliest observations of clinoforms in the south is dated as  
28  
29 14 Paleocene, and the youngest clinoforms are post mid-Miocene, a period of about 45 Ma. This implies  
30  
31 15 a slow northwards tilting of the Northeast Greenland shelf. Alternatively, it is possible that the  
32  
33 16 northwards tilting occurred much faster, but that the sedimentation occurred in pulses related to  
34  
35 17 hinterland uplift.

#### 38 18 **5.4 Effect of mantle plume path on deposition**

39  
40 19 The Icelandic hotspot and its effect in the North Atlantic realm, in particular in relation to the  
41  
42 20 continental breakup, has been the source of much debate (Campbell, 2007; Clift et al., 1998; Storey  
43  
44 21 et al., 2007). In the current study, it is suggested that the mantle plume system at present day  
45  
46 22 located beneath Iceland and Jan Mayen (Rickers et al., 2013), was instrumental in the uplift of the  
47  
48 23 inner Northeast Greenland shelf, and that it was responsible for a gradual, northwards shift of the  
49  
50 24 main sediment fairway. The central argument for this interpretation is that the Icelandic plume  
51  
52 25 system moved along a trajectory south of the study area during the Cenozoic, which is in good  
53  
54  
55  
56  
57  
58  
59  
60  
61  
62  
63  
64  
65

1  
2 1 agreement with the time-transgressive northward movement of the prograding units observed in  
3  
4 2 this study.  
5  
6  
7 3 The plume activity, its trajectory and its morphology are all influencing the depositional patterns  
8  
9 4 observed during the Cenozoic on the Northeast Greenland shelf. The plume underneath the North  
10  
11 5 Atlantic show a significant lateral extent, with an origin observed down to the lower mantle (Rickers  
12  
13 6 et al., 2013). Døssing et al (2016) concludes that the thermal perturbation at 2-15 Ma ( mid Miocene-  
14  
15 7 -Pliocene) is linked to the IMU (Intra Miocene Unconformity) observed around the East Greenland  
16  
17 8 Ridge, indicating a clear link between the thermal perturbations of the passing hotspot and tectonism  
18  
19 9 in the region.  
20  
21

22 10 The coupling between the Atlantic mantle plume system and the North Atlantic Igneous Province is  
23  
24 11 well established (e.g. Ganerød et al., 2010; Hansen et al., 2009; Larsen et al., 2014; Storey et al.,  
25  
26 12 2007). Onshore Northeast Greenland, the accurately dated igneous rocks show a distinct trend of  
27  
28 13 younger igneous rocks towards the north (Larsen et al., 2014). The youngest igneous rocks (40-20  
29  
30 14 Ma) observed according to Larsen et al.(2014) are all found north of 67° N (Fig. 13), further  
31  
32 15 indicating a south to north time transgressive impact of the passing Icelandic mantle plume system.  
33  
34 16 The location of the Icelandic and Jan Mayen hotspots directly south of the study area during mid  
35  
36 17 Miocene times (Fig. 13), is in very good agreement with uplift in the south and tilting of the margin  
37  
38 18 towards the north during the mid Miocene—Quaternary.  
39  
40

## 41 19 **6 CONCLUSIONS**

42  
43 20 This study utilizes a vast database of the most recent seismic data and presents a series of novel  
44  
45 21 observations on the tectonosedimentary development of the Northeast Greenland shelf following  
46  
47 22 the continental breakup. A summary of the tectonic and sedimentary events described in the current  
48  
49 23 study is presented in Fig. 15.  
50  
51  
52  
53  
54  
55  
56  
57  
58  
59  
60  
61  
62  
63  
64  
65

1  
2 1 It is demonstrated that significant vertical motion and associated extensional faulting are observed  
3  
4 2 after the continental breakup at *ca.* 55 Ma. Differential subsidence, some of which may be  
5  
6 3 attributed to deep-rooted faults, in the order of 1-2 ~~km~~ is observed along the west boundary of the  
7  
8 4 Thetis Basin, during the Eocene to post-Miocene times. The faulting occurred simultaneously with a  
9  
10 5 pronounced uplift and eastward tilt of the inner Northeast Greenland shelf.

11  
12  
13 6 Several progradational events are interpreted based on the seismic data. The earliest clinofolds are  
14  
15 7 of a pre-breakup age, and located in the south Danmarkshavn Basin. The clinofolds are however  
16  
17 8 more pronounced after the earliest Eocene breakup, where steep, rapidly prograding clinofolds  
18  
19 9 overstep the Danmarkshavn Ridge and prograde into the Thetis Basin. These clinofolds display a  
20  
21 10 northward migration over time, with a significant clinofold succession formed in the north of the  
22  
23 11 Thetis Basin sometime after the mid Miocene.

24  
25  
26 12 The Icelandic hot spot is suggested as the main cause of uplift, rotation and extensional faulting of  
27  
28 13 the shelf. The trajectory of the Icelandic hot spot south of the Northeast Greenland shelf during the  
29  
30 14 Neogene fits very well with a gradual, northwards shift of progradation due to thermally induced  
31  
32 15 uplift and dynamic topography, ~~which~~ This is observed in the seismic data as northwards tilting of  
33  
34 16 the shelf during post-breakup times. Lastly, the reactivation of the fault system separating the  
35  
36 17 Danmarkshavn Ridge and the Thetis Basin is also attributed to the thermal uplift caused by the  
37  
38 18 passage of the Icelandic hotspot.

#### 41 19 **Acknowledgements**

42  
43  
44 20 The author wishes to thank TGS and Spectrum for supplying the seismic database for this study, and  
45  
46 21 for allowing the publication of the data with very limited constraints. The author also wishes to  
47  
48 22 thank Schlumberger for providing the workstation software Petrel. For obvious reasons this study  
49  
50 23 could not have taken place without their support. This paper benefitted greatly from anonymous  
51  
52 24 reviews.

1  
2 1  
3  
4  
5  
6  
7  
8  
9  
10  
11  
12  
13  
14  
15  
16  
17  
18  
19  
20  
21  
22  
23  
24  
25  
26  
27  
28  
29  
30  
31  
32  
33  
34  
35  
36  
37  
38  
39  
40  
41  
42  
43  
44  
45  
46  
47  
48  
49  
50  
51  
52  
53  
54  
55  
56  
57  
58  
59  
60  
61  
62  
63  
64  
65

1  
2  
3  
4  
5  
6  
7  
8  
9  
10  
11  
12  
13  
14  
15  
16  
17  
18  
19  
20  
21  
22  
23  
24  
25  
26  
27  
28  
29  
30  
31  
32  
33  
34  
35  
36  
37  
38  
39  
40  
41  
42  
43  
44  
45  
46  
47  
48  
49  
50  
51  
52  
53  
54  
55  
56  
57  
58  
59  
60  
61  
62  
63  
64  
65

1 **Captions**

2 Fig. 1. Overview of the study area and the seismic database. The data are composed of two vintages.  
3 The AWI seismic data, collected during the nineties, and the TGS data collected 2008-2014. The TGS  
4 data are of both better quality and much higher density, as shown on the map. The AWI data covers  
5 the important transition from continental to oceanic crust however. All data are courtesy of TGS and  
6 Spectrum. Approximate locations of the seismic cross sections are also highlighted.

7 Fig. 2. Map of the main structural elements, traces of the interpreted faults, free air gravity  
8 anomalies, as well as magnetic isochrons. The map shows the NNE-SSW elongated Danmarkshavn  
9 Basin (DKHB), the Danmarkshavn Ridge (DKHR), right-lateral transfer zone (TS) and the Thetis Basin  
10 located on the easternmost side of the shelf. The East Greenland ~~Ridge~~Ridge (EGR), Store Koldewey  
11 (SKW) and Wollaston Forland (WSF) are also shown. Gravity data are courtesy of DTU Space  
12 DNSC08GRA and DTU10 data sets (Andersen 2010 and Andersen et al 2010).

13 Fig. 3. (a) Regional west to east oriented seismic profile through the northern part of the study area.  
14 The section shows a thick Palaeozoic and Mesozoic succession that overlies the northernmost extent  
15 of the Danmarkshavn Ridge basement high. The section shows a distinct step down of the Base  
16 Paleogene horizon from the Danmarkshavn Ridge and into the Thetis basin caused by ductile  
17 accommodation of normal reactivation of faults at the Danmarkshavn Ridge to Thetis Basin  
18 transition. To the west, in the Danmarkshavn Basin, the Cenozoic succession shows evidence of  
19 tilting and erosional incision, associated with pronounced progradation in the Thetis Basin, above  
20 the Intra Middle Miocene reflection. (b) Regional west to east oriented seismic profile through the  
21 southern part of the study area. The Cenozoic succession displays a significant uplift and tilt to the  
22 east across the Danmarkshavn Basin and Danmarkshavn Ridge. Faulting is present in the  
23 Danmarkshavn Basin, where it offsets the Cenozoic ~~succession~~succession (IDBF: Intra  
24 Danmarkshavn Basin Fault). Faulting is also present between the Danmarkshavn Ridge and Thetis  
25 Basin, as well as in the Thetis Basin, with the faults downfaulting the Cenozoic succession towards

1  
2 1 the East along the Intra Thetis Basin Fault (ITBF). Evidence of a steep erosional scar infilled with  
3  
4 2 prograding clinoforms is present across the Danmarkshavn Ridge. Seismic data are courtesy of TGS  
5  
6 3 and Spectrum.  
7  
8  
9 4 Fig. 4. Seismic examples of the Danmarkshavn Ridge to Thetis Basin transition at the southern  
10  
11 5 segment of the Danmarkshavn Ridge. (a) The Palaeocene to Miocene(?) seismic facies across the  
12  
13 6 Danmarkshavn Ridge is dominated by parallel, high amplitude reflections unconformably overlying  
14  
15 7 the Danmarkshavn Ridge. A concave erosional truncation of the Palaeocene to Miocene(?) marks the  
16  
17 8 transition from the Danmarkshavn Ridge to the Thetis Basin, where two east dipping normal faults  
18  
19 9 off sets the Paleogene succession by >1 s TWT down into the Thetis Basin. Steep, prograding  
20  
21 10 clinoforms fills out the accommodation space created by the erosional incision and extends out into  
22  
23 11 the Thetis Basin. (b) Seismic section further south compared to (a). The two faults still mark the  
24  
25 12 transition from the Danmarkshavn Ridge to the Thetis Basin. The prograding clinoforms persist,  
26  
27 13 reaching far out into the Thetis Basin. Small-scale faults intersect the succession between the Early  
28  
29 14 Eocene Unconformity and the Top upper prograding unit. (c) Seismic example from the  
30  
31 15 southernmost Danmarkshavn Ridge. Note the increase in distance between the Danmarkshavn Ridge  
32  
33 16 and the Intra Thetis Basin Fault (ITBF). The erosional incision is located east of the Danmarkshavn  
34  
35 17 Ridge, indicating that the ITBF triggered the incision. Note the pronounced angular unconformity  
36  
37 18 below the Early Eocene Unconformity to the far west. Seismic data are courtesy of TGS and  
38  
39 19 Spectrum.  
40  
41

42 20 Fig. 5. Seismic section through the central study area covering the Danmarkshavn Basin, the  
43  
44 21 Danmarkshavn Ridge and the Thetis Basin. The seismic section clearly show domal uplift and  
45  
46 22 truncation below the Early Eocene Unconformity in the Danmarkshavn Basin, with some indications  
47  
48 23 of minor compression and inversion are observed along the west margin of the Danmarkshavn  
49  
50 24 Ridge. To the far NW of the profile, disturbances in the reflections below the Early Eocene  
51  
52 25 Unconformity indicates gas venting and a pockmark associated with volcanic activity. The bounding  
53  
54  
55  
56  
57  
58  
59  
60  
61  
62  
63  
64  
65

1  
2 1 fault between the Danmarkshavn Ridge and the Thetis Basin offsets the entire succession above the  
3  
4 2 Base Paleogene, but the Erosional incision seismic horizon and prograding clinoforms are confined to  
5  
6 3 the Thetis Basin. Chaotic seismic facies indicate mass deposited sediments below the Erosional  
7  
8 4 incision reflection. Seismic data are courtesy of TGS and Spectrum.

9  
10  
11 5 Fig. 6. Seismic profile across the largest fault in the Danmarkshavn Basin, the Intra Danmarkshavn  
12  
13 6 Basin Fault (IDBF). There is a distinct offset of the Palaeogene succession along the fault, and several  
14  
15 7 minor associated faults are present. Also, notice the prograding clinoforms west of the fault. Seismic  
16  
17 8 data are courtesy of TGS and Spectrum.

18  
19  
20 9 Fig. 7. (a) Seismic example north of the Danmarkshavn Ridge. The structural style here is heavily  
21  
22 10 affected by the salt, which forms a detachment plane at the base of the faults. Salt diapirism is also  
23  
24 11 observed. (b) Seismic section showing the structural complexity of the Danmarkshavn Ridge in the  
25  
26 12 central part of the study area. Several eastwards dipping, listric faults comprise the Danmarkshavn  
27  
28 13 Ridge to Thetis Basin transition. At the westernmost edge of the profile, a salt diapier rises close to  
29  
30 14 the seafloor. Note how the main progradational event is now above the Intra Miocene  
31  
32 15 Unconformity. For comparison, see fig. 4. Seismic data are courtesy of TGS and Spectrum.

33  
34  
35 16 Fig. 8. (a) Structure map of the Base Palaeogene horizon in TWT with fault traces of the main faults  
36  
37 17 that outline the Danmarkshavn Ridge overlain. The map clearly shows the steep transition from the  
38  
39 18 relatively elevated Danmarkshavn Basin/Ridge area and lower lying Thetis Basin. Also, note the  
40  
41 19 coincidence between the faulting and the steep transition zone. (b) Structure map of the Upper  
42  
43 20 prograding unit horizon in TWT with fault traces of the main faults that outline the Danmarkshavn  
44  
45 21 Ridge trace overlain. The steep slope along the northern Danmarkshavn Ridge is due to steep,  
46  
47 22 prograding clinoforms rather than structural deformation. Note the eastwards movement of the  
48  
49 23 western limit of the unit.

50  
51  
52  
53  
54  
55  
56  
57  
58  
59  
60  
61  
62  
63  
64  
65



1  
2 1 Fig. 9. Overview and classification of the faults interpreted in this study overlain the free air gravity  
3  
4 2 data. Faults are subdivided into five categories: Main, ridge-delineating faults (type 1, black), Intra-  
5  
6 3 Danmarkshavn Basin faults (type 2, green), pre-Cenozoic faults that are not reactivated (type 3,  
7  
8 4 grey), Intra-Thetis Basin faults (type 4, blue), and salt related faults (type 5, magenta). The white  
9  
10 5 fault is a hybrid between the ridge delineating fault and the salt related fault types. The ridge  
11  
12 6 delineating faults are all located on the margins of the NE-SW oriented positive gravity anomaly  
13  
14 7 associated with the Danmarkshavn Ridge. A right-lateral transfer zone between the north and south  
15  
16 8 segments of the Danmarkshavn Ridge is highlighted. Note that all the salt related faults are located  
17  
18 9 in the northern part of the study area, where the gravity anomaly is relatively low. The westwards  
19  
20 10 erosional truncation of the Cenozoic deposits is also highlighted (grey line).

23 11 Fig. 10. Thickness map (in TWT) of the succession between the Early Eocene and the Base Paleogene,  
24  
25 12 corresponding to the Palaeocene—lower ~~most~~ Eocene. The main depo-center is located in the  
26  
27 13 southernmost part of the Thetis Basin, and thins substantially on the Danmarkshavn Ridge. A  
28  
29 14 potential northerly depo-center is also tentatively interpreted from the data. The Location of the  
30  
31 15 Danmarkshavn Ridge and the right-lateral transfer zone are shown for reference together with the  
32  
33 16 main, basin delineating faults.

36 17 Fig. 11. Thickness map (in TWT) of the succession between the Early Eocene and the Intra middle  
37  
38 18 Miocene horizons, corresponding to the Eocene—lower Miocene interval dominated by early  
39  
40 19 prograding clinoforms. The main depo-center is prominently located immediately west of the  
41  
42 20 southern segment of the Danmarkshavn Ridge. The Location of the Danmarkshavn Ridge and the  
43  
44 21 right-lateral transfer zone are shown for reference together with the main, basin delineating faults.

47 22 Fig. 12. Thickness map (in TWT) of the succession between the Intra middle Miocene and Upper  
48  
49 23 prograding unit horizons, dominated by the late prograding event. The upper age of this interval is  
50  
51 24 poorly constrained to a post-Miocene age. The depo-centre is located NE of the Danmarkshavn  
52  
53 25 Ridge. Compared to fig. 11, it is evident that the depo-center shifts further north and further into the

1  
2 1 Thetis Basin. The Location of the Danmarkshavn Ridge and the right-lateral transfer zone are shown  
3  
4 2 for reference together with the main, basin delineating faults.  
5

6  
7 3 Fig. 13. Overview map showing the path and estimated extent of the Jan Mayen-Iceland hotspot  
8  
9 4 system after Rickers et al. 2013, shown together with free air gravity anomalies. Ages of the  
10  
11 5 observed, onshore volcanics (Larsen et al. 2014) show a trend of younger magmatic rocks towards  
12  
13 6 the north (italics, stars and horizontal lines). A relatively good correlation between the passage of  
14  
15 7 the hot spots and the ages of the intrusions are seen, with the Jan Mayen plume branch a likely  
16  
17 8 candidate for the northern (and younger intrusions). The observed northwards shift in prograding  
18  
19 9 clinofolds, southwards deepening erosion during the latest Eocene and the area with seismic  
20  
21 10 observations of volcanics are shown as reference.  
22

23  
24 11 Fig. 14. Summary of tectonostratigraphic events during the early-mid Cenozoic period of the  
25  
26 12 Northeast Greenland shelf. Red arrows show uplift, blue arrows show normal faulting/subsidence.  
27  
28 13 Note how the clinofolds shift northwards during Eocene—Miocene period. The Thetis Basin is  
29  
30 14 dominated by varying degrees of subsidence (blue minus), but the Danmarkshavn Ridge and  
31  
32 15 Danmarkshavn Basin show a more complicated history of uplift (red plus) and erosion (grey  
33  
34 16 hatched).  
35

36  
37 17  
38  
39

## 40 18 **References**

41  
42  
43 19 ~~Andersen, O.B., 2010. The DTU10 Gravity field and Mean sea surface, in: Second International~~  
44  
45 20 ~~Symposium of the Gravity Field of the Earth (IGFS2). Fairbanks, Alaska.~~

46  
47  
48 21 ~~Andersen, O.B., Knudsen, P., Berry, P.A.M., 2010. The DNSC08GRA global marine gravity field from~~  
49  
50 22 ~~double retracked satellite altimetry. J. Geod. 84, 191–199. [https://doi.org/10.1007/s00190-](https://doi.org/10.1007/s00190-009-0355-9)~~  
51  
52 23 ~~009-0355-9~~  
53

1  
2  
3  
4  
5  
6  
7  
8  
9  
10  
11  
12  
13  
14  
15  
16  
17  
18  
19  
20  
21  
22  
23  
24  
25  
26  
27  
28  
29  
30  
31  
32  
33  
34  
35  
36  
37  
38  
39  
40  
41  
42  
43  
44  
45  
46  
47  
48  
49  
50  
51  
52  
53  
54  
55  
56  
57  
58  
59  
60  
61  
62  
63  
64  
65

1 Berger, D., Jokat, W., 2009. Sediment deposition in the northern basins of the North Atlantic and  
2 characteristic variations in shelf sedimentation along the East Greenland margin. *Mar. Pet.*  
3 *Geol.* 26, 1321–1337. <https://doi.org/10.1016/j.marpetgeo.2009.04.005>  
4  
5 Berger, D., Jokat, W., 2008. A seismic study along the East Greenland margin from 72°N to 77°N.  
6 *Geophys. J. Int.* 174, 733–748. <https://doi.org/10.1111/j.1365-246X.2008.03794.x>  
7  
8 Campbell, I.H., 2007. Testing the plume theory. *Chem. Geol.* 241, 153–176.  
9 <https://doi.org/10.1016/j.chemgeo.2007.01.024>  
10  
11 Clift, P.D., Carter, A., Hurford, A.J., P.D. Clift, A.C. and A.J.H., 1998. The erosional and uplift history of  
12 NE Atlantic passive margins: constraints on a passing plume. *J. Geol. Soc. London.* 155, 788–  
13 800. <https://doi.org/10.1144/gsjgs.155.5.0787>  
14  
15 Cloetingh, S., Burov, E., Matenco, L., Beekman, F., Roure, F., Ziegler, P.A., 2013. The Moho in  
16 extensional tectonic settings: Insights from thermo-mechanical models. *Tectonophysics* 609,  
17 558–604. <https://doi.org/10.1016/j.tecto.2013.06.010>  
18  
19 Cloetingh, S.A.P.L., Ziegler, P.A., Bogaard, P.J.F., Andriessen, P.A.M., Artemieva, I.M., Bada, G., van  
20 Balen, R.T., Beekman, F., Ben-Avraham, Z., Brun, J.P., Bunge, H.P., Burov, E.B., Carbonell, R.,  
21 Facenna, C., Friedrich, A., Gallart, J., Green, A.G., Heidbach, O., Jones, A.G., Matenco, L., Mosar,  
22 J., Oncken, O., Pascal, C., Peters, G., Sliapua, S., Soesoo, A., Spakman, W., Stephenson, R.A.,  
23 Thybo, H., Torsvik, T., de Vicente, G., Wenzel, F., Wortel, M.J.R., 2007. TOPO-EUROPE: The  
24 geoscience of coupled deep Earth-surface processes. *Glob. Planet. Change* 58, 1–118.  
25 <https://doi.org/10.1016/j.gloplacha.2007.02.008>  
26  
27 Døssing, A., Japsen, P., Watts, A.B., Nielsen, T., Jokat, W., Thybo, H., Dahl-Jensen, T., 2016. Miocene  
28 uplift of the NE Greenland margin linked to plate tectonics: Seismic evidence from the  
29 Greenland Fracture Zone, NE Atlantic. *Tectonics* 35, 257–282.

- 1  
2 1 <https://doi.org/10.1002/2015TC004079>  
3  
4  
5 2 Emery, D., Myers, K., Bertram, G.T., 1996. Sequence stratigraphy. Blackwell Science.  
6  
7  
8 3 Engen, Ø., Faleide, J.I., Dyreng, T.K., 2008. Opening of the Fram Strait gateway: A review of plate  
9  
10 4 tectonic constraints. *Tectonophysics* 450, 51–69. <https://doi.org/10.1016/j.tecto.2008.01.002>  
11  
12  
13 5 Funck, T., Erlendsson, Ö., Geissler, W.H., Gradmann, S., Kimbell, G.S., McDermott, K., Petersen, U.K.,  
14  
15 6 2017. A review of the NE Atlantic conjugate margins based on seismic refraction data. *Geol.*  
16  
17 7 *Soc. London, Spec. Publ.* 447, 171–205. <https://doi.org/10.1144/SP447.9>  
18  
19  
20 8 Gaina, C., Gernigon, L., Ball, P., 2009. Palaeocene–Recent plate boundaries in the NE Atlantic and the  
21  
22 9 formation of the Jan Mayen microcontinent. *J. Geol. Soc. London.* 166, 601–616.  
23  
24 10 <https://doi.org/10.1144/0016-76492008-112>  
25  
26  
27 11 Ganerød, M., Smethurst, M.A., Torsvik, T.H., Prestvik, T., Rouse, S., McKenna, C., van Hinsbergen,  
28  
29 12 D.J.J., Hendriks, B.W.H., 2010. The North Atlantic Igneous Province reconstructed and its  
30  
31 13 relation to the Plume Generation Zone: The Antrim Lava Group revisited. *Geophys. J. Int.* 182,  
32  
33 14 183–202. <https://doi.org/10.1111/j.1365-246X.2010.04620.x>  
34  
35  
36 15 Guarnieri, P., 2015. Pre-break-up palaeostress state along the East Greenland margin. *J. Geol. Soc.*  
37  
38 16 *London.* 172, 727–739. <https://doi.org/10.1144/jgs2015-053>  
39  
40  
41 17 Håkansson, E., Stemmerik, L., 1989. Wandel Sea Basin—a new synthesis of the Late Paleozoic to  
42  
43 18 Tertiary accumulation in North Greenland. *Geology* 17, 683–686.  
44  
45 19 [https://doi.org/10.1130/0091-7613\(1989\)017<0683:WSBANS>2.3.CO;2](https://doi.org/10.1130/0091-7613(1989)017<0683:WSBANS>2.3.CO;2)  
46  
47  
48 20 Hamann, N.E., Whittaker, R.C., Stemmerik, L., 2005. Geological development of the Northeast  
49  
50 21 Greenland Shelf, in: *Petroleum Geology: North-West Europe and Global Perspectives—*  
51  
52 22 *Proceedings of the 6th Petroleum Geology Conference.* pp. 887–902.  
53  
54  
55  
56  
57  
58  
59  
60  
61  
62  
63  
64  
65

1  
2  
3  
4  
5  
6  
7  
8  
9  
10  
11  
12  
13  
14  
15  
16  
17  
18  
19  
20  
21  
22  
23  
24  
25  
26  
27  
28  
29  
30  
31  
32  
33  
34  
35  
36  
37  
38  
39  
40  
41  
42  
43  
44  
45  
46  
47  
48  
49  
50  
51  
52  
53  
54  
55  
56  
57  
58  
59  
60  
61  
62  
63  
64  
65

1 <https://doi.org/10.1144/0060887>

2 Hansen, J., Jerram, D.A., McCaffrey, K., Passey, S.R., 2009. The onset of the North Atlantic Igneous  
3 Province in a rifting perspective. *Geol. Mag.* 146, 309–325.  
4 <https://doi.org/10.1017/S0016756809006347>

5 Larsen, L.M., Pedersen, A.K., Tegner, C., Duncan, R.A., 2014. Eocene to Miocene igneous activity in  
6 NE Greenland: northward younging of magmatism along the East Greenland margin. *J. Geol.  
7 Soc. London.* 171, 539–553. <https://doi.org/10.1144/jgs2013-118>

8 Lundin, E., Doré, A.G., 2002. Mid-Cenozoic post-breakup deformation in the 'passive' margins  
9 bordering the Norwegian-Greenland Sea 19, 79–93.

10 Matthews, K.J., Maloney, K.T., Zahirovic, S., Williams, S.E., Seton, M., Müller, R.D., 2016. Global plate  
11 boundary evolution and kinematics since the late Paleozoic. *Glob. Planet. Change* 146, 226–  
12 250. <https://doi.org/10.1016/j.gloplacha.2016.10.002>

13 McKenzie, D., 1978. Some remarks on the development of sedimentary basins. *Earth Planet. Sci.  
14 Lett.* 40, 25–32. [https://doi.org/10.1016/0012-821X\(78\)90071-7](https://doi.org/10.1016/0012-821X(78)90071-7)

15 Miller, K.G., Kominz, M.A., Browning, J.V., Wright, J.D., Mountain, G.S., Katz, M.E., Sugarman, P.J.,  
16 Cramer, B.S., Christie-Blick, N., Pekar, S.F., 2005. The phanerozoic record of global sea-level  
17 change. *Science (80-)*. 310, 1293–1298. <https://doi.org/10.1126/science.1116412>

18 Müller, R.D., Seton, M., Zahirovic, S., Williams, S.E., Matthews, K.J., Wright, N.M., Shephard, G.E.,  
19 Maloney, K.T., Barnett Moore, N., Hosseinpour, M., Bower, D.J., Cannon, J., 2016. Ocean Basin  
20 Evolution and Global Scale Plate Reorganization Events Since Pangea Breakup. *Annu. Rev. Earth  
21 Planet. Sci.* 44, 107–138. <https://doi.org/10.1146/annurev-earth-060115-012211>

22 Nøhr-Hansen, H., Nielsen, L.H., Sheldon, E., Hovikoski, J., Alsen, P., 2011. Palaeogene deposits in

1  
2 1 North-East Greenland. Geol. Surv. Denmark Greenl. Bull. 23, 61–64.  
3  
4  
5 2 Ogg, J.G., 2012. Geomagnetic Polarity Time Scale, The Geologic Time Scale 2012. Elsevier.  
6  
7 3 <https://doi.org/10.1016/B978-0-444-59425-9.00005-6>  
8  
9  
10 4 Olesen, O., Ebbing, J., Lundin, E., Møring, E., Skilbrei, J.R., Torsvik, T.H., Hansen, E.K., Henningsen,  
11 T., Midbøe, P., Sand, M., 2007. An improved tectonic model for the Eocene opening of the  
12 5 Norwegian-Greenland Sea: Use of modern magnetic data. Mar. Pet. Geol. 24, 53–66.  
13 6  
14 7 <https://doi.org/10.1016/j.marpetgeo.2006.10.008>  
15  
16 8 Petersen, T.G., Hamann, N.E., Stemmerik, L., 2016. Correlation of the Palaeogene successions on the  
17 9 North-East Greenland and Barents Sea margins. Bull. Geol. Soc. Denmark 64, 77–96.  
18  
19 10 Petersen, T.G., Hamann, N.E., Stemmerik, L., 2015. Tectono-sedimentary evolution of the Paleogene  
20 11 succession offshore Northeast Greenland. Mar. Pet. Geol. 67, 481–497.  
21 12 <https://doi.org/10.1016/j.marpetgeo.2015.05.033>  
22  
23  
24 13 Reynolds, P., Planke, S., Millett, J.M., Jerram, D.A., Trulsvik, M., Schofield, N., Myklebust, R., 2017.  
25 14 Hydrothermal vent complexes offshore Northeast Greenland: A potential role in driving the  
26 15 PETM. Earth Planet. Sci. Lett. 467, 72–78. <https://doi.org/10.1016/j.epsl.2017.03.031>  
27  
28 16 Rickers, F., Fichtner, A., Trampert, J., 2013. The Iceland-Jan Mayen plume system and its impact on  
29 17 mantle dynamics in the North Atlantic region: Evidence from full-waveform inversion. Earth  
30 18 Planet. Sci. Lett. 367, 39–51. <https://doi.org/10.1016/j.epsl.2013.02.022>  
31  
32  
33 19 Rowan, M.G., Lindsø, S., 2017. Salt Tectonics of the Norwegian Barents Sea and Northeast Greenland  
34 20 Shelf, Permo-Triassic Salt Provinces of Europe, North Africa and the Atlantic Margins: Tectonics  
35 21 and Hydrocarbon Potential. Elsevier Inc. <https://doi.org/10.1016/B978-0-12-809417-4.00013-6>  
36  
37  
38 22 Stemmerik, L., 2000. Late Palaeozoic evolution of the North Atlantic margin of Pangea. Palaeogeogr.  
39  
40  
41  
42  
43  
44  
45  
46  
47  
48  
49  
50  
51  
52  
53  
54  
55  
56  
57  
58  
59  
60  
61  
62  
63  
64  
65

1  
2 1 Palaeoclimatol. Palaeoecol. 161, 95–126. [https://doi.org/10.1016/S0031-0182\(00\)00119-X](https://doi.org/10.1016/S0031-0182(00)00119-X)  
3  
4  
5 2 Storey, M., Duncan, R.A., Tegner, C., 2007. Timing and duration of volcanism in the North Atlantic  
6  
7 3 Igneous Province: Implications for geodynamics and links to the Iceland hotspot. Chem. Geol.  
8  
9 4 241, 264–281. <https://doi.org/10.1016/j.chemgeo.2007.01.016>  
10  
11  
12 5 Talwani, M., Eldholm, O., 1977. Evolution of the Norwegian–Greenland Sea. Bull. Geol. Soc. Am. 88,  
13  
14 6 969–999. [https://doi.org/10.1130/0016-7606\(1977\)88<969:EOTNS>2.0.CO;2](https://doi.org/10.1130/0016-7606(1977)88<969:EOTNS>2.0.CO;2)  
15  
16  
17 7 Tegner, C., Storey, M., Holm, P.M., Thorarinsson, S.B., Zhao, X., Lo, C.H., Knudsen, M.F., 2011.  
18  
19 8 Magmatism and Eureka deformation in the High Arctic Large Igneous Province: 40Ar–39Ar age  
20  
21 9 of Kap Washington Group volcanics, North Greenland. Earth Planet. Sci. Lett. 303, 203–214.  
22  
23 10 <https://doi.org/10.1016/j.epsl.2010.12.047>  
24  
25  
26 11 Thiede, J., Myhre, A.M., Firth, J.V. and the S.S.P., 1995. Cenozoic northern hemisphere polar and  
27  
28 12 subpolar ocean paleoenvironments (summary of ODP Leg 151 drilling results). Proc. Ocean  
29  
30 13 Drill. Program, Initial Reports 151, 397–420.  
31  
32  
33 14 Tsikalas, F., Faleide, J.I., Eldholm, O., Antonio-Blaich, O., 2012. The NE Atlantic conjugate margins,  
34  
35 15 Regional Geology and Tectonics. <https://doi.org/10.1016/B978-0-444-56357-6.00004-4>  
36  
37  
38 16 Tsikalas, F., Faleide, J.I., Eldholm, O., Wilson, J., 2005. Late Mesozoic–Cenozoic structural and  
39  
40 17 stratigraphic correlations between the conjugate mid-Norway and NE Greenland continental  
41  
42 18 margins. Pet. Geol. North West Eur. Glob. Perspect. — Proc. 6th Pet. Geol. Conf. 785–801.  
43  
44 19 <https://doi.org/10.1144/0060785>  
45  
46  
47 20 Whittaker, J.M., Williams, S., Masterton, S.M., Afonso, J.C., Seton, M., Landgrebe, T.C., Coffin, M.F.,  
48  
49 21 Müller, D., 2013. Interactions among plumes, mantle circulation and mid-ocean ridges. AGU  
50  
51 22 Fall Meet. Abstr. D113A–04.  
52  
53  
54  
55  
56  
57  
58  
59  
60  
61  
62  
63  
64  
65

1  
2 1 ~~Ziegler, P.A., 1992. European Cenozoic rift system. Tectonophysics 208, 91–111.~~  
3  
4 2 ~~[https://doi.org/10.1016/0040-1951\(92\)90338-7](https://doi.org/10.1016/0040-1951(92)90338-7)~~  
5  
6  
7 3 ~~Ziegler, P.A., Cloetingh, S., 2004. Dynamic processes controlling evolution of rifted basins. Earth~~  
8  
9 4 ~~Science Rev. 64, 1–50. [https://doi.org/10.1016/S0012-8252\(03\)00041-2](https://doi.org/10.1016/S0012-8252(03)00041-2)~~  
10  
11  
12 5 Andersen, O.B., 2010. The DTU10 Gravity field and Mean sea surface, in: Second International  
13  
14 6 Symposium of the Gravity Field of the Earth (IGFS2). Fairbanks, Alaska.  
15  
16  
17 7 Andersen, O.B., Knudsen, P., Berry, P.A.M., 2010. The DNSCO8GRA global marine gravity field from  
18  
19 8 double retracked satellite altimetry. J. Geod. 84, 191–199. [https://doi.org/10.1007/s00190-](https://doi.org/10.1007/s00190-009-0355-9)  
20  
21 9 [009-0355-9](https://doi.org/10.1007/s00190-009-0355-9)  
22  
23  
24 10 Berger, D., Jokat, W., 2009. Sediment deposition in the northern basins of the North Atlantic and  
25  
26 11 characteristic variations in shelf sedimentation along the East Greenland margin. Mar. Pet.  
27  
28 12 Geol. 26, 1321–1337. <https://doi.org/10.1016/j.marpetgeo.2009.04.005>  
29  
30  
31 13 Berger, D., Jokat, W., 2008. A seismic study along the East Greenland margin from 72°N to 77°N.  
32  
33 14 Geophys. J. Int. 174, 733–748. <https://doi.org/10.1111/j.1365-246X.2008.03794.x>  
34  
35  
36 15 Campbell, I.H., 2007. Testing the plume theory. Chem. Geol. 241, 153–176.  
37  
38 16 <https://doi.org/10.1016/j.chemgeo.2007.01.024>  
39  
40  
41 17 Clift, P.D., Carter, A., Hurford, A.J., P.D. Clift, A.C. and A.J.H., 1998. The erosional and uplift history of  
42  
43 18 NE Atlantic passive margins: constraints on a passing plume. J. Geol. Soc. London. 155, 788–  
44  
45 19 800. <https://doi.org/10.1144/gsjgs.155.5.0787>  
46  
47  
48 20 Cloetingh, S., Burov, E., Matenco, L., Beekman, F., Roure, F., Ziegler, P.A., 2013. The Moho in  
49  
50 21 extensional tectonic settings: Insights from thermo-mechanical models. Tectonophysics 609,  
51  
52 22 558–604. <https://doi.org/10.1016/j.tecto.2013.06.010>  
53  
54  
55  
56  
57  
58  
59  
60  
61  
62  
63  
64  
65



- 1  
2 1 Cloetingh, S.A.P.L., Ziegler, P.A., Bogaard, P.J.F., Andriessen, P.A.M., Artemieva, I.M., Bada, G., van  
3  
4 2 Balen, R.T., Beekman, F., Ben-Avraham, Z., Brun, J.P., Bunge, H.P., Burov, E.B., Carbonell, R.,  
5  
6 3 Facenna, C., Friedrich, A., Gallart, J., Green, A.G., Heidbach, O., Jones, A.G., Matenco, L., Mosar,  
7  
8 4 J., Oncken, O., Pascal, C., Peters, G., Sliapua, S., Soesoo, A., Spakman, W., Stephenson, R.A.,  
9  
10 5 Thybo, H., Torsvik, T., de Vicente, G., Wenzel, F., Wortel, M.J.R., 2007. TOPO-EUROPE: The  
11  
12 6 geoscience of coupled deep Earth-surface processes. *Glob. Planet. Change* 58, 1–118.  
13  
14 7 <https://doi.org/10.1016/j.gloplacha.2007.02.008>  
15  
16  
17 8 Døssing, A., Japsen, P., Watts, A.B., Nielsen, T., Jokat, W., Thybo, H., Dahl-Jensen, T., 2016. Miocene  
18  
19 9 uplift of the NE Greenland margin linked to plate tectonics: Seismic evidence from the  
20  
21 10 Greenland Fracture Zone, NE Atlantic. *Tectonics* 35, 257–282.  
22  
23 11 <https://doi.org/10.1002/2015TC004079>  
24  
25  
26 12 Emery, D., Myers, K., Bertram, G.T., 1996. *Sequence stratigraphy*. Blackwell Science.  
27  
28  
29 13 Engen, Ø., Faleide, J.I., Dyreng, T.K., 2008. Opening of the Fram Strait gateway: A review of plate  
30  
31 14 tectonic constraints. *Tectonophysics* 450, 51–69. <https://doi.org/10.1016/j.tecto.2008.01.002>  
32  
33  
34 15 Funck, T., Erlendsson, Ö., Geissler, W.H., Gradmann, S., Kimbell, G.S., McDermott, K., Petersen, U.K.,  
35  
36 16 2017. A review of the NE Atlantic conjugate margins based on seismic refraction data. *Geol.*  
37  
38 17 *Soc. London, Spec. Publ.* 447, 171–205. <https://doi.org/10.1144/SP447.9>  
39  
40  
41 18 Gaina, C., Gernigon, L., Ball, P., 2009. Palaeocene-Recent plate boundaries in the NE Atlantic and the  
42  
43 19 formation of the Jan Mayen microcontinent. *J. Geol. Soc. London.* 166, 601–616.  
44  
45 20 <https://doi.org/10.1144/0016-76492008-112>  
46  
47  
48 21 Ganerød, M., Smethurst, M.A., Torsvik, T.H., Prestvik, T., Rouse, S., McKenna, C., van Hinsbergen,  
49  
50 22 D.J.J., Hendriks, B.W.H., 2010. The North Atlantic Igneous Province reconstructed and its  
51  
52 23 relation to the Plume Generation Zone: The Antrim Lava Group revisited. *Geophys. J. Int.* 182,  
53  
54  
55  
56  
57  
58  
59  
60  
61  
62  
63  
64  
65

- 1  
2 1 183–202. <https://doi.org/10.1111/j.1365-246X.2010.04620.x>  
3  
4  
5 2 Guarnieri, P., 2015. Pre-break-up palaeostress state along the East Greenland margin. *J. Geol. Soc.*  
6  
7 3 London. 172, 727–739. <https://doi.org/10.1144/jgs2015-053>  
8  
9  
10 4 Håkansson, E., Stemmerik, L., 1989. Wandel Sea Basin - a new synthesis of the Late Paleozoic to  
11  
12 5 Tertiary accumulation in North Greenland. *Geology* 17, 683–686.  
13  
14 6 [https://doi.org/10.1130/0091-7613\(1989\)017<0683:WSBANS>2.3.CO;2](https://doi.org/10.1130/0091-7613(1989)017<0683:WSBANS>2.3.CO;2)  
15  
16  
17 7 Hamann, N.E., Whittaker, R.C., Stemmerik, L., 2005. Geological development of the Northeast  
18  
19 8 Greenland Shelf, in: *Petroleum Geology: North-West Europe and Global Perspectives –*  
20  
21 9 *Proceedings of the 6th Petroleum Geology Conference.* pp. 887–902.  
22  
23 10 <https://doi.org/10.1144/0060887>  
24  
25  
26 11 Hansen, J., Jerram, D.A., McCaffrey, K., Passey, S.R., 2009. The onset of the North Atlantic Igneous  
27  
28 12 Province in a rifting perspective. *Geol. Mag.* 146, 309–325.  
29  
30 13 <https://doi.org/10.1017/S0016756809006347>  
31  
32  
33 14 Larsen, L.M., Pedersen, A.K., Tegner, C., Duncan, R.A., 2014. Eocene to Miocene igneous activity in  
34  
35 15 NE Greenland: northward younging of magmatism along the East Greenland margin. *J. Geol.*  
36  
37 16 *Soc. London.* 171, 539–553. <https://doi.org/10.1144/jgs2013-118>  
38  
39  
40 17 Lundin, E., Doré, A.G., 2002. Mid -Cenozoic post -breakup deformation in the `passive` margins  
41  
42 18 bordering the Norwegian- Greenland Sea 19, 79–93.  
43  
44  
45 19 Matthews, K.J., Maloney, K.T., Zahirovic, S., Williams, S.E., Seton, M., Müller, R.D., 2016. Global plate  
46  
47 20 boundary evolution and kinematics since the late Paleozoic. *Glob. Planet. Change* 146, 226–  
48  
49 21 250. <https://doi.org/10.1016/j.gloplacha.2016.10.002>  
50  
51  
52 22 McKenzie, D., 1978. Some remarks on the development of sedimentary basins. *Earth Planet. Sci.*  
53  
54  
55  
56  
57  
58  
59  
60  
61  
62  
63  
64  
65

- 1  
2 1 Lett. 40, 25–32. [https://doi.org/10.1016/0012-821X\(78\)90071-7](https://doi.org/10.1016/0012-821X(78)90071-7)  
3  
4  
5 2 Miller, K.G., Kominz, M.A., Browning, J. V., Wright, J.D., Mountain, G.S., Katz, M.E., Sugarman, P.J.,  
6  
7 3 Cramer, B.S., Christie-Blick, N., Pekar, S.F., 2005. The phanerozoic record of global sea-level  
8  
9 4 change. *Science (80-. )*. 310, 1293–1298. <https://doi.org/10.1126/science.1116412>  
10  
11  
12 5 Müller, R.D., Seton, M., Zahirovic, S., Williams, S.E., Matthews, K.J., Wright, N.M., Shephard, G.E.,  
13  
14 6 Maloney, K.T., Barnett-Moore, N., Hosseinpour, M., Bower, D.J., Cannon, J., 2016. Ocean Basin  
15  
16 7 Evolution and Global-Scale Plate Reorganization Events Since Pangea Breakup. *Annu. Rev. Earth*  
17  
18 8 *Planet. Sci.* 44, 107–138. <https://doi.org/10.1146/annurev-earth-060115-012211>  
19  
20  
21 9 Nøhr-Hansen, H., Nielsen, L.H., Sheldon, E., Hovikoski, J., Alsen, P., 2011. Palaeogene deposits in  
22  
23 10 North-East Greenland. *Geol. Surv. Denmark Greenl. Bull.* 23, 61–64.  
24  
25  
26 11 Ogg, J.G., 2012. *Geomagnetic Polarity Time Scale, The Geologic Time Scale 2012*. Elsevier.  
27  
28 12 <https://doi.org/10.1016/B978-0-444-59425-9.00005-6>  
29  
30  
31 13 Olesen, O., Ebbing, J., Lundin, E., Muring, E., Skilbrei, J.R., Torsvik, T.H., Hansen, E.K., Henningsen,  
32  
33 14 T., Midbøe, P., Sand, M., 2007. An improved tectonic model for the Eocene opening of the  
34  
35 15 Norwegian-Greenland Sea: Use of modern magnetic data. *Mar. Pet. Geol.* 24, 53–66.  
36  
37 16 <https://doi.org/10.1016/j.marpetgeo.2006.10.008>  
38  
39  
40 17 Petersen, T.G., Hamann, N.E., Stemmerik, L., 2016. Correlation of the Palaeogene successions on the  
41  
42 18 North-East Greenland and Barents Sea margins. *Bull. Geol. Soc. Denmark* 64, 77–96.  
43  
44  
45 19 Petersen, T.G., Hamann, N.E., Stemmerik, L., 2015. Tectono-sedimentary evolution of the Paleogene  
46  
47 20 succession offshore Northeast Greenland. *Mar. Pet. Geol.* 67, 481–497.  
48  
49 21 <https://doi.org/10.1016/j.marpetgeo.2015.05.033>  
50  
51  
52 22 Reynolds, P., Planke, S., Millett, J.M., Jerram, D.A., Trulsvik, M., Schofield, N., Myklebust, R., 2017.  
53  
54  
55  
56  
57  
58  
59  
60  
61  
62  
63  
64  
65

1  
2 1 Hydrothermal vent complexes offshore Northeast Greenland: A potential role in driving the  
3  
4 2 PETM. *Earth Planet. Sci. Lett.* 467, 72–78. <https://doi.org/10.1016/j.epsl.2017.03.031>  
5  
6  
7 3 Rickers, F., Fichtner, A., Trampert, J., 2013. The Iceland-Jan Mayen plume system and its impact on  
8  
9 4 mantle dynamics in the North Atlantic region: Evidence from full-waveform inversion. *Earth*  
10  
11 5 *Planet. Sci. Lett.* 367, 39–51. <https://doi.org/10.1016/j.epsl.2013.02.022>  
12  
13  
14 6 Rowan, M.G., Lindsø, S., 2017. Salt Tectonics of the Norwegian Barents Sea and Northeast Greenland  
15  
16 7 Shelf, Permo-Triassic Salt Provinces of Europe, North Africa and the Atlantic Margins: Tectonics  
17  
18 8 and Hydrocarbon Potential. Elsevier Inc. <https://doi.org/10.1016/B978-0-12-809417-4.00013-6>  
19  
20  
21 9 Stemmerik, L., 2000. Late Palaeozoic evolution of the North Atlantic margin of Pangea. *Palaeogeogr.*  
22  
23 10 *Palaeoclimatol. Palaeoecol.* 161, 95–126. [https://doi.org/10.1016/S0031-0182\(00\)00119-X](https://doi.org/10.1016/S0031-0182(00)00119-X)  
24  
25  
26 11 Storey, M., Duncan, R.A., Tegner, C., 2007. Timing and duration of volcanism in the North Atlantic  
27  
28 12 Igneous Province: Implications for geodynamics and links to the Iceland hotspot. *Chem. Geol.*  
29  
30 13 241, 264–281. <https://doi.org/10.1016/j.chemgeo.2007.01.016>  
31  
32  
33 14 Talwani, M., Eldholm, O., 1977. Evolution of the Norwegian-Greenland Sea. *Bull. Geol. Soc. Am.* 88,  
34  
35 15 969–999. [https://doi.org/10.1130/0016-7606\(1977\)88<969:EOTNS>2.0.CO;2](https://doi.org/10.1130/0016-7606(1977)88<969:EOTNS>2.0.CO;2)  
36  
37  
38 16 Tegner, C., Storey, M., Holm, P.M., Thorarinsson, S.B., Zhao, X., Lo, C.H., Knudsen, M.F., 2011.  
39  
40 17 Magmatism and Eureka deformation in the High Arctic Large Igneous Province: 40Ar-39Ar age  
41  
42 18 of Kap Washington Group volcanics, North Greenland. *Earth Planet. Sci. Lett.* 303, 203–214.  
43  
44 19 <https://doi.org/10.1016/j.epsl.2010.12.047>  
45  
46  
47 20 Thiede, J., Myhre, A.M., Firth, J.V. and the S.S.P., 1995. Cenozoic northern hemisphere polar and  
48  
49 21 subpolar ocean paleoenvironments (summary of ODP Leg 151 drilling results). *Proc. Ocean*  
50  
51 22 *Drill. Program, Initial Reports 151*, 397–420.  
52  
53  
54  
55  
56  
57  
58  
59  
60  
61  
62  
63  
64  
65

1  
2 1 Tsikalas, F., Faleide, J.I., Eldholm, O., Antonio Blaich, O., 2012. The NE Atlantic conjugate margins,  
3  
4 2 Regional Geology and Tectonics. <https://doi.org/10.1016/B978-0-444-56357-6.00004-4>  
5  
6  
7 3 Tsikalas, F., Faleide, J.I., Eldholm, O., Wilson, J., 2005. Late Mesozoic–Cenozoic structural and  
8  
9 4 stratigraphic correlations between the conjugate mid-Norway and NE Greenland continental  
10  
11 5 margins. *Pet. Geol. North-West Eur. Glob. Perspect. – Proc. 6th Pet. Geol. Conf.* 785–801.  
12  
13 6 <https://doi.org/10.1144/0060785>  
14  
15  
16 7 Whittaker, J.M., Williams, S., Masterton, S.M., Afonso, J.C., Seton, M., Landgrebe, T.C., Coffin, M.F.,  
17  
18 8 Müller, D., 2013. Interactions among plumes, mantle circulation and mid-ocean ridges. AGU  
19  
20 9 Fall Meet. Abstr. D113A–04.  
21  
22  
23 10 Ziegler, P.A., 1992. European Cenozoic rift system. *Tectonophysics* 208, 91–111.  
24  
25 11 [https://doi.org/10.1016/0040-1951\(92\)90338-7](https://doi.org/10.1016/0040-1951(92)90338-7)  
26  
27  
28 12 Ziegler, P.A., Cloetingh, S., 2004. Dynamic processes controlling evolution of rifted basins. *Earth-*  
29  
30 13 *Science Rev.* 64, 1–50. [https://doi.org/10.1016/S0012-8252\(03\)00041-2](https://doi.org/10.1016/S0012-8252(03)00041-2)  
31  
32

33 14 |  
34  
35

36  
37  
38  
39  
40  
41  
42  
43  
44  
45  
46  
47  
48  
49  
50  
51  
52  
53  
54  
55  
56  
57  
58  
59  
60  
61  
62  
63  
64  
65

Figure 1  
[Click here to download high resolution image](#)

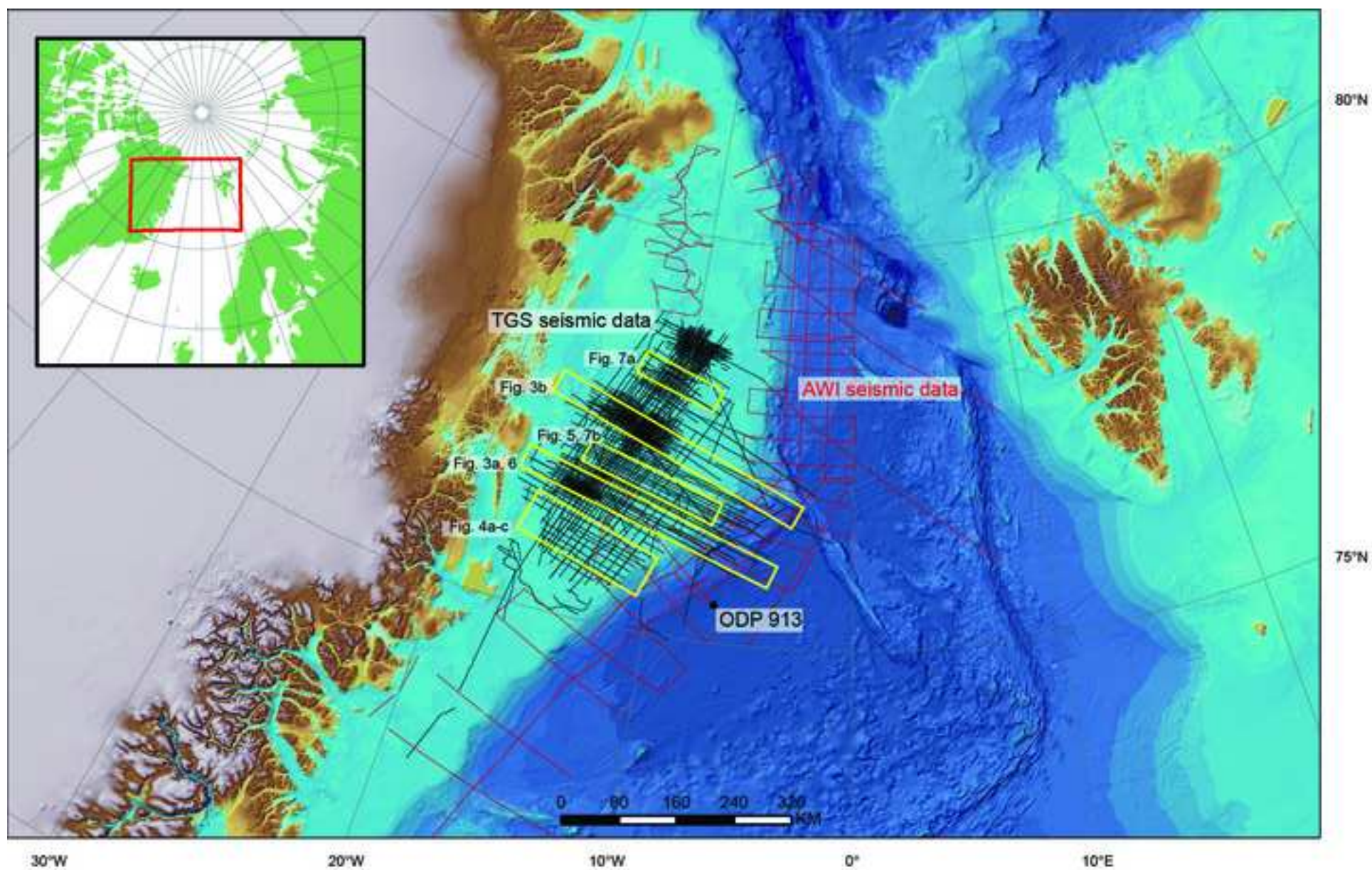


Figure 2  
[Click here to download high resolution image](#)

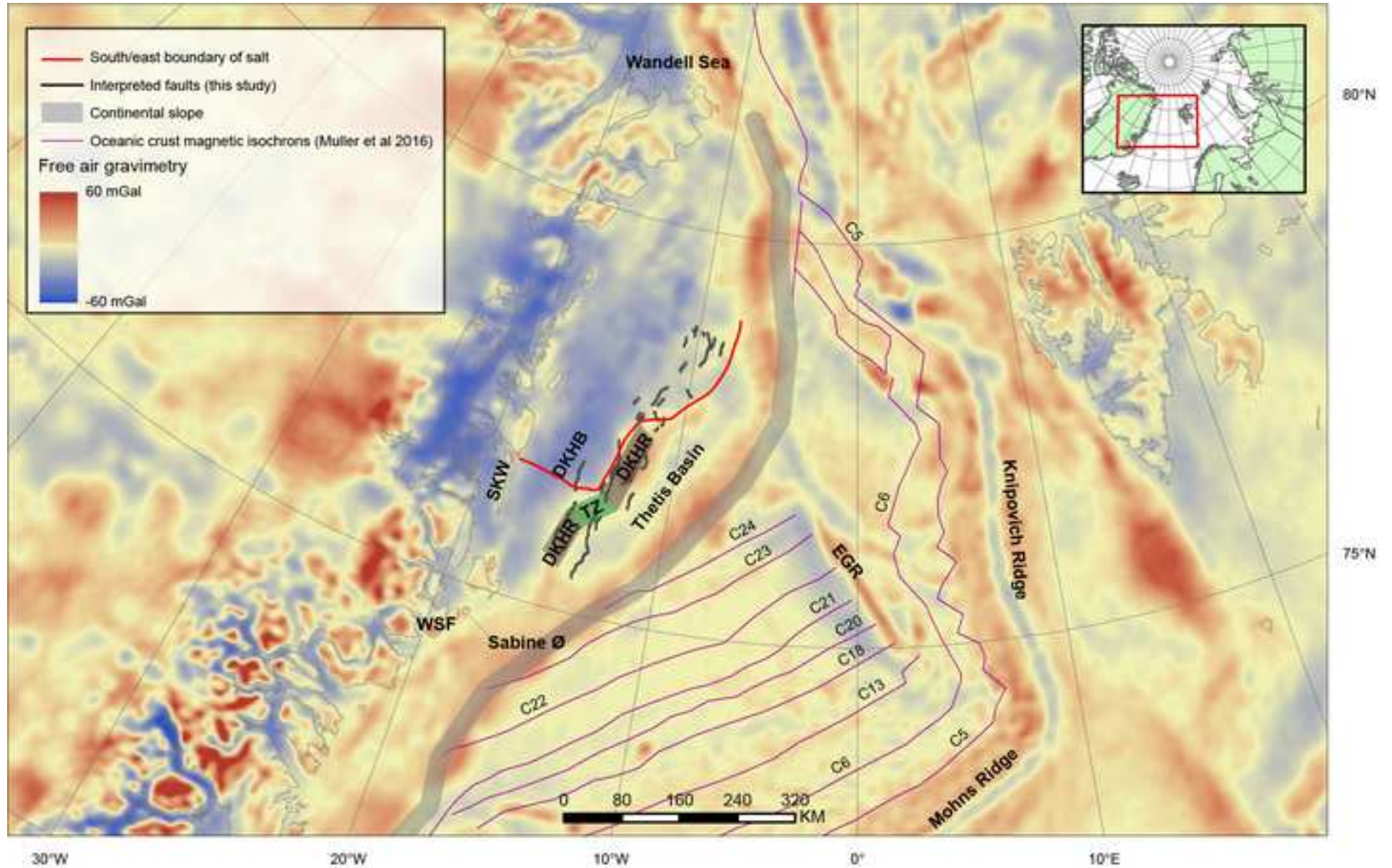


Figure 3a  
[Click here to download high resolution image](#)

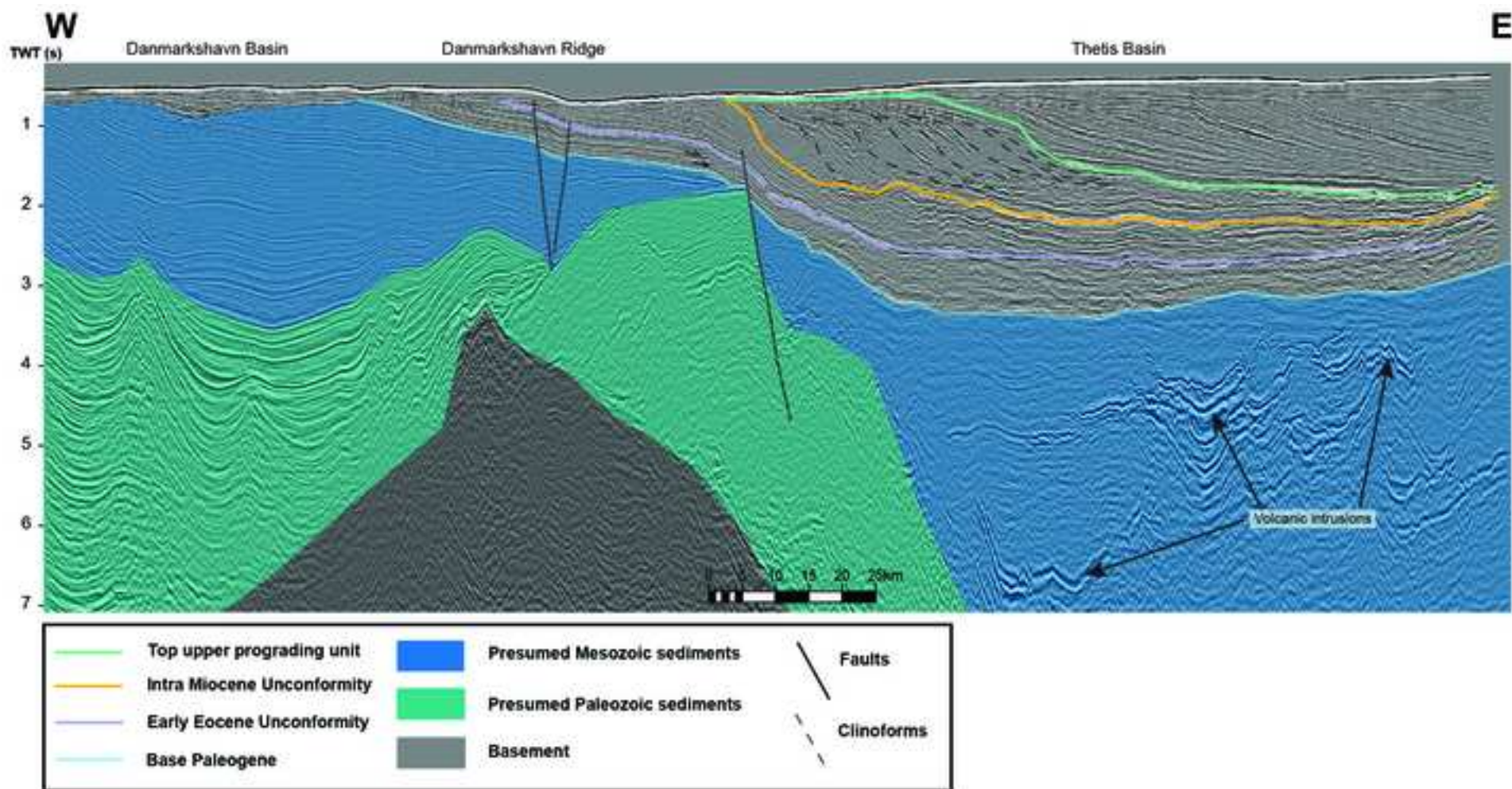




Figure 3b  
[Click here to download high resolution image](#)

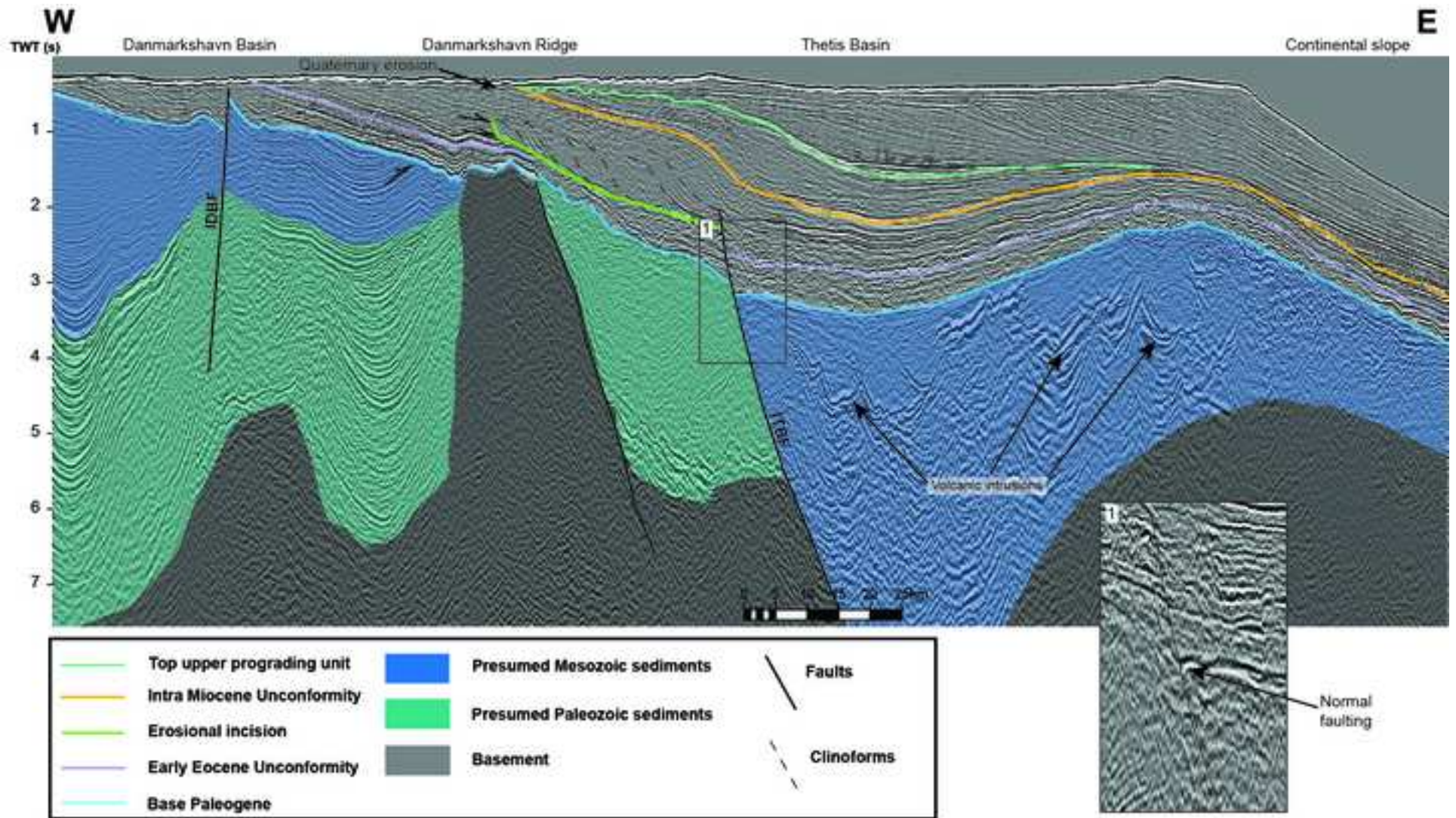


Figure 4

[Click here to download high resolution image](#)

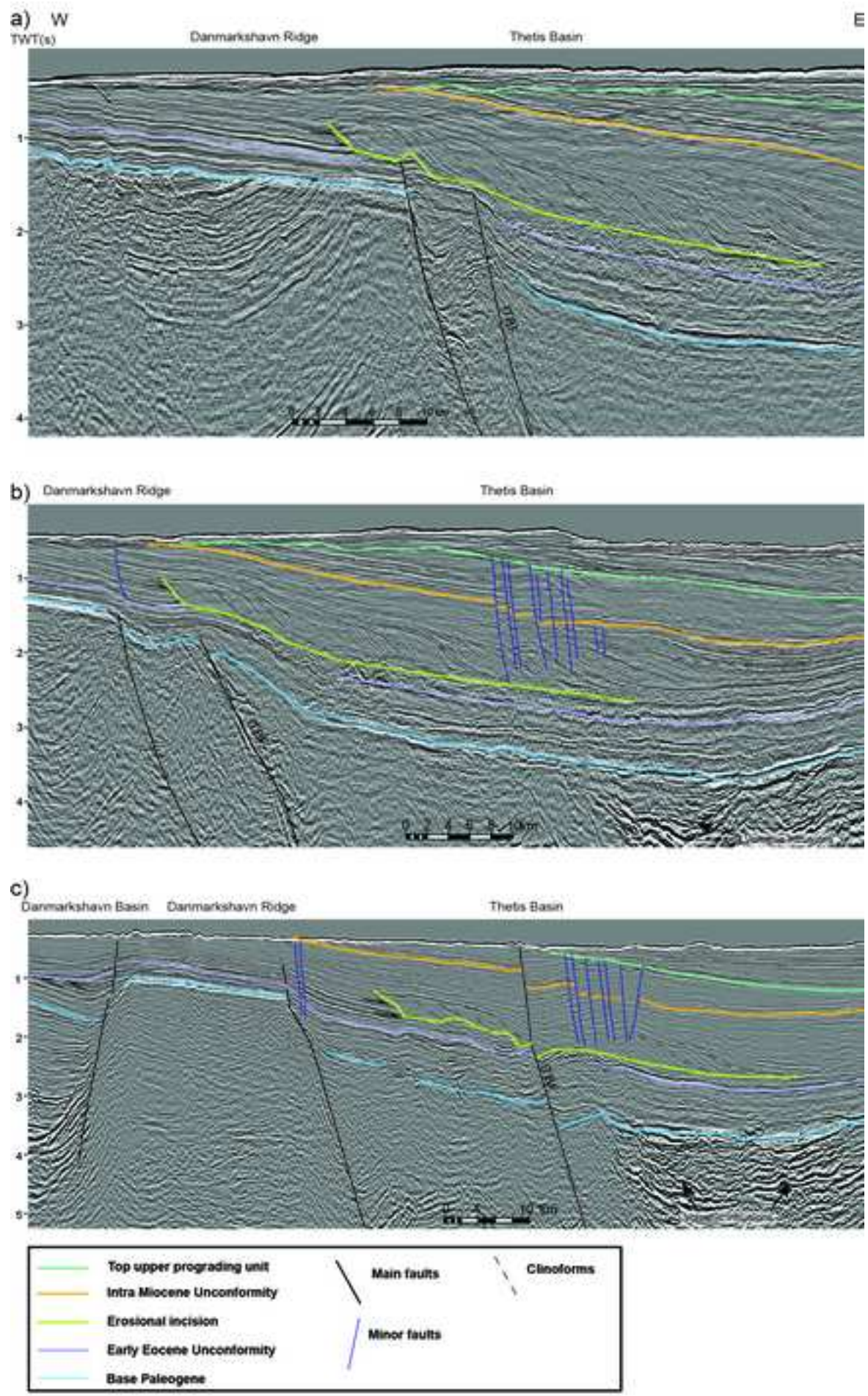


Figure 5  
[Click here to download high resolution image](#)

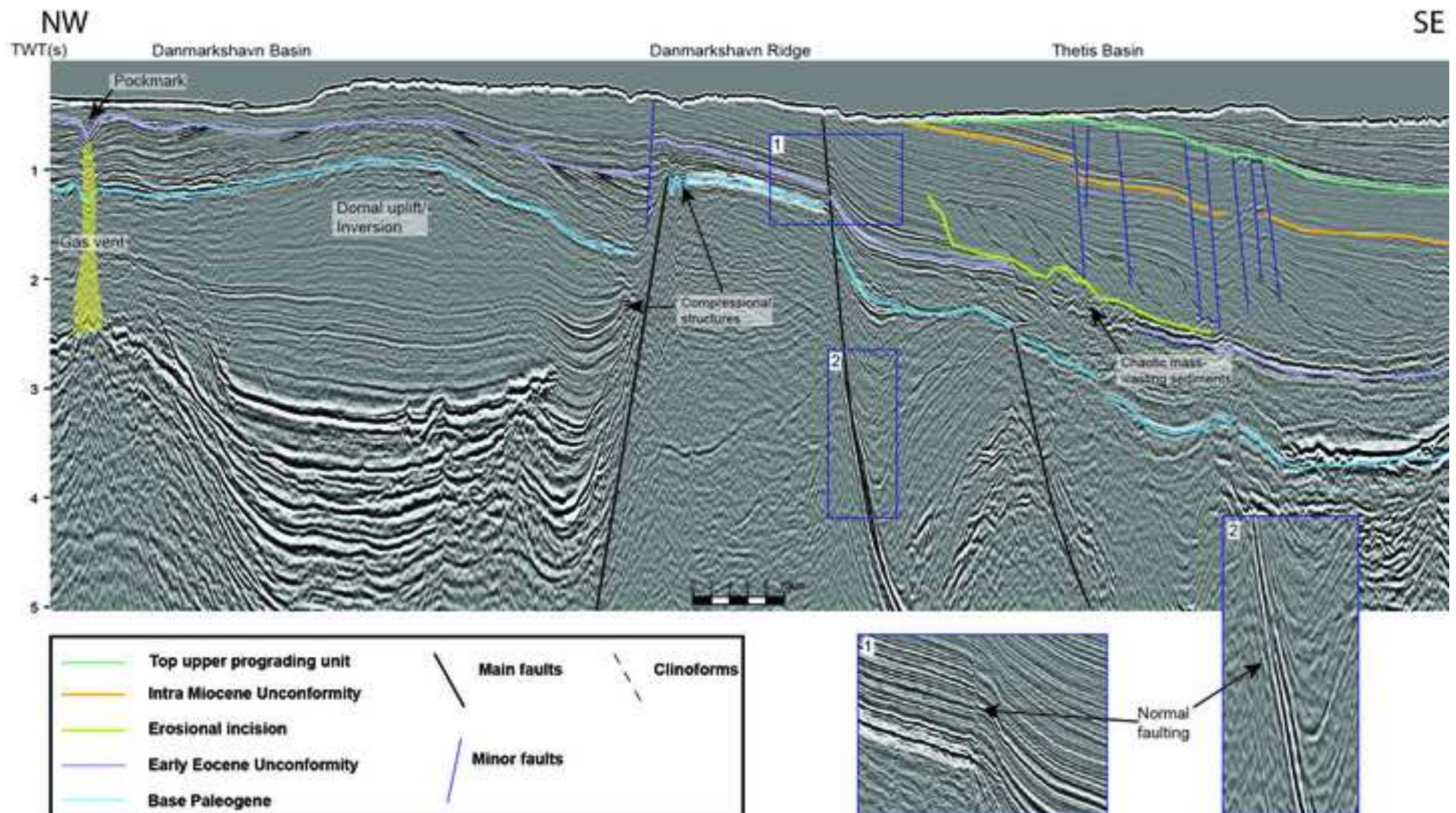


Figure 6  
[Click here to download high resolution image](#)

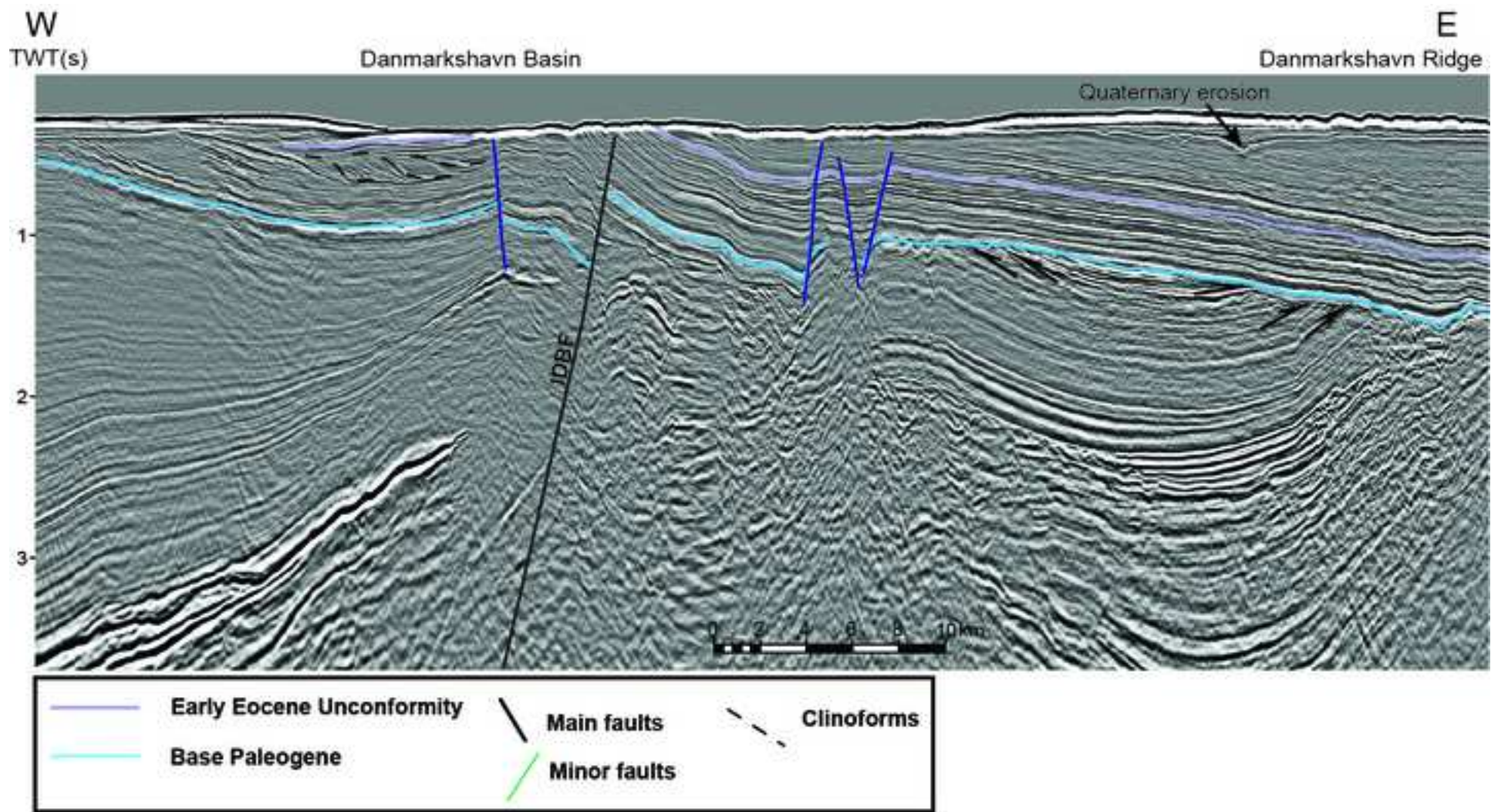


Figure 7  
[Click here to download high resolution image](#)

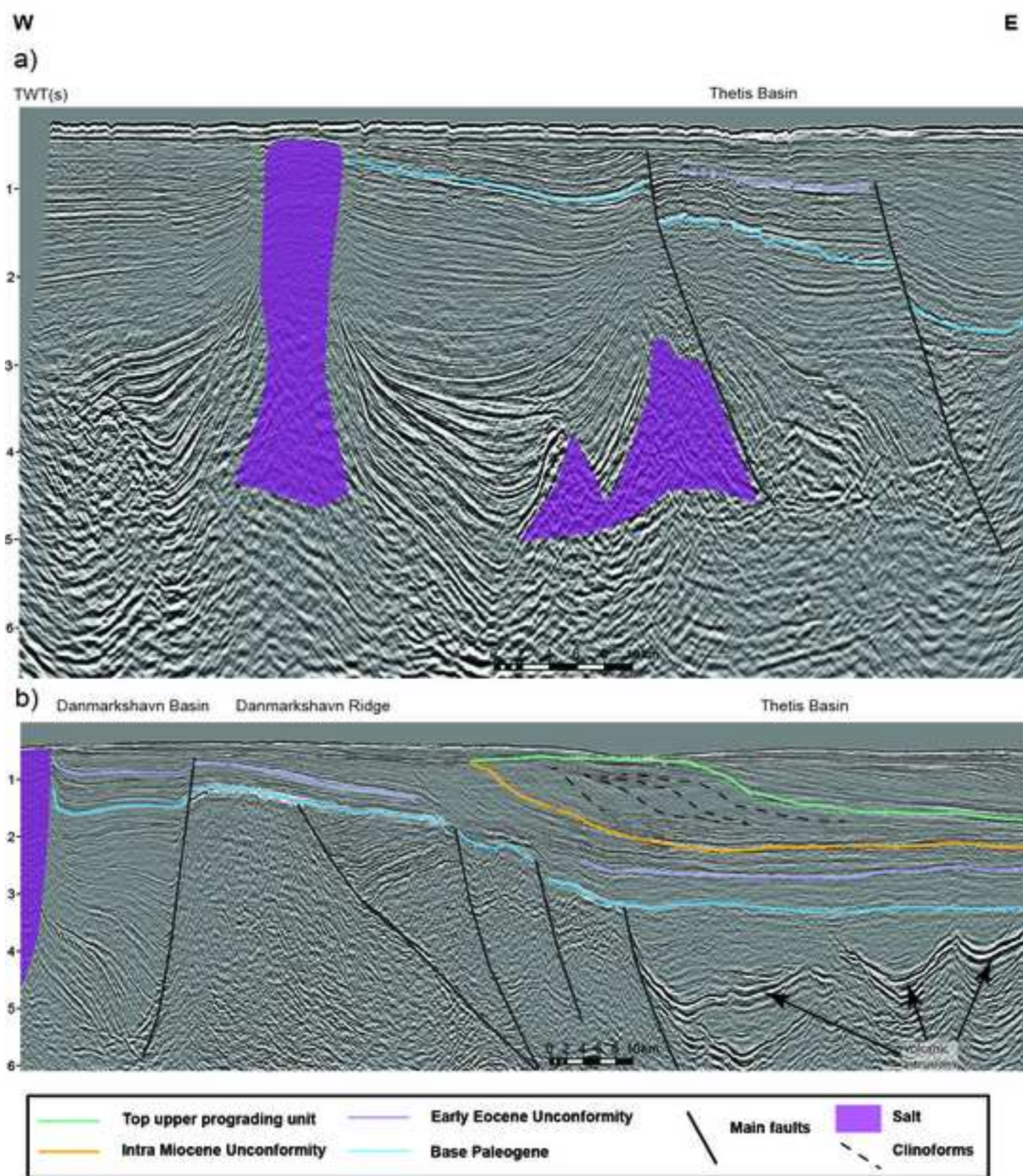


Figure 8  
[Click here to download high resolution image](#)

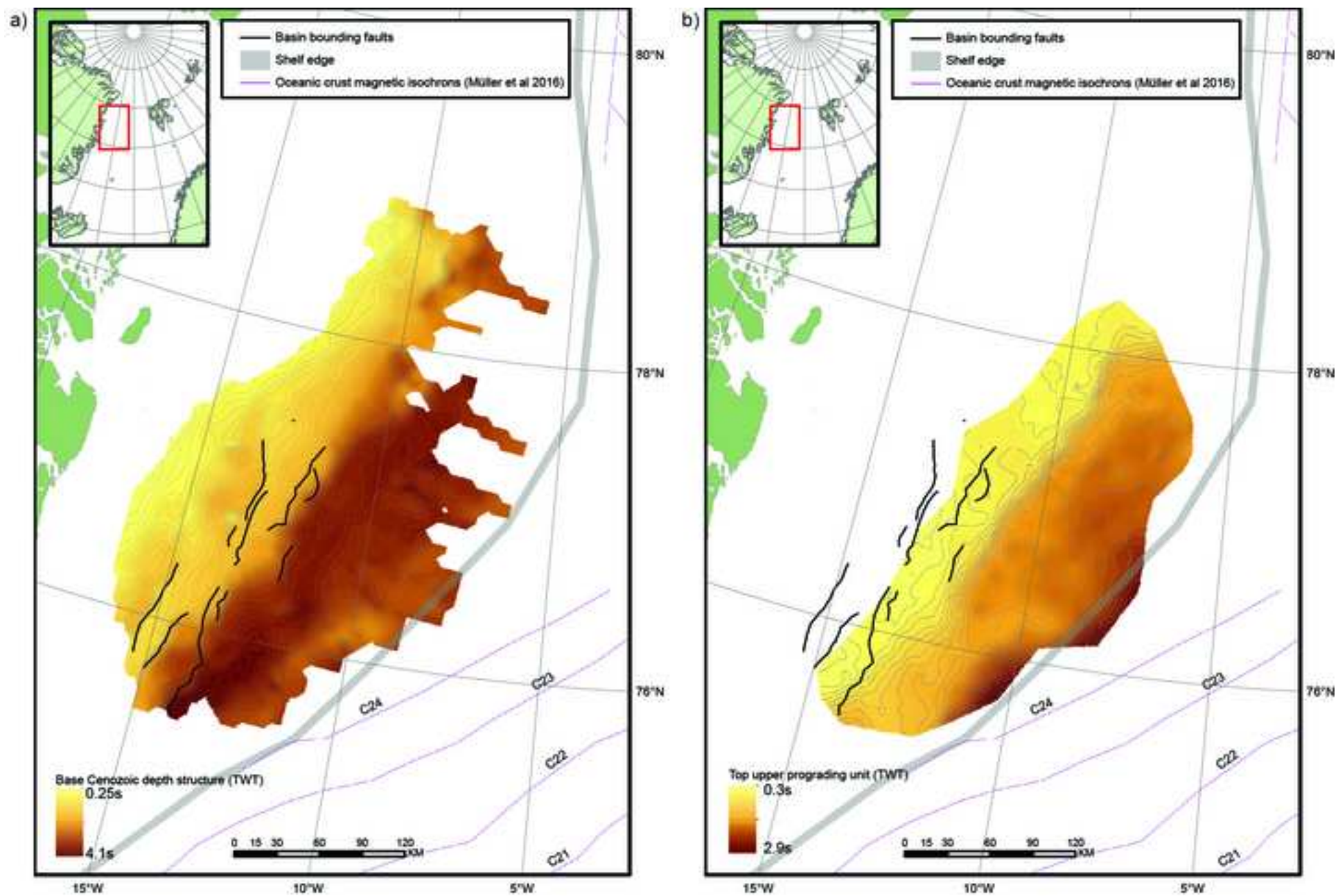


Figure 9

[Click here to download high resolution image](#)

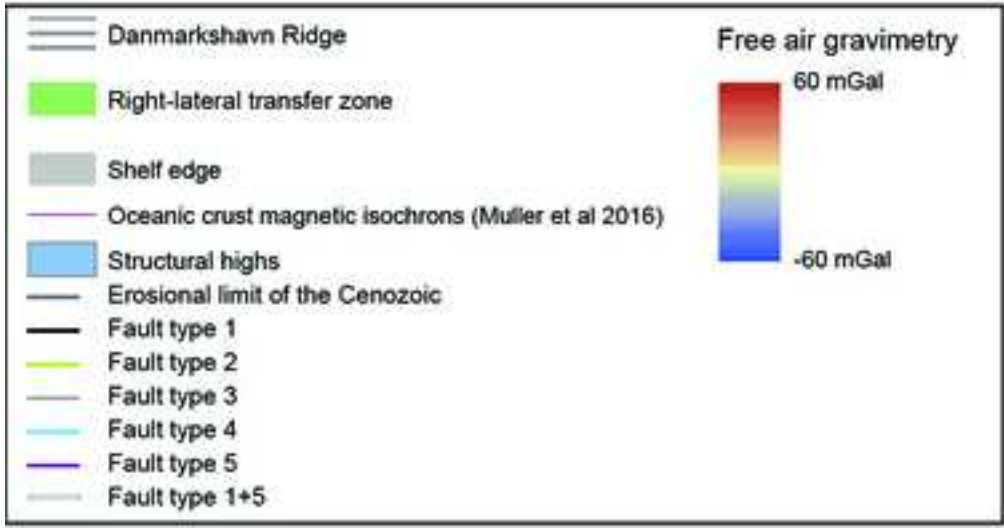
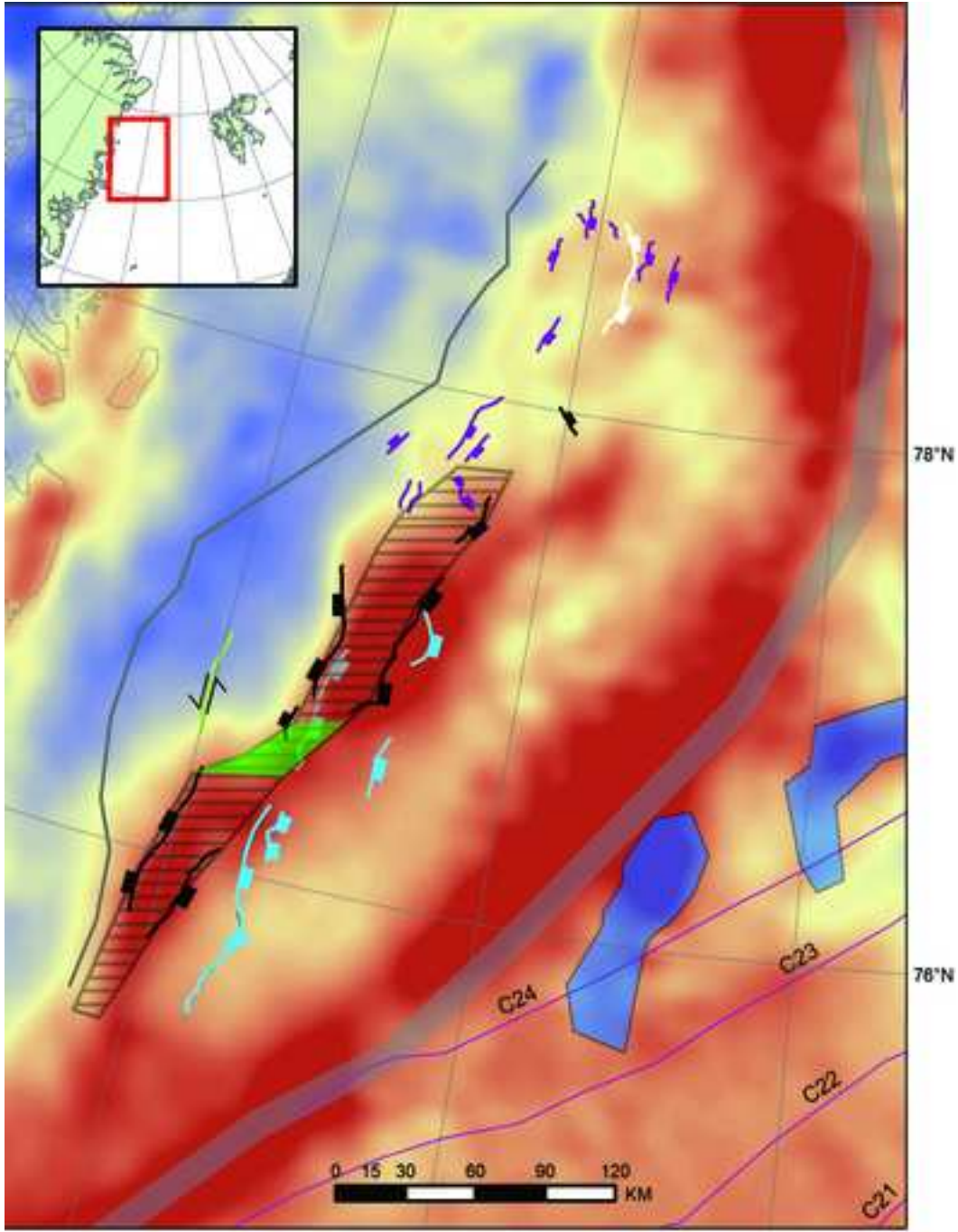


Figure 10

[Click here to download high resolution image](#)

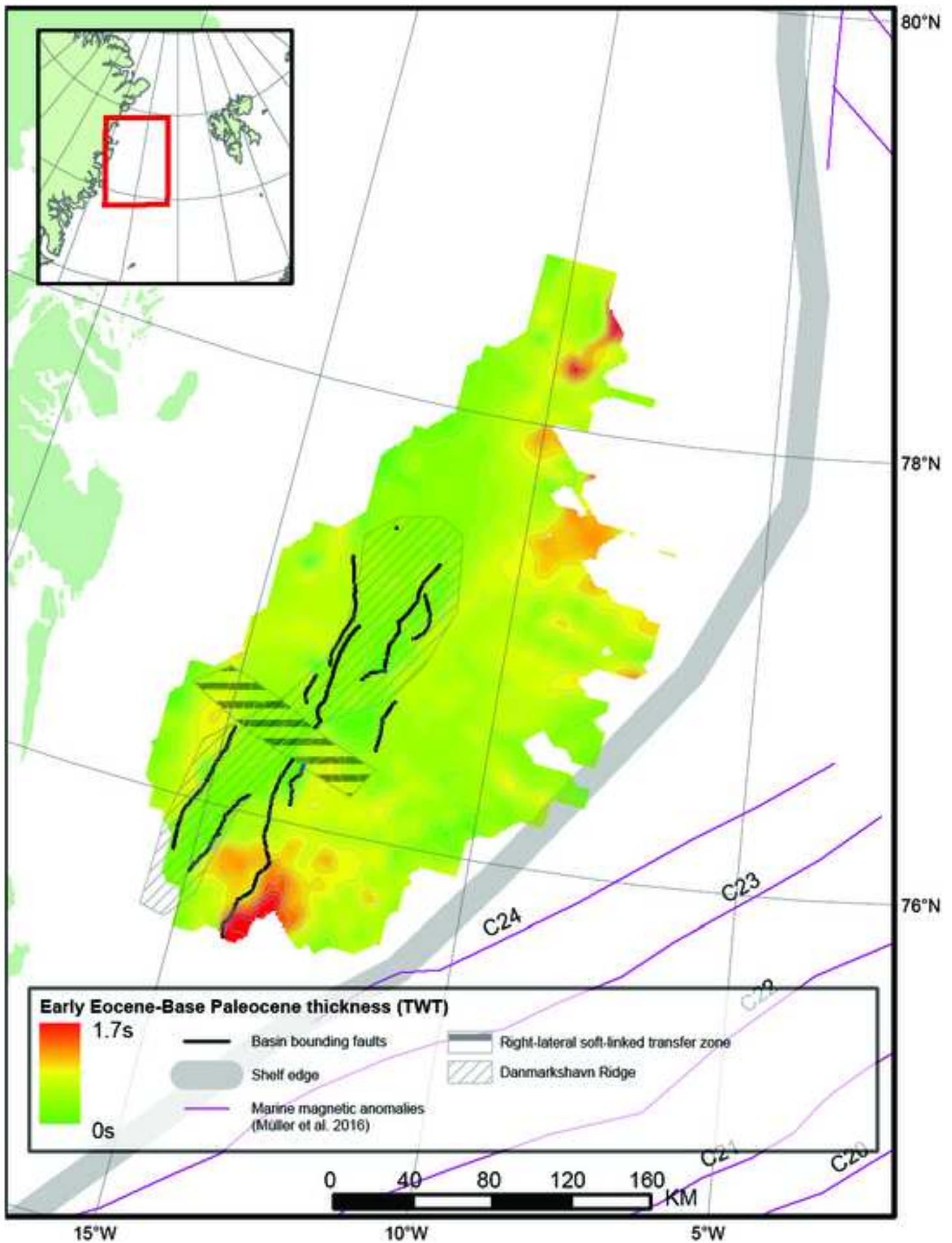




Figure 11  
[Click here to download high resolution image](#)

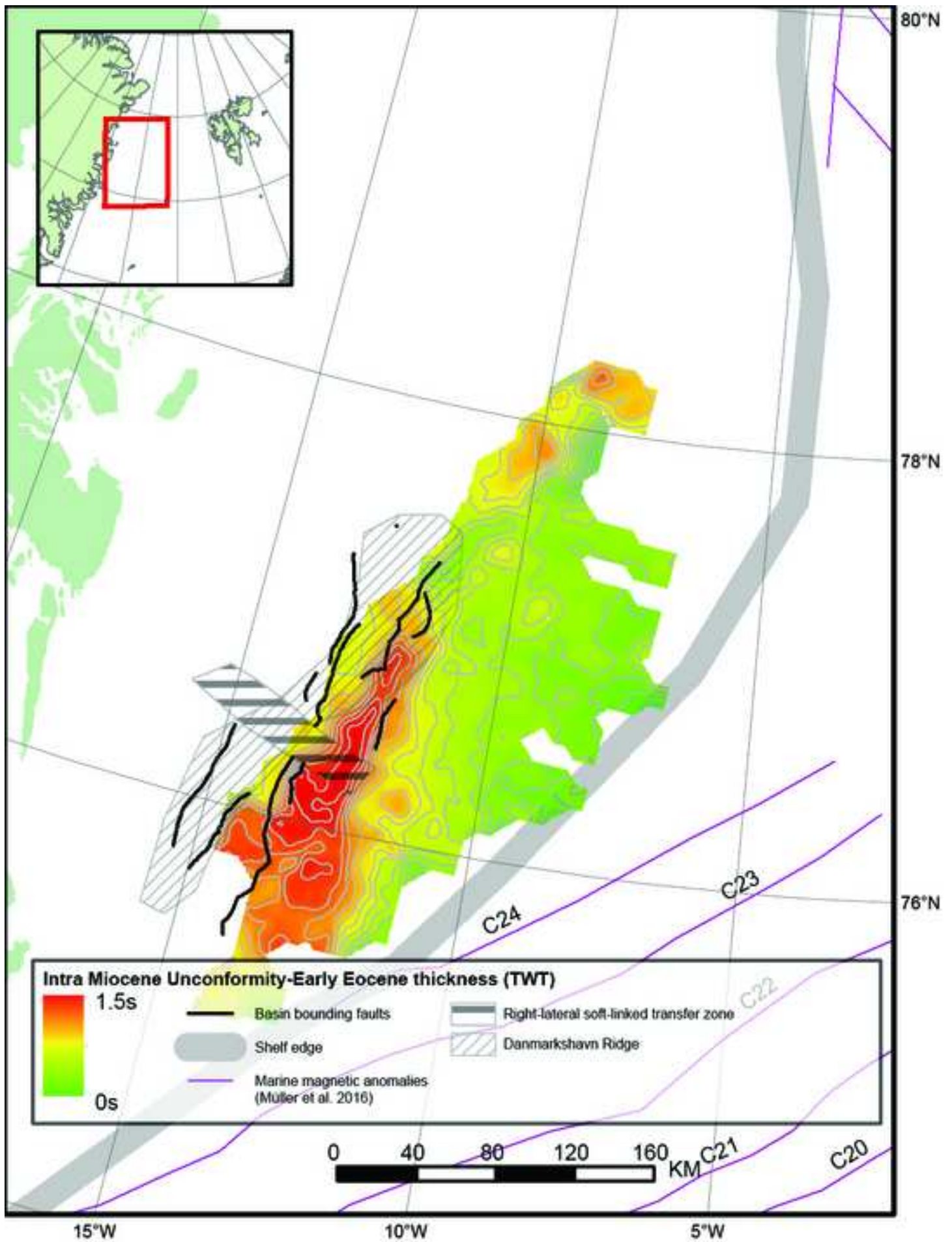


Figure 12

[Click here to download high resolution image](#)

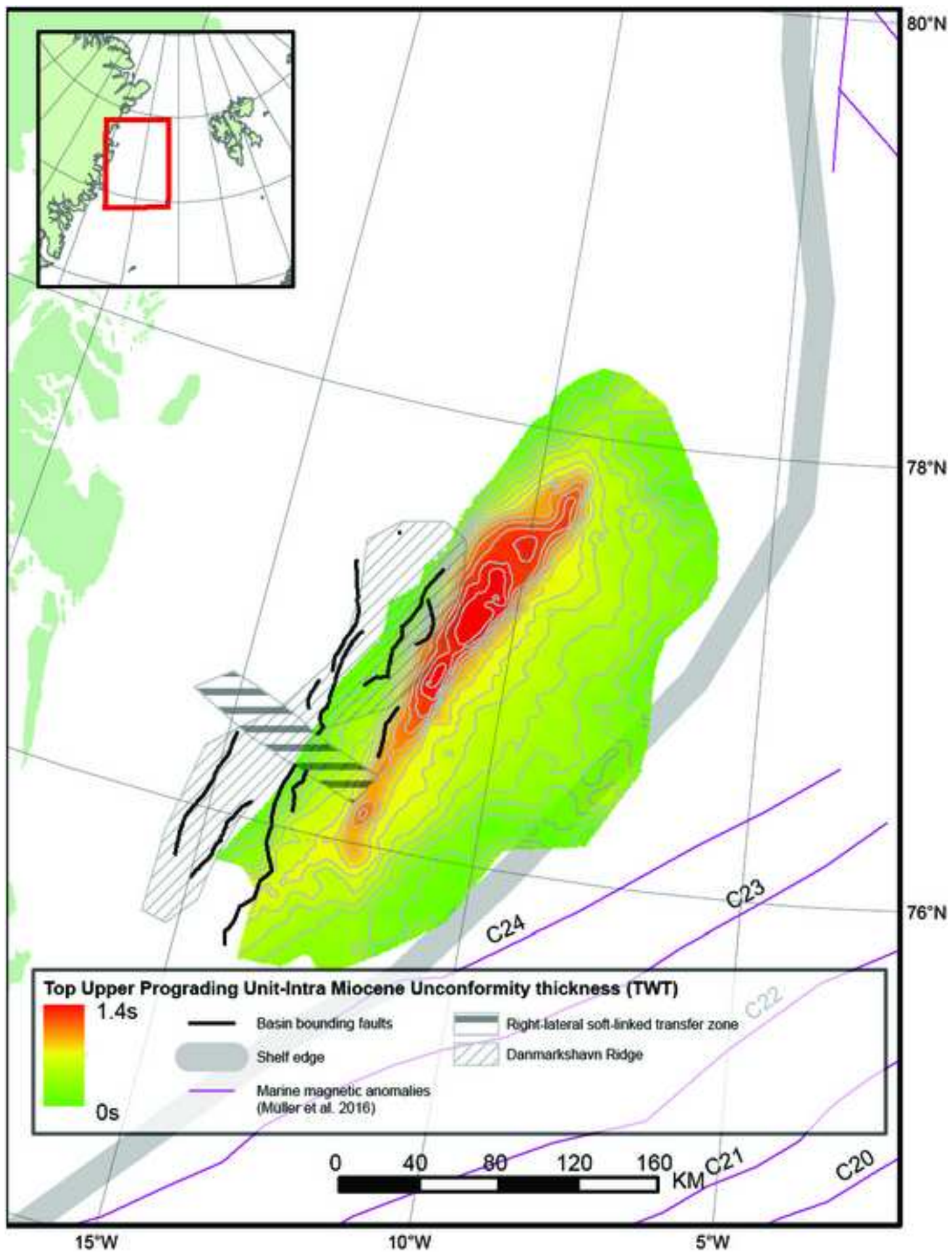


Figure 13

[Click here to download high resolution image](#)

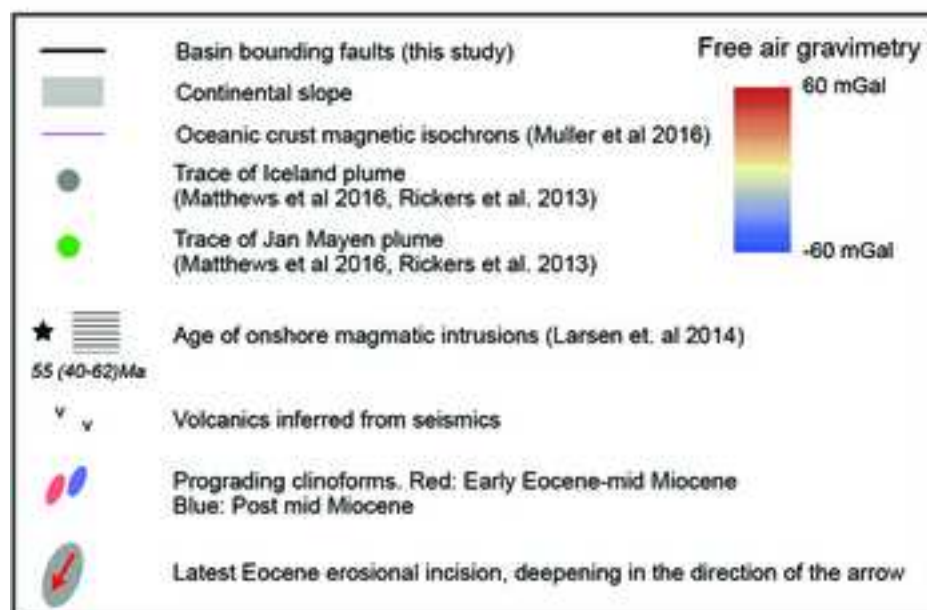
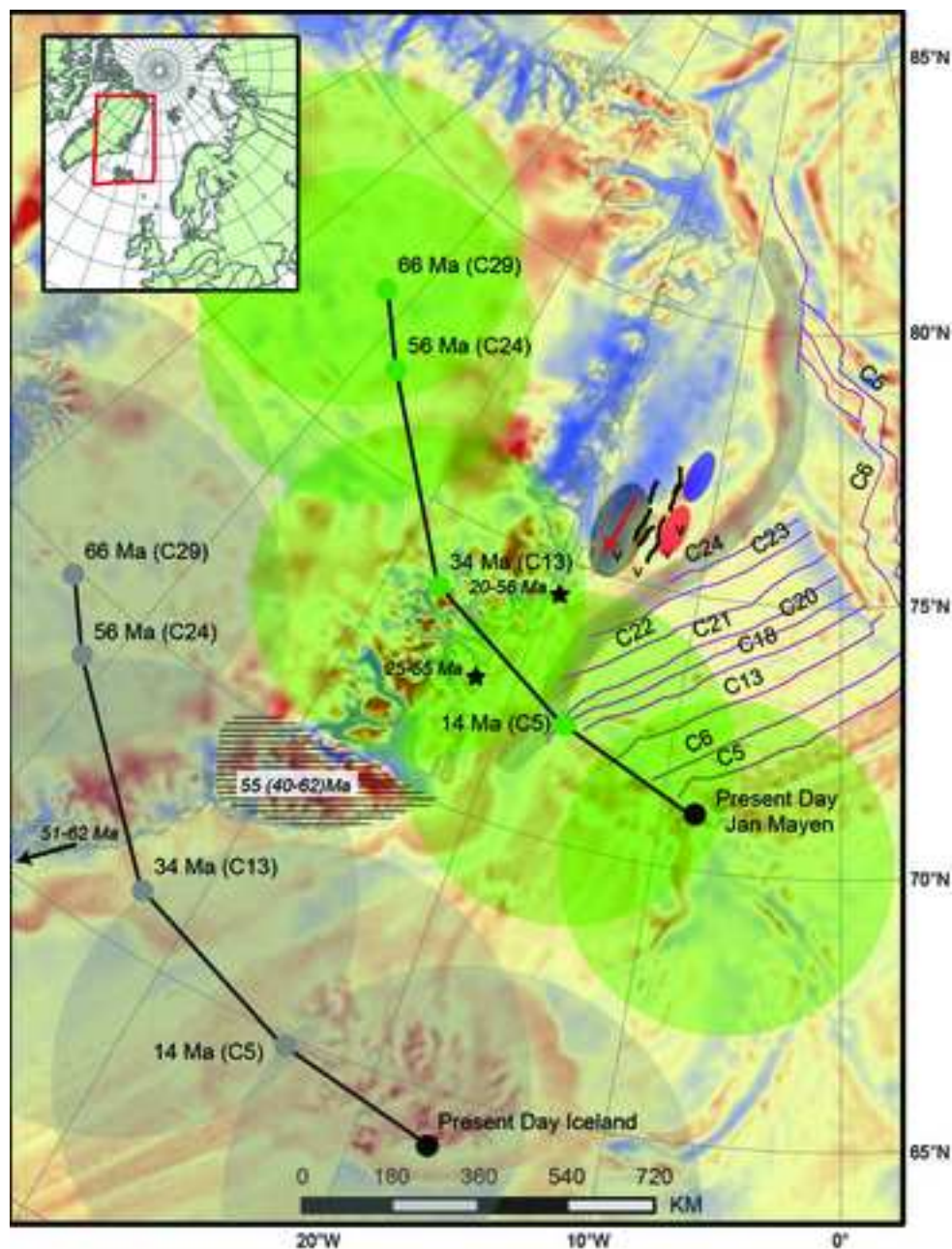


Figure 14

[Click here to download high resolution image](#)

